SAPIENZA
UNIVERSITÀ DI ROMA

University of Rome La Sapienza

Dept. Chemical Engineering Materials and Environment

Photobioremediation of agro-industrial wastewaters by microalgae and cyanobacteria: simultaneous production of biomass and high added value secondary metabolites

PhD in chemical engineering environment and safety

XXVI cycle

Candidate

Agnese Cicci

Tutor

Prof. Marco Bravi

A mia figlia

Summary

1. Introduction 5

2. PhotoBioReactors (PBR) for microalgal cultivation 8

2.1 Microalgal cultivation systems 8

2.1.1. Raceway PBR 8

2.1.2. Closed PBR 9

2.2. Light: an essential parameter 14

3. Microalgal technology 19

3.1. Biofuel from microalgae 19

3.2. Nutraceutics from microalgae 21

3.2.1. Chlorella vulgaris 21

3.2.2. Arthrospira platensis 22

3.2.3. Dunaliella 23

3.3. Pharmaceutics from microalgae 23

3.4. Microalgal wastewaters treatment 26

4. Materials and methods 29

4.1. Set up for microalgal cultivation in synthetic media 29

4.1.1. Cellular concentration , dry weight and pH 29

4.2. OMWW pre -treatment 29

4.2.1. OMWW feedstocks production by membrane separation 30

4.2.2. Set up microalgal cultivation in OMWW and its fractions 31

4.3. Cattle digestate pre-treatment 32

4.3.1. Set up microalgal cultivation in cattle digestate 32

4.4. Carbohydrates and proteins essays 32

4.5. C-phycocyanin extraction 32

4.6. Determination of cholorophills A, B and total carotenoids 33

4.7. Lipid extraction 33

4.8. Media analysis 33

4.9. Experimental equipment for the fluid dynamic investigation on the local recirculation photobioreactor 34

4.10. Local Recirculation PBR for microalgal culture 36

4.11. Experimental set up microalgal cultivation in Local Recirculation PBR (LR-PBR) out-door 37

5. Results and discussion 38

5.1. Microalgal growths in synthetic media in air and air with 5% of CO_2 38

5.1.1. *Scenedesmus dimorphus* 1237 growth 38

5.1.2. *Arthrospira platensis* growth 40

5.2. Microalgal growth rates on olive oil mill wastewater (OMWW) 41

5.2.1. Microalgal growth rates on OMWW and its fractions diluted with 50% of synthetic media: polyphenols and phenol analysis 42

5.2.2. Microalgal growth rates on OMWW and its fractions diluted with 50% of synthetic media: biomass profiles and supernatant analysis 45

5.2.3. *S. dimorphus 1237* growth in OMWW and its fractions diluted (1:1 v/v) with synthetic medium 46

5.2.4. *A. platensis* growth in OMWW and its fractions diluted (1:1 v/v) with synthetic medium 50

5.3. Preliminary data of *S. dimorphus 1237* and *Arthrospira platensis* growth rates in digestate. 53

5.3.1. *S. dimorphus 1237* specific growth rates in digestate diluted at 50% by volume with synthetic medium 54

5.3.2. *A. platensis* growth rates in digestate diluted at 50% in volume with synthetic medium 58

5.4. Analysis of extracted species-specific metabolites: lipids from *S. dimorphus* 1237 and C-phycocyanin from *A. platensis* 60

5.5. Light supply and microalgal growth 61

5.6. Fluid dynamic study of Local Recirculating PBR (LR-PBR) by particle tracking velocimetry (FT) 68

5.7. Microalgal growth tests in the Local Recirculation PhotoBioreactor (LR-PBR) 79

6. Conclusions 81

7. References 82

1. Introduction

Microalgae are primary producers of food chain ecosystems and are considered as a low utility group. These microorganisms are able to enhance the nutritional content of conventional food preparations and hence, to positively affect the health of humans and animals. (Spolaore et al. 2006; Bravi et al. 2012). As the basis of the natural food chain, microalgae play a key role in aquaculture, especially mariculture, being the food source for larvae of many species of mollusks, crustaceans and fish (Pulz et al. 2004). In particular, some species of freshwater and marine algae contain large amounts of high-quality PUFAs and are currently widely used to produce PUFAs for aquaculture operations (Guschina et al. 2006).

Microalgae are also considered one of the most promising feedstocks for biofuels. The productivity of these photosynthetic microorganisms in converting carbon dioxide into carbon-rich lipids, only a step or two away from biodiesel, greatly exceeds that of agricultural oleaginous crops, without competing for arable land faced with stresses such as nutrient deprivation, algae store chemical energy in the form of oils such as neutral lipids or triglycerides The algal oil can be extracted from the organisms and converted into biodiesel by transesterification with short-chain alcohols or by hydrogenation of fatty acids into linear hydrocarbons.

Economics is considered a key barrier to full-scale algal biodiesel production as a drop-in fuel, energy source, and commodity. The possibility to couple microalgal production with other revenue streams and/or with other forms of energy production, opens new perspectives for the massive production of microalgal biomass. The potential use of waste waters generated by agro-food operations (e.g. olive oil mill wastewater from olive oil production) or biomass-based electric utilities (e.g. digestate from anaerobic digestors) in microalgal cultivation depends on the nutrients (and substrates, if a mixotrophic microalgal species is adopted and microbiological competing contaminants can be controlled) content of these scraps. The exact composition of the waste liquor is therefore essential in determining the suitability for the planned culturing destination. OMWW organic matter content includes polysaccharides, sugars, phenolic compounds, polyalcohols, nitrogenous compounds, organic acids, oil and a considerable amount of suspended solids (Markou et al. 2011); the phenolic fraction is mainly constituted by tyrosol

and hydroxytyrosol. Anaerobic digestion creates a nutrient-rich waste stream, the so-called digestate, which can be spread as a crop fertilizer but has the potential to be used as a nutrient source for micro-algal growth (Chisti, 2013).

A further major cost in the current production technologies of microalgae is represented by the relatively low productivity of commercial photobioreactors (PBRs), which is almost one order of magnitude lower than the theoretical one (Morweiser et al., 2010; Acién Fernández et al., 2013). Volumetric productivity in outdoor photobioreactors is strongly limited by a combination of factors, among which the scarce illumination of large part of the (often thick) suspension volume and the so called 'light saturation effect' dominate. The light saturation effect indicates the fact that microalgae reach their maximum photosynthetic activity at roughly 1/10 of the maximum irradiation recorded in summer days and suffer photoinhibition, and in some cases photooxidation, above saturation irradiation. Microalgal cultures have been shown to exhibit a higher photosynthetic activity when a luminous energy exceeding the saturation is supplied in high frequency pulses rather than in a continuous flow (Kok, 1957). Many studies aimed at exploiting the productivity boost potential of hydrodynamic light pulsation (Park and Lee, 2001; Yoshimoto et al., 2005; Sato et al., 2010); however, while it is relatively simple on a small scale (laboratory) PBR achieving a turbulence resulting in millisecond-scale light/dark (L/D) cycles, only photobioreactors with a short-light path (SLP <50 mm), where the L/D frequencies could be shortened from 10 s to 10 ms, seem viable in any large scale application (Grobbelaar, 2009).

Torzillo et al. (2010) proposed a novel photobioreactor design featuring a sloping, wavy-bottomed surface; this photobioreactor configuration might provide light/dark cycles to the microalgae swirling within the vanes. However, the extent and stability of these recirculating streams had not been characterised.

In this study we investigated a possible reuse and valorization of two waste waters and a new photobioreactor design for microalgal growth.

For the first aim, we selected a cattle digestate liquid fraction and olive oil mill wastewater (OMWW); OMWW as such (after some pretreatments) and ultra- and nanofiltration membrane concentrates of OMWW were used as media for culturing microalgae and cyanobacteria. *Scenedesmus dimorphus* and *Arthrospira platensis*, usable as a food, feed, and feedstock for producing nutraceutical components or biofuels, were selected for this investigation. The former, *S. dimorphus*, is an eucaryotic oleaginous microalga, capable of producing lipids that can be used

as biofuel or biodiesel feedstock. The latter, *A. platensis*, is a cyanobacterium, particularly rich in proteins valuable for the human and animal nutrition, and carbohydrates with a potential medical and nutraceutical application.

The two goals for this part of the thesis work were:

- Phytoremediation of agricultural and zoo-technical wastewater: COD – N – P species
- Biomass production for sustainable biofuels, food, feed nutraceutical products.

An extensive experimentation was carried out to outline the opportunities and the limits of such wastewaters for said use.

For the second aim, an experimental study was carried out on Torzillo's novel photobioreactor design with the goal to provide a detailed description of the fluid kinematics which establishes in a wavy-bottomed photobioreactor as a dependence of the imposed flow rate and inclination. State of the art techniques such as Particle Tracking Velocimetry (PTV) and novel image processing and velocity field reconstruction algorithms were applied to determine the main features of the local recirculation flow, such as the size of the recirculation zone, the local fluid velocity and the recirculation period. Subsequently, the results obtained from the PTV analysis were used to assign the installation geometry and the operating conditions of a small scale (0.34 m^2) photobioreactor which was installed outdoor and was operated with both *S. dimorphus 1237* and *A. platensis*.

2. PhotoBioReactors (PBR) for microalgal cultivation

2.1 Microalgal cultivation systems

Local populations living in the neighbourhood of the Chad lake in Africa and of the Texcoco lake in Mexico have harvested Spirulina growing and floating spontaneously on the lake surfaceand used it as a superfood for ages before the World Health Organisation officially recognised this cyanobacterium a very special value for human and animal feeding. However, that was spontaneous and uncontrolled growth. The earliest microalgal cultivation systems were developed during the second World War with the purpose of producing a food integrator.
With the subsequent industrialization, these systems were proposed for the removal of CO_2 at the Carnegie Institute of Washington in 1953 (Carvalho et al. 2006). During the Seventies, in Japan, East Europe and Israel the development of algal cultivations operations were carried out for commercial applications. In the U.S.A. algal cultivation systems were developed to study a possible use of algae for waste water purification. Recently the unicellular algae are arousing interest for the production of high value molecules as pharmacological, cosmetic and as feed (Bozarthet al. 2009; Gouveia 2009).
The microalgal cultivation systems can be "open" or "closed" (to the atmosphere) pieces of equipment. In every case it is necessary to minimize the contaminations of the crop, to furnish suitable CO_2, nutrients and illumination, and maintain the required cultural conditions (pH, temperature, salinity etc), to reduce the capital and maintenance costs (Eriksen 2008).

2.1.1. Raceway PBR

This type of systems, constituted by artificial or natural tanks directly illuminated by sunlight, have been the first ones studied and currently they are the only ones deployed for the algal cultivation in commercial premises (with very few exceptions). They are really simple and economic systems, both during the start-up and and the maintenance phase, but have some negative features: low productivity, exposure to microbial contaminations, remarkable evaporative water loss, scarce CO_2 mass transfer coefficient, large areal requirement, high biomass recovery cost, due to the very low prevailing cellular density and to the consequnt need to treat very large volumes of suspension per unit of recovered product (Fig. 2.1.1.).

Open ponds

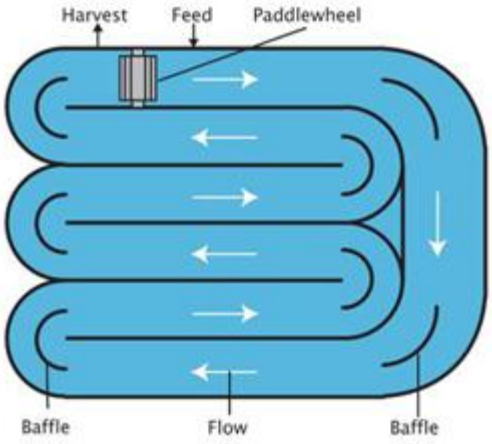

Fig.2.1.1.raceway PBR

Most common open PBR systems are: circular puddles and raceway ponds. Circular puddles are the simplest and they consist in tubs exposed to the solar light. Currently they are used especially in extreme east, where for their simplicity and the low cost of the land, they result a practicable solution. The raceway ponds have the form of closed ring (a "raceway") with a depth of ~30 cm, in which a paddle wheel (or another suitable mechanic system) moves the culture. In these systems it is possible to achieve a biomass concentration of 1 g/L and a biomass production of 60-100 mg/L d.

In some open cultivation systems an organic carbon substrate, such as acetate, is continually supplied in small quantities to maintain high biomass concentrations and hinder bacterial proliferation. In these systems both light and heating come from solar irradiation and, considering the climatic variability at one site and between sites at different latitudes irradiation cannot be maintained at a constant value, unless artificial auxiliary equipment is installed (Doucha et al. 2009).

2.1.2. Closed PBR

Closed microalgal cultivation systems are aimed at creating a controlled culturing environment where the optimal growth conditions for the desired microalgal species can be maintained from the operating conditions (temperature, pH and medium composition) and microbiological axenicity can be ensured. They date back to the Fifties and can be as simple as traditional mechanically agitated biological reactors, which were optimised for heterotrophic cultures but do

not lend themselves to an efficient adaptation to the culture of photosynthetic microorganisms. Furthermore, traditional biological reactors are rarely employed for microalgal cultivation because microalgae are less efficient than other microorganisms as bacteria and yeasts under heterotrophic growth conditions.

Nowadays, therefore, most often photobioreactors are specific equipment aimed at maximising the light energy transfer to the culture volume and that, in general terms, can be naturally (sunlight) or artificially illuminated, or both. Therefore, they are designed to be enclosed volumes which also maximise the enclosing surface per unit volume and require that the enclosing material be of maximal transparency and sufficient mechanical and thermal strength to cope with the requirements of the desired installation (indoor or outdoor). If they are designed for natural illumination, as it is generally for minimising the running costs of biomass production, they are also designed for maximising sunlight capture. (Posten 2009, Lehr et al. 2009).

The high operating cost and a few specific technical difficulties of these systems have restrained the industrial deployment of closed facilities to a few sites dedicated to the production of high valued products which can offset the (currently very high) installation and operating costs and leave fairly high economic margins to their operators.

The current high installation and operating costs have fueled the continuous spring of new types of photobioreactors, resorting to new ideas and to the reviving of old ones. Revived old ideas include the maximisation of mass transfer coefficients, in order to minimise "hidden", local or diffused, limitation (substrate and/or nutrient-related) or toxic (product, that is released oxygen) situations. Novel ideas include the supply of light in short pulses, that can be, in a sense, 'Eulerian', that is, uniformly tied to the entire fluid volume, or 'Lagrangian', that is, tied to the individual cell moving through locations of the fluid volume where local irradiation differs (generally because of the absorbance of the culture itself).

The construction materials generally used are glass, PVC, Plexiglass, polycarbonate, PET. They differ in mechanic strength, stiffness, fragility, physical and chemical stability, so that they may be self-sufficient from a mechanical point of view (that is, they may support the mechanical forces that derive from the liquid head, the weight of the unit itself plus the suspension contained therein, the flectional loads that may derive from the chosen orientation of the unit−such as horizontally or inclined stacked pipes, the horizontal forces that may applied by the wind), or may require external, generally metallic, stiffening structures. Natural illumination may be directly provided by exposition of the enclosing surface to the sunlight or by such exotheric devices as solar concentrators, optical fibres and light redistributors, generally aimed at concentrating the photobioreactor volume in a compact device and allowing provisions for mixed natural/artificial illumination and ensuring a location- and season-indipendent target illumination. Artificial illumination has been provided by high efficiency illumination devices such as fluorescent tubes, halogen lamps and, more recently, high-power light emitting diodes which have permitted a couple of previously impossible developments, such as the tailoring of the light spectrum (light quality) and the tailoring of the light supply time profile (light pulsing, as

described above). Together with light emitting sources, electric power supplies, light intensity measuring devices and regulators of the light intensity are required.
The suspension circulation in the plant has the purpose to ensure an uniform exposure of all the cells to the optimal cultural conditions (light availability, uniform composition of the medium, uniform aeration). Enclosed photobioreactors differ significantly in this respect because some try to behave as a mixed reactor while others behave as a plug flow reactor. The former types may suffer from dead spots (where chemical properties uniform is less than desired) and are often thick while the latter types (generally, pipes) are prone to nutrient limitation and toxic buildup.

- **Tubular PBR**

Tubular PBR are constituted by long transparent pipes with diameter of several centimeters (Fig.2.1.2.1.A); pumps or air insufflation move the suspension as plug-flow model. Usually peristaltic pumps are chosen for their ability to enliven the biomass without damaging the cells; the gas produced during the photosynthesis is freed in a separator, connected to the reactor. This type of phtotobioreactors is among the most suitable to develop algal biomass productions (Chiu et al. 2009). This type of reactors shows several problems about dissolved gases; during the pipes it is possible that accumulation of O_2 areas are created, with consequent inhibition of the photosynthesis or impoverishment of CO_2 areas, with consequent lack of carbon. Blending problems also exist, due to the length of the system, partially solved with the mixers installation inside the plant. Tubular PBR, can be realized in three different configurations: vertical horizontal and helical disposition. The vertical tubular PBR include the bubbling PBR and PBR with air-lift system. In these PBRs air has insufflated in the lower part of the PBR, blending the culture and suitable restocking of CO_2 and O_2 removal (Greque et al. 2007).

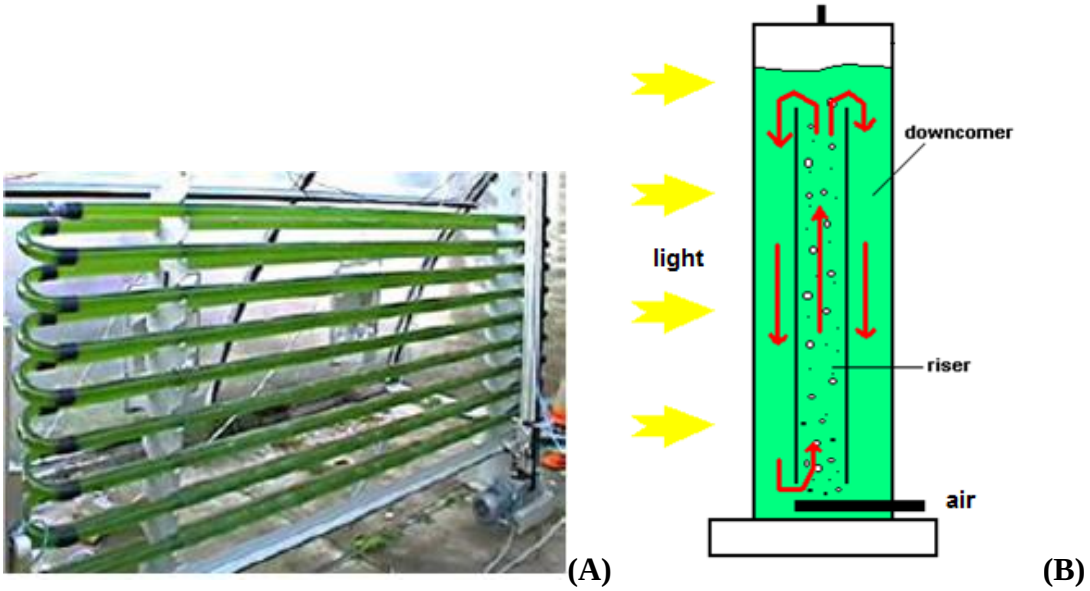

Fig.2.1.2.1. A) Tubular PBR. B) tubular PBR with air lift system.

❖ **PBR with air-lift system**

Two typologies of these reactors exist, internal and external loops, that introduces notable differences in the form and accordingly in the lines of flow of the liquid (Loubiere et al. 2009). The air lift PBRs (Fig.2.1.2.1.B) have the advantage that mechanical agitation system is not required, constructive simplicity, good transport coefficients, easy temperature control easy control of the. Another advantage is constituted by the lower part efforts of cut (absence of the agitator) that make him/it attractive for the crop of sensitive cells.

Air-lift reactors are able to assume both vertical and horizontal disposition; in the vertical position they show a best removal of the oxygen produced in comparison to those horizontally configuration; this is due to the transfer coefficient gas / liquid phase that assumes best values in the vertical position (Evens et al. 2000). As result it has a photoinhibition and photooxidation reduction effects, caused by gas accumulation and intense light radiation.

- **Flat plate PBR:**

  These PBR consist in thin plexiglas parallelepiped (Fig.2.1.2.2.A). They dispose of an elevated surface / volume ratio, increasing the portion of volume exposed at light (Issarapayup et al. 2009). They are usually conceived for being installed to the open one and to exploit the solar light in optimal way; it is possible to tilt these PBRs to maintain the perpendicular solar rays to the surface of exposure. nevertheless this type of system introduces the disadvantage that biofilm has generated inside surface exposed to the illumination.


(A)

(B)

Fig.2.1.2.2. A) flat panel PBR. B) thin layer PBR.

- **Thin layer PBR:**

This type of PBR is constituted by a harvest tank, a pumping system and one or more tilted surfaces (Fig.2.1.2.2.B). The culture is distributed on the plan, being uniform and in thin (less than 1 cm) layer; The plan can be in metal, plexiglass, polypropylene or glass. This geometry has been projected with the purpose to increase the biomass productivity (Doucha et al. 2005) incrementing the light penetration in so thin volume of the culture.

In the table 2.1.2.1. Jorquera et al. (2010) shows the results of the comparative energy analysis for the production of Nannochloropsis sp. biomass, using the three different cultivation systems: raceway open ponds, flat-plate photobioreactors and tubular horizontal photobioreactors. All systems were compared at the 100.000 kg/year biomass production level, assuming a lipid content of 29.6%, yielding 32.9 m^3 or 206.97 barrels per year. In this case the microalgal species is an oleaginose microalga able to produce lipids for biodiesel production.
From the comparison of these reactors it's possible to extrapolate that:

- ➢ the shaken reactors have a good light distribution, but they have low ratio of the illuminated surface / volume and they show low productivities to do industrial scale-up.

- ➢ the tubular reactors, both horizontal and vertical, occupy space and they are relatively expensive, both to build them whether to maintain them.

- ➢ the vertical reactors (column) have a good transport coefficient and the O_2, produced by photosynthesis, is removed, avoiding photooxidation phenomenon. This last, is well present instead in the tubular reactors with diameters 0,08 ms, and horizontal (those to vertical axle have a good behavior): in the reactors with air-lift system storages a maximum of the 115% of O_2, while in tubular PBR with small diameter storages a maximum of the 400% of O_2. The photooxidation phenomenon reaches importance in the summer period because of the elevated light irradiation; at the same illumination conditions, productivity is higher in the reactors with air-lift in comparison with tubular PBRs.
- ➢ the air-lift reactors show, in comparison with tubular PBRs, a good gas exchange, a good efficiency of exposure of the cells to the light (there is, in fact, a best distribution of the light in the riser and in the downcomer), a smaller superficial occupation, an easy management. Furthermore these PBRs, in comparison with a bubble column PBR, have the following advantages: a good blending (not too much energetic to avoid phenomena of breakup stress), best lines of flow, lower operational costs.

Table 2.1.2.1: From Jorquera et al. (2010); Comparative analysis of microalgal biomass and bio-oil production using three different cultivation systems: raceway ponds, tubular photobioreactors and flat-plate photobioreactors.

Variable	Raceway ponds	Flat-plate photobioreactors	Tubular photobioreactors
Annual biomass production (kg/year)	100,000	100,000	100,000
Volumetric productivity (g/l × d) or (kg/m^3 × d)	0.035	0.27	0.56
Illuminated areal productivity (kg/m^2 × d)	0.011	0.0142	0.0081
Occupied areal productivity (kg/m^2 × d)	0.011	0.027	0.025
Occupied areal productivity (t/ha x year)	38.5	98.6	92.9
Illuminated areal volume (m^{-2})	301	50	14.46
Illuminated Area/volume ratio (m^{-1})	3.32	19.01	69.15
Occupied Area/volume ratio (m^{-1})	2.3	10	22
Biomass concentration (g/l) or (kg/m^3)	0.35	2.7	1.02
Dilution rate, D (d^{-1})	0.1	0.1	0.1
Space required for a biomass annual production of 100,000 kg/year (m^2)	25,988.25	10,147.00[a]	10,763.20
Reactor volume required to support a biomass annual production of 100,000 kg/year (m^3)	7827.79	1014.71	489.24
Flow rate required to maintain a 0.1 d^{-1} dilution rate (m^3/d)	782.79	101.47	48.9
Hydraulic retention time (volume/ flow rate)	10	10	10
Relative oil content (%)	29.6	29.6	29.6
Net oil yield (m^3/year)	32.9	32.9	32.9
Oil yield per area (m^3/ha x year)	12.65	31.6	30.56
Energy consumption (W/m^3)	3.72	53	2500
Energy consumption required for accumulation of 100,000 kg/year biomass (W)	29,119.37	53,779.80	1,223,091.98
Total energy consumption (KWh/months)[b]	8735.81	16,133.94	366,927.6
Total energy consumption (GJ/year)	378.45	698.94	15,895.8
Energy produced as oil (GJ/year)[c]	1155.49	1155.49	1155.49
Total energy content in 100,000.00 kg biomass (GJ/year)	3155.30	3155.30	3155.30
NER for oil production	3.05	1.65	0.07
NER for biomass production	8.34	4.51	0.20

2.2. Light: an essential parameter

Attaining a high photosynthetic efficiency in microalgae culture systems is not a matter of concern when the objective is to produce high value products such as pigments (e.g. lutein, astaxathin, phycocyanin, etc.), PUFAs (DHA, EPA), that sell for hundreds of dollars a kilogram, but it is critical in the design of efficient photobioreactors (PBR) for the production of biofuels at an affordable price (Chisti, 2007). Food and feed (i.e., aquaculture) lie somewhat in-between: the whole replacement of vegetal (e.g., soy) meal with Spirulina is not economically feasible at the current prices and market appeal of farmed fish (Belay, 2009).

Exploiting solar irradiation, which penetrates the culture from the enclosure, also entails the problem that the inner volume of the culture is darker than the external ones. Often it turns out that only a small portion of the suspension volume facing the enclosure and just a few millimeters thick is actually able to carry out photosynthesis at an acceptable pace. Sunlight energy capture should be maximised to minimise operating costs, and this can be done either keeping a low cell density throughout a long light path or in the opposite way. In either case, light entering the culture is intensely attenuated and an important fraction of the PBR volume becomes dark enough to cause photosynthesis to cease, due to the so-called effect of mutual shading, while the cells placed near the external part of the PBR result exposed to over-saturating light intensities which cannot be efficiently assimilated, or to photoinhibition, a phenomenon that involves a partial, reversible deactivation of the photosynthetic apparatus, leading to an intense decrease in photosynthetic efficiency and, eventually, to a deleterious effect known as photooxidation, which is usually destructive for the microalgal culture. Collectively, at the base

of these phenomena, there is a mismatch between light capture and conversion time constants within the photosynthetic systems.

In order to avoid the above phenomena, the strategy of light dilution, consisting in spreading the sunlight falling on a given ground area is spread over a larger reactor surface area. As a result, more algae are exposed to lower intensities, being able to maximize their photosynthetic efficiency (Posten, 2009). This light dilution effect is implemented nowadays within different new photobioreactor designs developed by, for example, Subitec (Germany), Solix Biofuels (USA) or Proviron (Belgium) (Morweiser et al., 2010).

An effective mixing, beyond ensuring spatial homogeneity and helping avoid limitations and toxicities, can serve the purpose of avoiding the overload of photosynthetic by moving the cells between photic and dark zones of the PBR. This accomodates the different time constants involved in energy transfer, thus allowing photosynthesis to take place in the dark volume of the PBR and helping to prevent photoinhibition. Light is effectively 'diluted' (Richmond et al. 2003) in the time domain (as opposed to being diluted in the space domain) as long as the residence time in light or dark zones is short enough to avoid either saturation or limitation (Brindley et al. 2011).

Time-domain dilution is strictly connected with light integration, a concept discussed mathematically by Terry (1986) and stated verbally by Weller and Frank (1941) who suggested that the maximum contribution of flashing light to improved photosynthetic efficiency is an integration of the light intensity experienced by the cells. When flashes are sufficiently rapid, if the photosynthetic rate is determined by the average rather than by the instantaneous light intensity. In Figure 2.2.1, for a flashing light regime of illuminated proportion $\Phi = t_{light} / (t_{light} + t_{darkness})$, $\Phi \cdot P_G(I)$ represents the gross photosynthetic rate that would be expected with no integration (that is, photosynthetic rate is determined by the instantaneous light intensity experienced by the cells), while $P_G(\Phi \cdot I)$ represents the photosynthetic rate that would be expected with full integration (photosynthetic rate is determined by the time-averaged light intensity experienced by the cells).

Grobbelar (1995) studied the turbulence role in light:dark fluctuations that the biomass undergoes; he defined three ranges of intermittent illumination (light/dark cycles) that influence growth: (1) high frequency fluctuations of 100 ms (l0 Hz) and less; (2) medium frequency fluctuations of seconds to minutes; (3) low frequency cycles of hours (or more).

High frequency fluctuations (> 10Hz) give rise to the 'flashing light effect' (Kok, 1953; Friedrickson et al., 1970; Terry, 1986), whereby the rate and efficiency of photosynthesis are increased under specific conditions of illumination. Legendre et al. (1986) included frequencies of between 0.1 and l0 Hz in their definition of high frequency light fluctuations. Low frequency fluctuations influence the periodicity of cell division, where synchronous populations would establish under light/dark cycles similar to that of day/night cycles. He concluded that a high turbulence enhances nutrient exchange and the light:dark fluctuations, increasing the productivity and the photosynthetic efficiency.

In the photosynthetic rate versus irradiance response curve (Figure 2.2.1.) that is usually been used to describe the algal response three distinct are discernable: a light limited region, a light saturated region and photoinhibition region. Photoinhibition is a defense mechanism respect at high light irradiance, reducing PSII systems that are present in redundant numbers and all light energy are dissipated under heat form. In limitation light the mechanism is activated in the opposite sense, that is, the photosynthetic units are increased and the photons harvesting antennae are enlarged to permit photon capture. The continuous passage between these two regions entails a dynamic acclimation that algal population sustain.

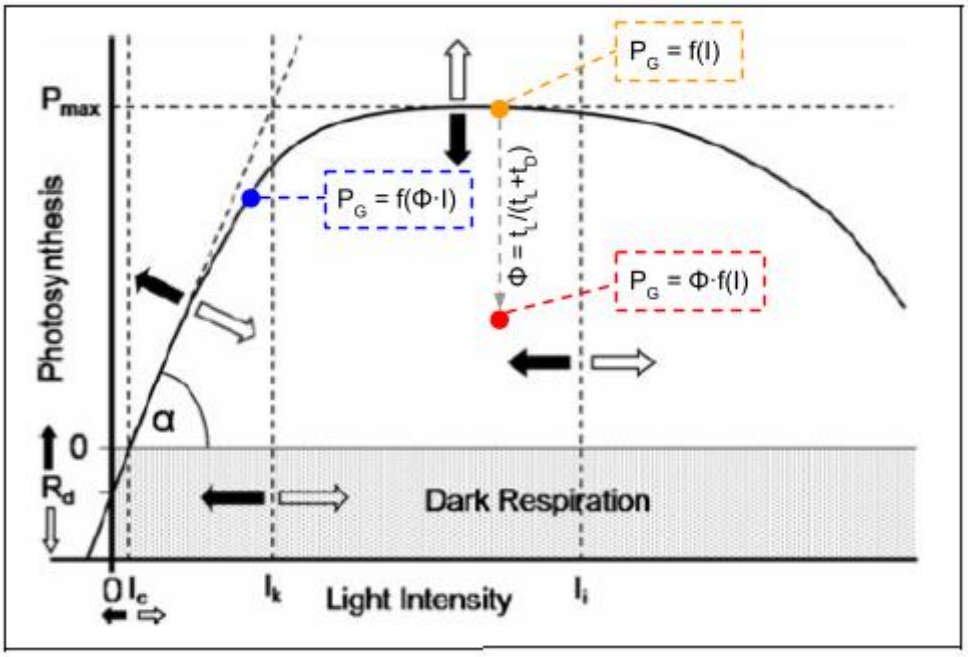

Figure 2.2.1. P/I or the light response curve of photosynthesis versus light intensity. Pmax, the maximum photosynthetic rate measured at saturated I; Rd, dark respiration; a, maximum photosynthetic efficiency; Ik, the transition light intensity between light dependant and light saturated photosynthesis; and Pi, photoinhibition. Solid arrows indicate the affect of dark acclimation and open arrows the response to light acclimation (adapted from Grobbelaar, 2006 with inclusions from Terry, 1986).

The light regime is strictly a continuous variation of irradiance versus time, I(t), has been characterized in a simplified form by several parameters, such as dark/light residence times, cycle time, frequency of exposition, duty cycle and average light (Terry, 1986; Nedbal et al., 1996). Most analyses divide the photobioreactor into well illuminated and substantially obscure zones (with/without enough light to support photosynthesis); depending on the optical length and the cellular density inside the culture, the photobioreactor may receive substantial lighting in all of its volume, may exaust light at a single point of its volume or may lack enough light for photosynthesis in a substantial fraction of its volume (Figure 2.2.2). Furthermore, depending on the regular, or turbulent (more often) streams of liquid establishing inside the photobioreactor

volume, their length and their velocity, each photobioreactor, be it open or closed, features its own very special set of L:D ratio and L/D alternation frequency.

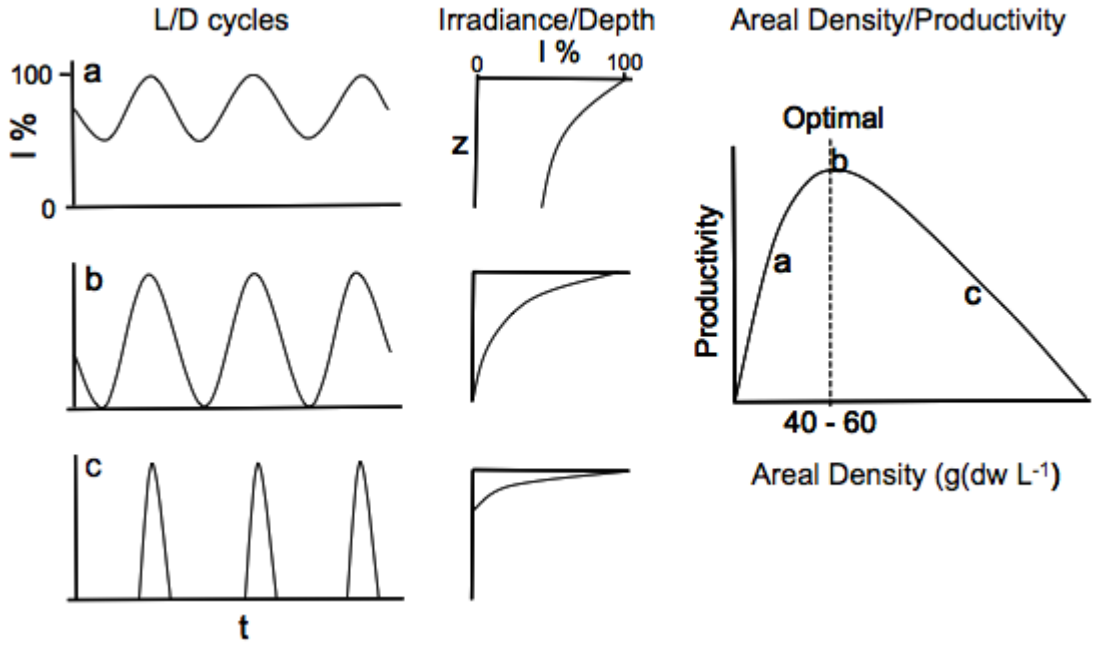

Figure 2.2.2. L/D cycles as a function of the biomass load inside the photobioreactor, for a given value of the eexternal irradiance hitting the photobioreactorand, and of the optical length of this latter (Grobbelaar, 2006).

The time profile of irradiation for a moving cell entrained by a liquid stream flowing inside the photobioreactor is therefore not abruptly changing from zero to the maximum value and to zero again, and it is difficult to characterise photobioreactors that differ from the geometric and fluid dynamic point of view. To help in comparing different situations, Brindley et al. (2011) introduced a definition of L:D ratio, which is normally written as $\Phi = t_{light} / (t_{light} + t_{dark})$, rather as $\Phi = I_{av} / I_o$, which permits to easily compare differently operating photobioreactors as far as their flashing light performance is concerned.

Brindley et al. (2011) observed that the experiments done with square-wave cycles (i.e., the largest part of experiments carried out so far) may overestimate the effect of the bad mixing and would lead to overestimate the mixing intensity needed to avoid or ameliorate the decrease in the performance caused by the inadequate light regime. They also observed that the condition defined as full integration of light by Terry ($\Gamma = 1$) is not an upper limit but can be exceeded when very low L:D ratios apply, that is, for highly concentrated biomass inside the

photobioreactor. This shows that cells in a highly concentrated biomass, although potentially leading to operating the photobioreactor at a supraoptimal areal density, may actually work in a very favourable light use condition.

3. Microalgal technology

Microalgae and cyanobacteria are unicellular photoautrophic organisms that use CO_2 and light energy to produce sugars and oxygen. In aquatic environments, they provide an important link in the food chain of marine ecosystems, ensuring the mass and energy flows necessary for the maintenance of heterotrophic organisms (Kim and Lee 2005). The high content in protein is the main reason to consider them as non-conventional sources of protein, because they are able to synthesize all the aminoacids, providing essential proteins for man and animals (Spolalore et al. 2006). Carbohydrates in microalgae are in the form of starch , glucose, other sugars and polysaccharides; their digestibility is high, in fact there are no limits to use dried microalgae in food or feed. Algal lipid content varies between 1% and 70%, but can reach 90 % of the dry weight in specific conditions. Algal lipids are composed of glycerol, esterified with saturated or unsaturated fatty acids (from 12 to 22 carbon atom). ω3 and ω6 fatty acids are particularly interesting; the total amount and the relative percentage of fatty acids can be affected by nutritional and environmental factors (i.e. nitrogen limitation). Microalgae are a source of almost all the essential vitamins (such as A, B1, B2, B6, B12, C, E, nicotinate, biotin, folic acid and pantothenic acid); their proportion varying with environmental factors, the biomass collection and drying systems. Microalgae are also rich in pigments such as chlorophyll (0.5% to 1 % of dry weight) and carotenoids (14% dry weight).

Nowadays many applications for microalgal and microalgal-derived products with added values are being developed; these include pharmaceutical, biomedical and diagnostic, cosmetic, aquaculture, food and animal feed and energetic.

However, despite the variety of applications already identified by microalgae and molecules extracted, microalgae have not yet been discovered completely; although there are more than 10.000 existing species, only a few hundred species were studied and only a small number of this species are grown in sufficient quantities for possible commercial applications. The microalgal biotechnology can be divided into several key application areas:

- biofuels
- nutraceuticals for human, feed integrators for animals and farmed fish diet
- pharmaceutical products
- wastewater treatment

3.1. Biofuel from microalgae

Microalgal organisms are also considered one of the most promising feedstocks for biofuels. The productivity of these photosynthetic microorganisms in converting carbon dioxide into carbon-rich lipids, only a step or two away from biodiesel, greatly exceeds that of agricultural oleaginous crops, without competing for arable land. Faced with physiological stresses such as nutrient deprivation, algae store chemical energy in the form of oils such as neutral lipids or

triglycerides, by switching from carbohydrates metabolism to lipids metabolism. The algal oil can be extracted from the organisms and converted into biodiesel by transesterification with short-chain alcohols, or by hydrogenation of fatty acids into linear hydrocarbons.

Eukaryotic and prokaryotic lipid species were formed in the two pathways which involved cytoplasmic and chloroplastic lipids. Cytoplasmic linoleoyl- phosphatidyl choline might be converted into either arachidonyl- phosphatidyl choline in the x-6 pathway or into EPA-PC, which would then have their diacylglycerol (DAG) moieties transferred to chloroplasts. In the chloroplasts, the DAGs could be galactosylated to the respective monogalactosyl diacylglycerol (MGDG) molecular species and further desaturation of C20:4(n-6)-MGDG by a chloroplastic D17 (x-3) desaturase would then result in the formation of EPA-containing galactolipids (Khozin et al. 1997). The high acidic value of microalgal oil makes them an inconvenient raw material for the traditional biodiesel production. However, by means of a sequential acidic esterification/alkaline transesterification, coupled with a heat integration strategy, the opportunities of accepting microalgae oil as a biodiesel precursor will increase. Biodiesel production from non-edible sources has been extensively studied. Microalgae oil (MAO) can be transformed into biodiesel by several routes. MAO composition have shown high potential for biodiesel production although its free fatty acid (FFA) and poly-unsaturated fatty acid (PUFA, like linolenic acid, C18:3), makes it somewhat technologically troublesome compared to other traditional crops. To cope with that issue a process have been developed in such a form that before the basic transesterification takes place, there is an esterification of the FFA's with an alcohol in the presence of an acidic catalyst, so fatty acid alkyl esters and water are obtained and separated. At this point, an alkali-transesterification of the triacylglycerides with an alcohol will take place faster and with fewer technical difficulties (Sanchez et al. 2011). Recovery of oil from microalgal biomass and conversion of oil to biodiesel are not affected by whether the biomass is produced in raceways or photobioreactors. Hence, the cost of producing the biomass is the only relevant factor for a comparative assessment of photobioreactors and raceways for producing microalgal biodiesel (Chisti, 2007). The high cost of algae lipids is largely due to the lower-than-expected lipid yield (LY) of algae culture. Nitrogen source and concentration in the growth media greatly influence algae lipid yield. In nitrogen-limited situations, algae lipid content usually increases because lipid-synthesizing enzymes are less susceptible to disorganization than carbohydrate synthesizing enzymes due to nitrogen deprivation; thus, most carbon ends up to be bound in lipids. However, biomass growth is often inhibited in nitrogen-lacking situations, so that each algal strain usually exhibits a lipid yield peak at (species-specific) concentrations of nitrogen-carrying molecules (Shen et al. 2009). Moreover one of the main obstacles to fully taking advantage of lipid-producing microalgae, is the ability to successfully and efficiently extract oil from the cell biomass. Additionally, there is the concern of extracting oil in the safest and most environmentally sustainable manner; therefore, solvent extraction may not always be the optimal solution for recovering oil from the microalgal biomass. Algae also synthesize other fuel products, such as hydrogen, ethanol and long-chain hydrocarbons, that resemble crude oil,

or the algal biomass can be converted to biogas through anaerobic fermentation (Wijffels and Barbosa, 2010).

3.2. Nutraceutics from microalgae

The microalgae have in practice an interesting composition in regard to main components such as protein, polyunsaturated fatty acids (PUFA), pigments, and carbohydrates (Doucha 2009). The protein content is consistently high in microalgae. Some cyanobacteria (blue-green algae) are characterised by a high protein content (60-65%), not commonly found among higher plants. But, for full utilisation of the protein, special treatment of the microalgae is generally necessary. Moreover, microalgae are excellent producers of essential amino acids. Microalgae are also used in a very widespread as a source of food for marine fish and shellfish breeding (Pulz and Gross 2004). In particular some species of freshwater and marine algae contain large amounts of high-quality Poly Unsatured Fatty Acids (PUFAs) and are widely used for fish feed (Guschina and Harwood, 2006). Worldwide, there are thousands of marine hatcheries , which produce billions of fish and shellfish per year. For this purpose it has been adapted a relatively small number (~ 6-10) of species of microalgae easy to breed. In many cases, the microalgae are grown by the hatchery operators and served live to the larvae of fish and shellfish. In this scenario, the opportunity to sell to hatcheries consists primarily in equipment and consumables required for production of microalgae: photobioreactors, pumps, lights, nutrients, etc. . However, hatcheries are increasingly buying concentrated microalgae in order to simplify the operations on site. These concentrates are manufactured by companies that specialize in large-scale production and processing of microalgae.
Up to date only three species are cultivated on industrial scale level: these are the cyanobacterium *Arthrospira*, and the green algae *Chlorella* and *Dunaliella*. Their biomass is used for production of a rather limited range of products, most of them are directed to the nutraceutical market. The success of these three species is due to the fact that they can be grown in a very selective medium (*Arthrospira* and *Dunaliella*), therefore, contamination of parasites or competing organisms (microalgae, fungi, and others) is naturally prevented even in open reactors where it is possible to ensure a low cost of production for the biomass (Boussiba and Affalo, 2005), while *Chlorella* is endowed with a remarkably high growth rate sustained by organic acid addition in fermentor.

3.2.1. Chlorella vulgaris

Chlorella vulgaris cells contain β-1,3-glucan, polysaccharides and also a rich source of proteins, 8 essential amino acids, vitamins (B-complex, ascorbic acid), minerals (potassium, sodium, magnesium, iron, and calcium), β-carotene, chlorophyll, 'CGF' (Chlorella growth factor), as well as other health-promoting substances. β-1,3-glucan is an active immunostimulator, a free-radical scavenger and a reducer of blood lipids (Ryll et al., 2003). However, various other health-

promoting effects have been clarified (efficacy on gastric ulcers, wounds, and constipation; preventive action against atherosclerosis and hypercholesterolemia and antitumor action). Chlorella vulgaris biomass has colouring properties and has been tested with success as a pigment source for farmed products with functional activity (e.g. as antioxidants). The total annual production of Chlorella is estimated to be about 2000 t. The production process is based on the mixotrophic nature of the Chlorella strains and uses acetic acid as a carbon source. The production cost of biomass is not clear. However, based on claims that in those systems a high biomass concentration is achieved (more than 10 g/l) one may reach the conclusion that the production cost may be a figure close to those of open pond systems (10 -15 US$/Kg). However, the cost can raise to up to 30 US$/Kg, for example in the Central part of Europe where the adverse climatic conditions do not allow to grow the alga all the year around. Up to about 10 years ago most of the production took place in Taiwan and only 10-15% of the total production was carried out in green houses in Japan. The market for Chlorella products is limited to the Far East, mainly Japan. In some early works it was reported that Chlorella extracts may have affect the growth and production of lactic acid by lactic bacteria. The growth facilities are based on round concrete ponds mixed by a rotating arm which also provides CO_2 and acetic acid supply. Another development that should be mentioned is the attempt to set up new facilities for culturing Chlorella in Europe. One of them is located in Czech Republic (2 tons a year production capacity; Bravi et al., 2012) and is based on inclined reactors that allow to maintain a fast flow rate of a thin layer culture and, as a result, enables the maintenance of high biomass concentrations and high volumetric productivity (Masojidek et al. 2010). The second facility is located in Germany, and uses tubular photobioreactors made with glass tubes arranged on a vertical fence and placed in a greenhouse. The total annual capacity is claimed to reach 150 tons per year (Pulz 2001). Although Chlorella market is still the largest one in term of gross revenue US$, one can expect that without developing new products and reducing the production cost a sine qua non condition for use of Chlorella biomass as feed additive in the animal feed market, it is difficult to expect an expansion of the production capacity.

3.2.2. *Arthrospira platensis*

Presently *Arthrospira* (commercially indicated as Spirulina) represents the second most important commercial microalga in term of total market value US$ (after Chlorella), while in terms of total biomass produced, the *Arthrospira* market is twice or more of that occupied by *Chlorella* (Torzillo and Vonshak 2003). The major producers of Arthrospira are the DIC group of companies, Earthrise in California, USA, Hainan DIC Marketing in Hainan Island, China. On the whole these facilities produce about 1000 metric tons of *Arthrospira* annually (Belay et al. 2008; Sili et al. 2012). Another important *Arthrospira* producer is Cyanotech Corporation of Hawaii with an annual production of 300 tons. Other producers are located mainly in the Asia-Pacific region, particularly in China and India (Lee 1997). The highest production capacity of Arthrospira biomass takes place in China. Recent estimates are that the total potential of the

different sites of this country may exceed 2000 t. Production is carried out in raceway ponds of 2000-5000 m^2 in size and may contain between 400 and 1000 m^3 of culture according to the dept adopted which can vary between 15 and 40 cm depending on season, desired algal density and, to a certain extent, the desired biochemical composition of the final product (Belay et. al 2008). The major share of the market for this organism is for health food involving crude biomass production. This has the advantages of simple processing (harvest and rudimentary handling) keeping production costs reasonably low, and of eluding the competition of the chemical industry which cannot match the wealth in nutritional bioactive components and attractiveness of natural products (Boussiba and Affalo 2005). *Arthrospira platensis* (Harun et. al 2010) has commercialized as nutraceutical food, also a strong immune-stimulated molecule, Immulina®, can be extracted from it (Grzanna et. al 2006).

3.2.3. *Dunaliella*

This species is being grown as a source of beta-carotene. this carotenoid can accumulate in the cells grown under nutrient limitation and high sun light up to 12% of the dry weight (Ben-Amoz and Avron 1973). This pro-vitamin A product is widely used in the feed and food industry. Today, the product is available mainly in two forms: dried or extracted. Dried Dunaliella, in powder or pill form, is considered to be highest quality. The product is harvested by means of concentration and centrifugation, and thereafter dried by spraydrying. In this form, the product is mainly addressed to health food market for direct human consumption. The price is based on the beta-carotene content, and can reach about 2000 US$ per Kg of beta-carotene. The second kind of product is beta-carotene extracted into a vegetal oil. This product can be applied as a food colorant and a pro-vitamin additive for human consumption, for fish and poultry feed, or in the cosmetic industry as an additive to sunscreen products. From few reports it is estimated that the price, on the basis of beta-carotene content, varies in the range of US$ 500-600 per Kg of beta-carotene.

3.3. Pharmaceuticals from microalgae

In the last decade the screening of microalgae, especially the cyanobacteria (blue-green algae), for antibiotics and pharmacologically active compounds has received ever increasing interest. A large number of antibiotic compounds, many with novel structures, have been isolated and characterised. Similarly many cyanobacteria have been shown to produce antiviral and antineoplastic compounds. A range of pharmacological activities have also been observed with extracts of microalgae, however the active principles are as yet unknown in most cases. Several of the bioactive compounds may find application in human or veterinary medicine or in agriculture. Others should find application as research tools or as structural models for the development of new drugs. The microalgae are particularly attractive as natural sources of

bioactive molecules since these algae have the potential to produce these compounds in culture which enables the production of structurally complex molecules which are difficult or impossible to produce by chemical synthesis.
Pharmacologycal compounds extracted from microalgae can categorized in three groups:

- ➢ antimicrobials
- ➢ antivirals
- ➢ Toxins and pharmacologically active compounds

A large number of microalgal extracts and/or extracellular products have been found to have antimicrobial (antibacterial, antifungal, antialgal, antiprotozooal) activity, although for many of these the structure and identity of the active constituent is not yet known (Pesando, 1990). Antibacterial and antifungal substances identified are listed in table 3.3.1.:

Table 3.3.1. principal antimicrobial molecules extracted from gree-nblu microalgae

molecules	Species or Strains	References
fatty acids	Stichococcus bacillaris Protosiphon botryoides Navicula delognei.	(Harder & Opperman, 1953; Findlay & Patil, 1984)
glycolipids carbohydrates	Bacillariophyceae Chrysophyceae,Cryptophyceae	(Duff et al., 1966)
acrylic acid	Phaeocystis	(Sieburth, 1959)
phenolics and bromophenols	Nostoc muscorum. Calothrix brevissima	(De Cano et al., 1990; Pedersen & DaSilva, 1973)
N-glycosides	Tolypothrix tjipanasensis	(Bonjouklian et al., 1991)
polysaccharides	Chaetoceras lauderi Chlorella vulgaris	(Pesando et al., 1980; Pratt and Fong, 1940)
peptides	Stichochrysis immobilis	(Berland et al.,1972)
acrolyl-choline	Amphidinium carteri	(Taylor et al., 1974)

Unfortunately, most of the studies have only used in vitro assays and, in analogy with macroalgae, it is likely that most of these compounds will have little or no application in medicine as they are either too toxic or are inactive in vivo (Reichelt & Borowitzka, 1984). They may, however serve as useful leads to new synthetic antibiotics or may find application in agriculture. For example, the tjipanazoles, isolated from the cyanobacterium, Tolypothrix

tjipanensis, are indolo [2,3-a] carbazoles, similar to those found in actinomycetes and slime moulds, but without a pyrrolo [3,4-c] ring (Bonjouklian et al., 1991).

A number of cyanobacteria and very few other microalgae, have been screened for antiviral activity; Rinehart et al.(1981) have found that over 5% of the extracts of cultured cyanobacteria screened by them showed antiviral activity against Herpes simplex virus type II, and >5% had activity against respiratory syncytial virus.

Table 3.3.2. anti-HIV activity of extracts of, and compound isolated from green brown and red algae (Scaeffer and Krylov 2000).

Reference	Species[a]	Compounds isolated	Other compounds tested
Nakashima *et al.* (1987b)	*Schizymenia pacifica* (red seaweed)	Extract, polysachharide MW, 10^2 kDa	
Nakashima *et al.* (1987a)	*Schizymenia pacifica* (red seaweed)	SAE MW, 2×10^3 kDa	Chondroitin sulfate A, dermatan sulfate, heparin sulfate, and keratan polysulfate inhibited RT of avian myeloblastosis virus
Beress *et al.* (1993)	*Fucus vesiculosus* (brown seaweed)	Polysachharides, fucoidan, polyphenols	AZT
Moen and Clark (1993)	*Fucus vesiculosus* (brown seaweed)	Fucoidan and water-soluble, noncarbohydrate component of fucoidan	
Hoshino *et al.* (1998)	*Sargassum horneri* (brown seaweed)	Sulfated polysaccharide with fucose as the main component sugar	Dextran sulfate (50 kDa)
Witvrouw and De Clercq (1997)	Marine algae (review); Red seaweeds: *Nothogenia fastigiata*, *Agardhiella tenera*, *Eucheuma cottonii*, *Gigartina aciculaire*, *Gigartina pistillata*	Xylomannan, Galactan sulfate, κ-, λ-Carrageenan	Dextran sulfate, pentosan sulfate, dermatan sulfate
Damonte (1996)	Alga	Not directly relevant	
Hasui *et al.* (1995)	*Cochlodinium polykrikoides*	Sulfated polysachharides	
Damonte *et al.* (1994)	*Nothogenia fastigiata* (red seaweed)	Sulphated xylomannan	
Baba *et al.* (1988b, 1990)	Purchased compounds	Fucoidan, κ-, λ-Carrageenan	Dextran sulfate (10^3 to 500 kDa), pentosan polysulfate (3.1 kDa), dermatin sulfate (31 kDa), heparin (30 kDa), mannan sulfate (30 kDa), suramin (1.4 kDa), PAA (27 kDa), COAM (150 kDa)
Sugawara *et al.* (1989); Mizumoto *et al.* (1988)		Fucoidan	Dextran sulfate, DEAE dextran (diethyla-minoethyldextran)
Parish *et al.* (1990)		Fucoidan, κ-, λ-, ι-Carrageenan	Chondroitin 4-sulfate, chondroitin 6-sulfate heparin, dextran sulfate (5, 500 kDa), polyvinyl sulfate, polyanethole sulfonate, pentosan sulfate
McClure *et al.* (1992)		Fucoidan	Dextrin sulfate, dextran sulfate
Ohta *et al.* (1998)	*Gigartina tenella* (red seaweed)	Sulfoquinovosyldiacylglycerol	
Loya *et al.* (1995)	*Peyssonelia* sp. (red seaweed)	Peyssonol A. Peyssonol B (sesquiterpene hydroquinones)	
Bagasra *et al.* (1989)		Carrageenan, fucoidan	Dextran sulfate, heparin, heparin sulfate, chondriotin sulfate, pentosan polysulfate, D-glucosamine 2-sulfate, D-glucosamine 6-sulfate, D-glucosamine 2,6-disulfate, inositol hexasulfate
Elias *et al.* (1997)		ι-Carrageenan	

[a]When "Species" column is blank, compounds were purchased rather than isolated.

Lau et al. (1993) have also screened extracts of over 900 strains of cyanobacteria for inhibition of reverse transcriptases of avian myeloblastosis virus and human immunodeficiency virus type 1, and they found that over 2% of these algae showed promising activities. Compounds extracted from algae have in vitro or in vivo activity against a wide range of retroviruses, including herpes viruses (HSV-1, HSV-2, HCMV), togaviruses (Sindbis virus, Semliki Forest virus), paramyxoviruses (RSV), rhabdoviruses (vesicular stomatitis virus [VSV]), and human immune

deficiency viruses (SIV, HIV). Compounds isolated from algae that have been tested against HIV (Table3.3.2.) include steroids and sulfoglycolipids, but most of the research has used natural and synthetic sulfated polysaccharides (Schaeffer and Krylov, 2000).
However it's necessary to perform studies of the anti-HIV activity of compounds from aquatic and terrestrial algae and cyanobacteria, to understand their different modes of toxic action (e.g., antimicrotubule and antimitotic agents, steroids, and other classes).

3.4. Microalgal wastewaters treatment

Excess nitrogen and phosphorus in discharged wastewaters can lead to downstream eutrophication and ecosystem damage (Correll, 1998). The negative effects of such nutrient overloading of receiver systems include nuisance algae, low dissolved oxygen concentrations and fish kills, undesirable pH shifts, and cyanotoxin production. While chemical and physical based technologies are available to remove these nutrients, they consume significant amounts of energy and chemicals, making them costly processes (Tchobanoglous and Burton, 1991).The energy and cost required for tertiary treatment of wastewater remain a problem for industries and municipalities.
Compared to physical and chemical treatment processes, algae based treatment can potentially achieve nutrient removal in a less expensive and ecologically safer way with the added benefits of resource recovery and recycling (Graham et al., 2009; Oswald, 2003) The use of wastewater can offset the cost of commercial fertilizers otherwise needed for the production of algae, and wastewater treatment revenues can offset algae production costs (Christenson and Sims, 2011). Furthermore microalgae, as photosynthetic microorganisms, are able to remove of CO_2 from industrial flue gases by algae bio-fixation and reduce the GHG emission (Wang et al. 2008).
When it comes to growing microalgae for low-valued applications, the impact of every cost item should be minimised and any growth promotion potential should be exploited. Byproducts from agro-food processing are prime candidate for reuse both because they convey nutrients and sometimes organic carbon which are required (or may be used) by the microalgal biomass and because they need to be treated before discharge anyway. There is a need to couple microalgal production with other revenue streams and/or with other forms of energy production, such as anaerobic digestion (Chisti, 2013). Christenson and Sims (2011) reported in table below (Table 3.4.1) the potential production of algal biomasses correlated at nitrogen and phosphorous concentrations and their ratio.

Table. 3.4.1. Characterization of typical wastewaters with respect to algal nutrients nitrogen and phosphorus (Christenson and Sims, 2011).

Wastewater type	Nitrogen[a] ($mg\ l^{-1}$)	Phosphorus[b] ($mg\ l^{-1}$)	Reference	N:P (molar ratio)	Theoretical algae biomass production[c,d]
Weak domestic	20[e]	4	Tchobanoglous and Burton (1991)	11	0.3 g
Medium domestic	40[e]	8	Tchobanoglous and Burton (1991)	11	0.6 g
Strong domestic	85[e]	15	Tchobanoglous and Burton (1991)	13	1.4 g
Beef cattle feedlot	63	14	Bradford et al. (2008)	10	1.0 g
Dairy	185	30	Bradford et al. (2008)	14	2.9 g
Poultry feedlot	802	50	Bradford et al. (2008)	36	5.7 g
Swine feedlot	2430	324	Bradford et al. (2008)	17	37.1 g
Swine feedlot	895	168	Vanotti and Szogi (2008)	12	14.2 g
Coffee production	85	38[f]	Olguin et al. (2003)	5	1.3 g
Coke plant	757	0.5[f]	Vazquez et al. (2007)	3352	0.1 g
Distillery	2700[e]	680[f]	Basu (1975)	9	42.8 g
Paper mill	11[e]	0.6	Pokhrel and Viraraghavan (2004)	41	0.1 g
Tannery	273	21[f]	Durai and Rajasimman (2011)	29	2.4 g
Textile	90	18	Fongsatitkul et al. (2004)	11	1.4 g
Winery	110	52	Mosse et al. (2011)	5	1.7 g

[a] Total Kjeldahl nitrogen (TKN) unless specified.
[b] Total phosphorus unless specified.
[c] Based on limiting nutrient assuming a formula of $C_{106}H_{181}O_{45}N_{16}P$ (Stumm and Morgan, 1981).
[d] Based on the nutrients (N and P) contained in one liter of wastewater.
[e] Total nitrogen.
[f] Phosphorus as phosphate (PO_4–P).

Many algae have a very good capability to adsorb metals, and there is considerable potential for using them to treat wastewaters. In this case a metal-rich biomass is obtained, which excludes it from most of the above mentioned uses.

Metal sorption involves binding on the cell surface and to intracellular ligands. The adsorbed metal is several times greater than intracellular metal. Carboxyl group is most important for metal binding. Concentration of metal and biomass in solution, pH, temperature, cations, anions and metabolic stage of the organism affect metal sorption. Algae can effectively remove metals from multi-metal solutions. Dead cells adsorb more metal than live cells. Various pretreatments enhance metal sorption capacity of algae. $CaCl_2$ pretreatment is the most suitable and economic method for activation of algal biomass. Algal periphyton has great potential for removing metals from wastewaters. An immobilized or granulated biomass-filled column can be used for several sorption/desorption cycles with unaltered or slightly decreased metal removal. For commercial application of algal technology for metal removal from wastewaters, emphasis should be given to: (i) selection of strains with high metal sorption capacity, (ii) adequate understanding of sorption mechanisms, (iii) development of low-cost methods for cell immobilization, (iv) development of better models for predicting metal sorption, (v) genetic manipulation of algae for increased number of surface groups or over expression of metal binding proteins, and (vi) economic feasibility (Mehta and Gaur, 2005).

The use of immobilized microalgal biomass has some advantages; in fact one of the major and practical limitations in algal treatment systems is the need of treating very large volumes of water to separate the algal biomass from the treated water discharge; an efficient removal of algal biomass is essential for recycling of the wastewater. Numerous efforts have been devoted to develop a suitable technology for harvesting microalgae ranging from simple sand filtration to energy-intensive centrifugation (Oswald, 1988). Application of immobilization technology to algal wastewater treatment provides more flexibility in the reactor design when compared with conventional suspension systems. Moreover, accelerated reaction rates due to increased cell density, increased cell wall permeability, no washout of cells and better operational stability are

the additional advantages of immobilized cells over their free-living counterparts (Brouers et al. 1989).

There are indications that immobilization affects the cell behaviour, but many of the observations, particularly with respect to productivity are contradictory. Therefore, there is a need of a deeper understanding of the effects of immobilization on algal cell. The leakage problem is one of the key concerns in cell immobilization since it obviates the primary purpose of delimiting viable cells in a confined matrix. Hallow-fiber cartridges seem to be good enough to solve this problem. When metal recovery is of economic interest, destructive recovery may be accomplished by treatment of biomass with strong acids. Attention has to be foccussed towards non-destructive desorption from loaded biomass and regeneration of biomass for reuse (Mallick, 2002).

4. Materials and methods

4.1. Set up for microalgal cultivation in synthetic media

S. dimorphus (UTEX 1237) was obtained from the Culture Collection of Algae at the University of Texas at Austin, USA. The strain on agar was inoculated into a Modified Basal (MB) medium that in a liter contained: $CaCl_2$ 0.17 mM, $NaNO_3$ 8.82 mM, $MgSO_4x7H_2O$ 0.3 mM, K_2HPO_4 0.43 mM, KH_2PO_4 1.29 mM, NaCl 0.43 mM, $Na_2EDTAx2H_2O$ 2 mM, $FeCl_3x6H_2O$ 0.36 mM, $MnCl_2x4H_2O$ 0.21 mM, $ZnCl_2$ 0.037 mM, $CoCl_2x6H_2O$ 0.0084 mM and $Na_2MoO_4x2H_2O$ 0.017 mM).
A. platensis was obtained from the culture collection of CNR-ISE (Sesto Fiorentino, Italy). The strains on agar was inoculated into Zarrouk medium (1996); a liter has g/L of: $NaHCO_3$ 16.8, K_2HPO_4 0.5, $CaCl_2$ 0.04, $NaNO_3$ 2.5, $MgSO_4x7H_2O$ 0.2, K_2SO_4 1, NaCl 0.43; microelements in mg/l: $MnCl_2x4H_2O$ 1.81, H_3BO_5 2.86, $ZnSO_4x7H_2O$ 0.22, $CoCl_2x6H_2O$ 0.035, $CuSO_4x5H_2O$ 0.08 and Na2MoO_4x2H_2O 0.23; finally, 1 ml/L of solution of FeEDTA (29.954 g of Na_2EDTA and 24.9 g of $FeSO_4x7H_2O$ in 500 ml distilled water).
Cultures were grown in 400-mL cylindrical glass tubes, with a diameter of 6 cm, fed with filtered and humidified air and air with CO_2 5%V/V; flow rate was $130*10^3 Nm^3/h$. Photoperiod of light provided by cold white fluorescent lamps (400-700 nm, 865 K, 32 W, 80 mmol photons m^2 s^{-1}) 16 h followed by a period of darkness equal to 8 h. The temperature was maintained constant at 28 ±1 °C.

4.1.1. Cellular concentration , dry weight and pH

The cellular density was correlated with the absorbance measured at a wavelength of 690 nm, corresponding to the absorption peak of chlorophyll by means of a spectrophotometer
(UV-1800PC by Shanghai Mapada Instruments Co., Ltd). Biomass was transferred in a humidity free glass flask and dried in a vacuum oven for 4 h; dry weight was determined gravimetrically. The pH values were determined by means of a pHmeter instrument, supplied by Hanna Instruments, model HI8418.

4.2. OMWW pre -treatment

The raw OMWW was pretreated by means of sieving with a cut-size of 300 micron, a flocculation by means of acidification with nitric acid to pH values near 3.0, centrifugation and photocatalysis; the clarified stream was processed by photocatalysis using home-made composite magnetic nanoparticles with size of 79 nm coated by titania, irradiated by UV light for 4 h.

4.2.1. OMWW feedstocks production by membrane separation

The plant consist of a 100 L feed tank FT1, in which the pretreated feedstock is stored. The centrifugal booster pump P1 and the volumetric pump P2 drive the wastewater stream over the used spiral-wound membranes, supplied by Osmonics, fitted in the housing M1, at an average flow rate equal to 600 L/h, active membrane area of each module is equal to 2.51 m^2.

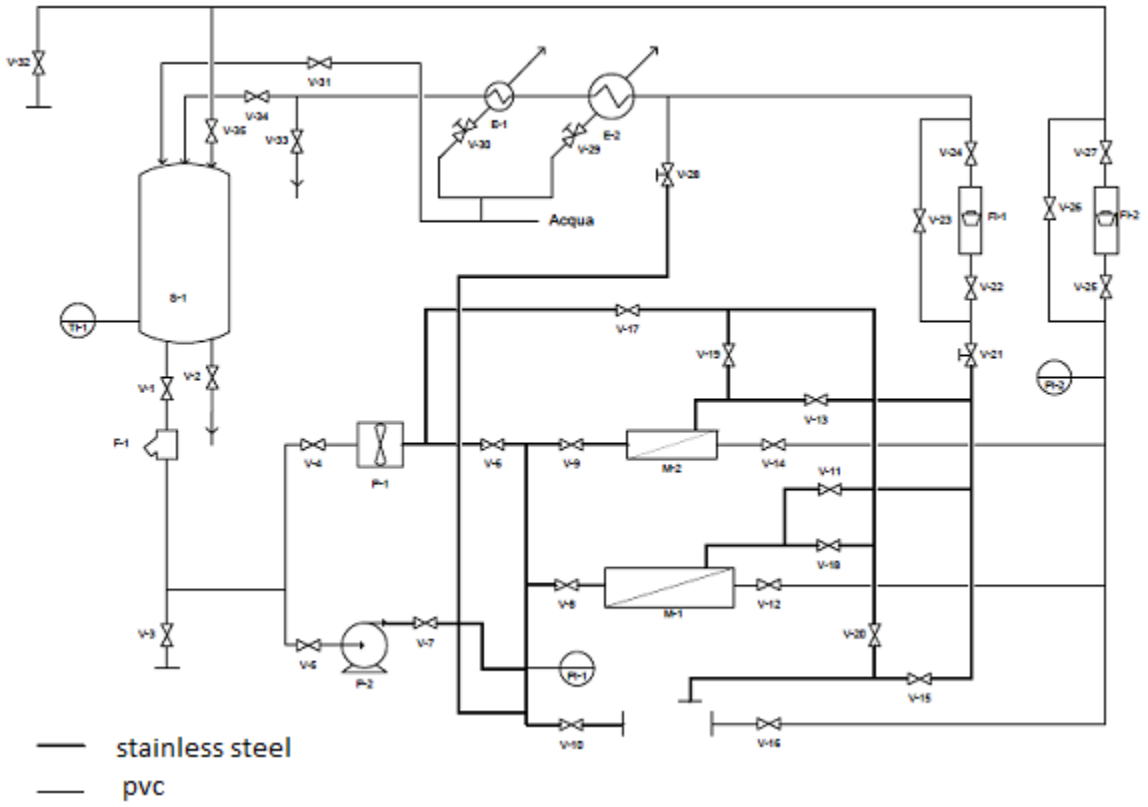

Figure 4.2.1. the scheme of membrane pilot plant.

The maximum one that can be obtained constantly on this system. The used membranes in this work are of ultrafiltration("UF"), nanofiltration ("NF") and reverse osmosis ("RO") type, as reported in Table 4.2.1 and are characterized, when new, by their pure water permeability value mw, the average pore size Dp and the maximum operating pressure Pmax. The active membrane area of each module is equal to 2.51 m^2. The membrane modules were old, each used below threshold flux conditions for at least 1000 operating hours, and for this reason each module exhibits reduced pure water permeability values if compared to new ones. Acting on the regulation valves V1 and V2 it is possible to set the desired operating pressure P_{ExT} over the membrane

maintaining the feed flow rate constant with an accuracy of 0.5 bar. Both permeate and concentrate streams are cooled down to the feedstock temperature, mixed together and recycled back to the feedstock. In this way, the feedstock composition is kept constant during each experimental batch run. The temperature was controlled for all experiments at the value of 20 °C ±1 °C (Cicci et al. 2013).

Table 4.2.1. Membrane characteristics of the used membrane modules.

Type	Id	m_w [l/hm^{2}bar]	m_w [l/hm^{2}bar]	Dp [nm]	P_{max} [bar]
UF	Osmonics model GM	16.3	4.8	2.0	16
NF	Osmonics model DK	7.9	5.2	0.5	32
RO	Osmonics model SC	2.7	2.6	<0.1	65

The application of the pretreatment processes aims at the reduction of the TSS and the organic matter content measured by the COD. In table 4.2.2. the obtained results were reported, together with the reduction D% expressed as percentage with reference to the previous step.

Table 4.2.2. Pretreatment of the raw omww.

Stream	COD		TSS		pH
	[g/l]	Δ%	[g/l]	Δ%	
Raw OMWW	32.4	–	33.0	–	5.2
After flocculation	22.2	31.5	10.9	66.9	3.1
After centrifugation	19.2	13.5	8.4	22.9	–
After photocatalysis	16.5	14.1	5.2	38.1	–

4.2.2. Set up microalgal cultivation in OMWW and its fractions

Three set of experiments were performed for following feedstocks: OMWW, concentrate of ultrafiltration and concentrate of nanofiltration. They were sterilized and diluted 1:1 by volume, for each species, with the relevant media; pH was regulated, at a value of 9 for A. platensis and 6.7 for *S. dimorphus 1237*. Cultures were grown in 400-mL cylindrical glass tubes, with a diameter of 6 cm, fed with filtered and humidified air; flow rate was 130 *10^3Nm^3/h. The cultures were carried on for a batch time of 5 days, switching between a period of light provided by cold white fluorescent lamps (400-700 nm, 865 K, 32 W, 80 mmol photons m^2 s^1) 16 h followed by a period of darkness equal to 8 h. The temperature was maintained constant at 28 1 C. At the end of the batch, the biomass was collected, centrifuged and washed two times with distilled water. Afterwards, the collect algae were transferred in a humidity free glass flask and dried in a vacuum oven for 4 h, and measured on its dry weight.

4.3. Cattle digestate pre-treatment

The feedstock used is the liquid fraction obtained from the mechanical separation of the product of an anaerobic co-digestion of cow manure and agricultural products carried out in a 1-MW plant located in Cicerale (Southern Italy). The digestate was subsequently sieved at a 710 μm aperture to get rid of suspended solids and micro-filtered with a poliammide (type JX) (pore size 0.3 μm). Finally, the digestate was thermally sterilized (20 minutes at 120 °C).

4.3.1. Set up microalgal cultivation in cattle digestate

Scenedesmus dimorphus (UTEX 1237) strain on agar was inoculated into a Modified Basal (MB); *A. platensis* (CNR-ISE Sesto Fiorentino, Italy) strain on agar was inoculated into Zarrouk medium (Zarrouk 1996). Three set of experiments were performed for the digestate feedstock. The sterilised digestate was diluted 1:1, 1:5, 1:10 and 1:20 by volume, for each species, with the species-relevant media and with tap water, and then used for algal growth experiments. The cultures were bubbled with air and air supplemented with 5% CO_2; pH was adjusted to a value of 9.0 for *A. platensis* and 6.7 for *S. dimorphus 1237*. Cultures were grown in 400-mL cylindrical glass tubes, with diameter 6.5 cm, fed with filtered and humidified air; flow rate was 130 NL/h. The batch cultures were carried on for 5 days, with daily switching between lighting (16 h), provided by cold white fluorescent lamps (400 - 700 nm, 32 W, 80 μmol photons m^2 s^{-1}), and darkness (8 h). The temperature was maintained constant at 24 ± 1 °C. At the end of the batch, the biomass was collected, centrifuged and washed twice with distilled water. Afterwards, the collected microalgal biomass was transferred in a dry glass flask, dried in a vacuum oven for 4 hours, and weighed.

4.4. Carbohydrates and proteins essays

Carbohydrates and proteins were quantified spectrophotometrically; total carbohydrates were quantified by Dobois assay (Dobois et al. 1956) and total proteins were measured by Lowry assay (Lowry et al. 1951).

4.5. C-phycocyanin extraction

To estimate C-phycocyanin content, washed cell pellets, harvested at 96 hours, were resuspended to a total volume of 20 ml with 0.01 M sodium phosphate, pH 7 0.15 M NaCl cold buffer (5°C); at cell suspensions were cells disrupted with bead-beating extraction method.
were transferred to Beckman polycarbonate tubes and centrifuged at 4 ° C and 20.000 g for 45 min .
The supernatant (crude extract), containing the phycobiliproteins and other soluble proteins,

were collected and were determined spectrophotometrically adopting follow equations (Bennett and Bogorad, 1973):

$$[PC] = \frac{OD_{615} - 0.474(OD_{652})}{5.34}$$

4.6. Determination of chlolorophills A, B and total carotenoids

Cell disruption: biomass was disrupted by thermic shock and vortexing with glass beads in cold methanol; the cholorophylls and carotenoids were determined spectrophotometrically adopting follow equations (Wellburn A. 1994):

$$C_a = 16.72A_{665.2} - 9.16A_{652.4}$$
$$C_b = 34.09A_{652.4} - 15.28A_{665.2}$$
$$C_{x+c} = (1000A_{470} - 1.63C_a - 104.96C_b)/221$$

4.7. Lipid extraction

Bead-beating extraction system was adopted; the biomass was harvested, washed twice with distilled water, centrifuged and suspended in dichloromethane/methanol (2:1, v/v) with glass beads. The system was mixed for 30 minutes and shaken for 24 h at 130 rpm. After 1 h from stopping the agitation three layers could be identified; the topmost, corresponding to the lipid fraction, was withdrawn and evaporated using a rotary evaporator. The lipid weight in each sample was measured gravimetrically.

4.8. Media analysis

- COD: it was measured by means of the Dr. Lange test kit (LCK414).
- Quantification of phenolic acids by HPLC: At zero time and after 96 h an aliquot of the cultures was collected and centrifuged at 2647 g for 10 min. The supernatant was filtered through a cellulose acetate membrane filter (0.20 mm, Schleicher & Schuell) and used for analysis. A 25 mL portion of the filtrate was injected into the HPLC system and eluted as described below. The analysis were performed on an Agilent Technologies 1200 HPLC system fitted with a SUPELCOSIL LC-18 column (length 250 mm, diameter 4.6 mm, packaging size 5 mm). The column temperature was set equal to 20 C. The mobile phase consisted of an aqueous solution of 1%vol acetic acid (“A”) and acetic nitrile (“B”). Elution

was performed by following this protocol: at start and lasting for the first 2 min of the run, 100% of A. from 2 min to 60 min after run start a linear ramp was used, targeting 40% of A and 60% of B. The flow rate was set equal to 1mL/min. Polyphenols were detected by a UV detector (280 nm). Beforehand, the retention times of the polyphenolic compounds of interest were measured by using of single polyphenol standard solutions.

- Quantification of nitrate, nitrite, chloride, orthophosphate and nitrogen ammonia ions: UNI EN 10304-1: 2009 and APAT/IRSA CNR 2003-4030-A2.

4.9. Experimental equipment for the fluid dynamic investigation on the local recirculation photobioreactor

The core of the experimental set-up is one 120 cm long waved surface made from commercial fiberglass semi-finished material, provided with 10 cm high side transparent glass rims, which was installed with the ridges laying on a (virtual) plane inclined with respect to a horizontal plane, as shown in Fig. 4.9.1. The waved surface comprises 15 complete vanes. Its bottom surface is connected to a screw jack allowing several inclinations to be set. Four angles have been investigated, namely 0, 3, 6 and 9°. The inclination of 6° of this wavy surface reflects the angle set for the 5 m^2 outdoor pilot unit installed at CNR-ISE and described by Torzillo et al. (2010).

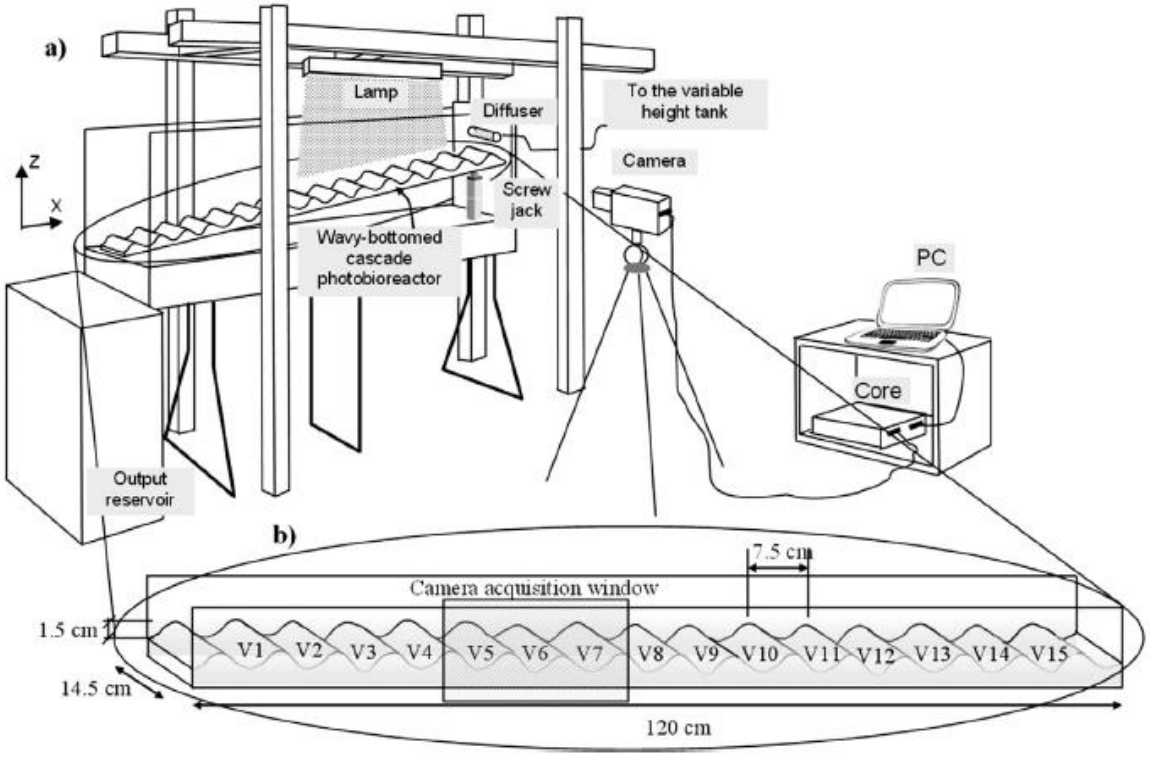

Figure 4.9.1. a) Experimental set-up comprising the wavy-bottomed cascade photobioreactor and the equipment for image analysis (camera, illumination and image acquisition/processing system); b) zoom in

the photobioreactor to visualize the acquisition window.

The channel is fed via a variable height tank connected to a diffuser installed in the topmost vane of the wavy surface and water is dumped at the exit into an output reservoir. The water level within the tank is controlled through an overflow exit. The average flow rate depends on the hydraulic head at the inlet diffuser. Experiments were conducted at three different elevations of the tank (0.84 m, 1.84 m and 2.69 m, referred to the inlet diffuser height). Table 4.9.1 shows the flow rates per unit width measured for each slope of the bottom plate and height of the tank. The last rows of the table present the average and the maximum differences of the flow rate values for the same height of the tank and different bottom plate slopes. As expected, for the same tank height, the flow rate does not depend on the bottom slope. Furthermore, higher tank heights determine a larger volume of water flowing through the apparatus per unit time. In the following discussion, we use the symbols Q1, Q2 and Q3 to indicate the tank heights and the corresponding specific flow rates. The water was seeded with a well-reflecting neutrally buoyant
passive tracer to allow qualitative visualization of the flow and quantitative estimation of the velocity field.

Table 4.9.1. Specific flow rates per unit width measured for each slope and height of the tank (values in L/s/m).

Slope	Q1 (L/s/m)	Q2 (L/s/m)	Q3 (L/s/m)
0°	0.713	0.941	1.174
3°	0.715	0.943	1.167
6°	0.705	0.939	1.169
9°	0.711	0.944	1.169
Average	0.711	0.943	1.169
Maximum difference	0.006	0.004	0.005

The seeding particles were yellow-green fluorescent microspheres (Cospheric), with a diameter in the range 53-63 mm. Proper illumination was ensured through the use of a LED based Linescan Illuminator (COBRA Slim) positioned above the wavy surface.Alight sheet 40 cm long and 1 cm thick oriented in the longitudinal direction, i.e.,parallel to theme a flow field and close to the lower discharge section to minimize the boundary effects from the distributor section was generated. The image acquisition system consisted of a high-speed, high-resolution camera (Mikrotron EoSens) equipped with a Nikon 50-mm focal length lens capturing gray-scale images at up to 500 fps with a resolution of 1280x1024 pixels (for the present set of measurements, images were acquired at 400 fps) and a high-speed Camera Link digital video recorder operating in Full configuration (IO Industries DVR Express Core) to manage data acquisition and storage. The captured images were transferred to a personal computer under the control of the Express Core software. The camera acquisition window contains 3 vanes of the wavy-bottomed cascade photobioreactor (gray shaded area in Fig.4.9.1). The whole apparatus described thereupon was enclosed in a dark room made by a thick dark plastic sheet to minimize light interference from

external sources. The duration of each experiment was approximately 60 s, i.e., the time required for the tracer particles introduced in the topmost vane of the wavy surface to pass through the test section and for a consistent amount of data to be recorded ensuring robust enough statistics to be computed.
The image analysis technique Feature Tracking (FT) was employed to reconstruct the trajectories of tracer particles seeding the fluid under investigation and to determine the velocity field evolution with time. The velocity field obtained by image analysis techniques is frequently an intermediate result in the investigation of complex flow phenomena. Further post-processing is required to extract important fluid mechanical quantities often valuable for understanding fluid motion, i.e., streamlines. A streamline is a curve that is instantaneously tangent to the fluid velocity throughout the flow field. The analysis of streamlines provides a topological description of fluid dynamic field highlighting the presence of critical points, i.e., nodes, saddles and foci (Cicci et al. 2013). After determining the velocity field, all the potential sources of high frequency light/dark alternation within the vanes of the photobioreactor exposed to sunlight were spotted and analysed by using the velocity fields themselves.

4.10. Local Recirculation PBR for microalgal culture

The photobioreactor is composed by two 120 cm long waved surfaces made from commercial fiberglass semifinished material, provided with 10 cm high side transparent glass rims; every waved surface comprises 15 complete vanes and has an inclination of 6° respect horizontal plane (Figure 4.10.1.A). The total surface exposed to the sunlight is 0.35 m^2; recirculation is supported by air pumped at the bottom of the riser pipe (air lift). At the end of the second wavy surface has been installed a collection tank with a geometry suited to minimize both the settling of biomass and the variation of the liquid level which would make the liquid rate recirculated by the air-lift pump unstable (Figure 4.10.1.B). A liquid level sensor was inserted in the tank to control the evaporation rate of the water; the sensor activates a valve collected to tank with water, keeping the volume at the preset level.

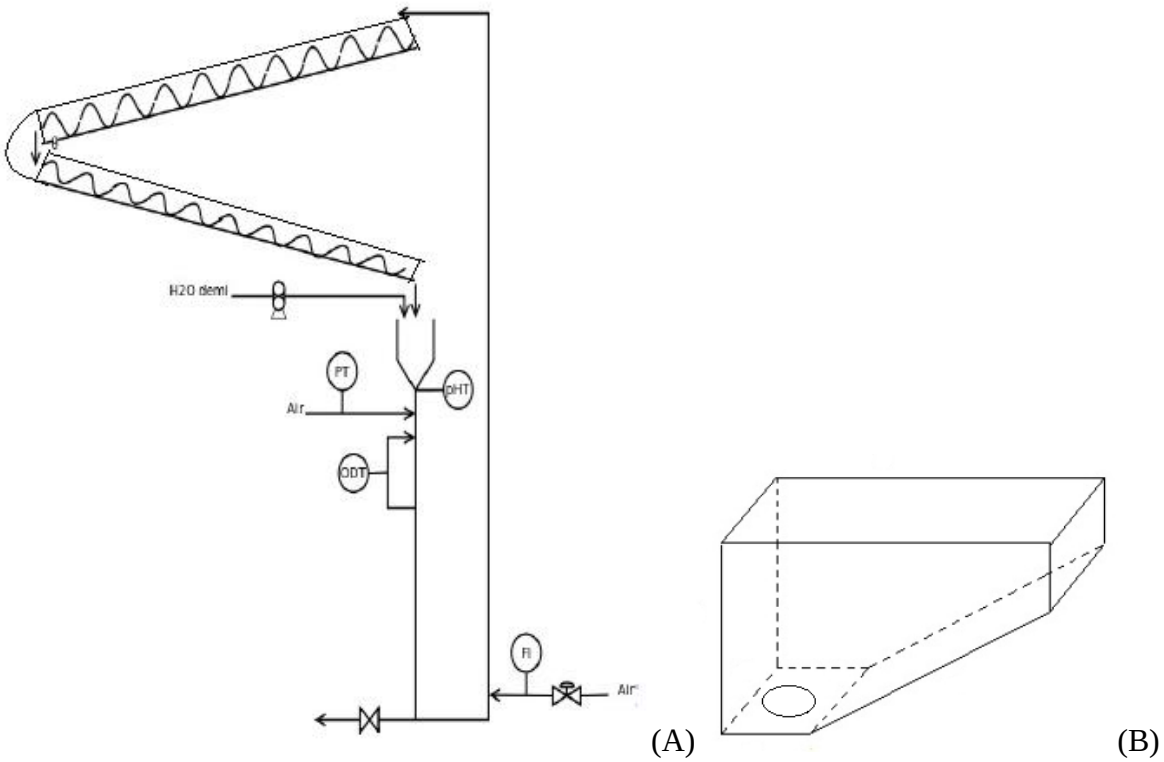

Figure 4.10.1. (A): LR-PBR plant. (B): collected tank.

4.11. Experimental set up microalgal cultivation in Local Recirculation PBR (LR-PBR) out-door

Cultures were grown in 400-mL cylindrical glass tubes, with a diameter of 6 cm, fed with filtered and humidified air at flow og $130*10^3 Nm^3/h$. Photo-period of light provided by cold white fluorescent lamps (400-700 nm, 865 K, 32 W, 80 mmol photons m^2 s^{-1}) 16 h followed by a period of darkness equal to 8 h. The temperature was maintained constant at 25 ±1 °C. After 15 days cultures were carried out in a cylindrical photobioreactor of capacity 8 liters; after this step the cylindrical PBR was transferred outdoor, on the roof of the building, for photoperiod and temperature acclimation.After 7 days of acclimation the cultures were used as inoculum in LR-PBR. The total volume of the transferred cultures was 7 l, 4.5 of which made up the total (static plus operating) hold up on the active (i.e., the wavy-bottomed channels exposed to sunlight) area. The adopted recirculation rate (and which the total active hold up refers to) was set at 1100 l/h and required an air flow rate of 2500 l/h. Biomass growth was monitored sampling the photobioreactor from the volume buffer tank and measuring sample at absorbance of 690 nm; temperature inside and outside the reactor were monitored daily. Due to logistic constraints, the growth test of both species took place in very unfavourable climate conditions (in March for *S. dimorphus*, in September-October for *A. platensis*).

5. Results and discussion

5.1 Microalgal growths in synthetic media in air and air with 5% of CO_2

The cellular density of the two species, *Scenedesmus dimorphus e Arthrospira platensis*, was inferred from the absorbance measured at a wavelength of 690 nm (corresponding to the absorption peak of chlorophyll). Measurements were taken every 24 hours from the onset of the culture.

5.1.1. *Scenedesmus dimorphus 1237* growth

The relationship between cellular density (g/l) and the absorbance measured at a wavelength of 690 nm was determined by the correlation line:

$D = 1.05 * Abs_{690}$ $R = 0.98$

Different synthetic media were tested to study the growth rate as a function of different nitrate and phosphate concentrations. This study was required to elucidate the possibility to apply nitrate starvation condition to produce lipids.

Table 5.1.1.1. *S. dimorphus 1237* growth rates in media at different nitrogen and phosphorus concentrations.

Samples	NO_3^-	N:P	PO_4^{3-}	$\mu(d^{-1})$
CTR	8.82 mM	5:1	1.76 mM	0.57
A	8.82 mM	20:1	0.441 mM	0.65
B	0.88 mM	5:1	0.176 mM	0.48
C	0.88 mM	1:2	1.76 mM	0.51

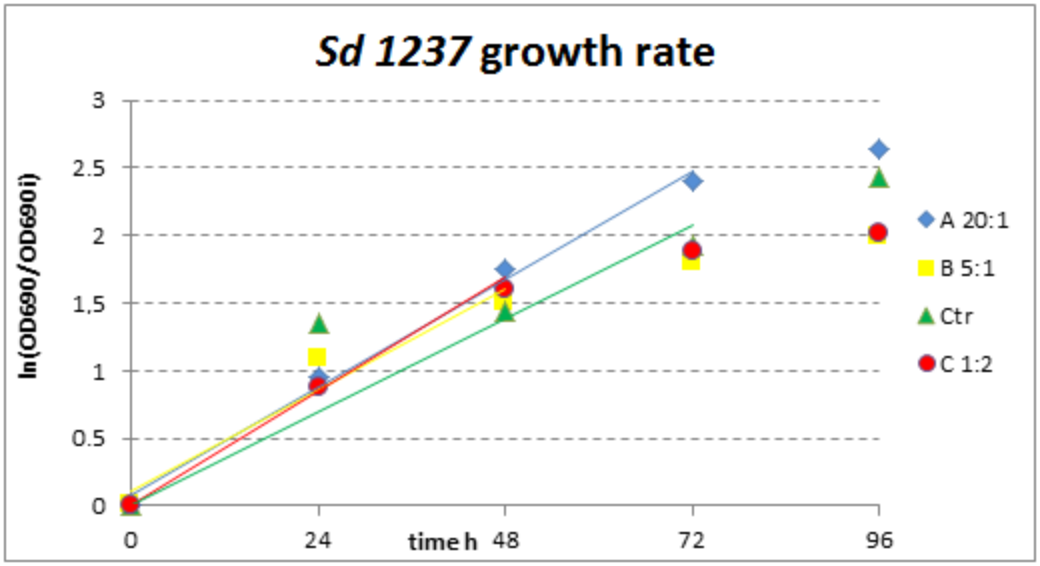

Figure 5.1.1.1. *S. dimorphus 1237* growth rates in synthetic media with different nitrogen and phosphorus concentrations. Medium A: $N=N_{Ctr}$; N:P = 1:20; Medium B: (N,P) = 1/10 (N_{Ctr},P_{Ctr}); Medium C: $N=N_{Ctr}/2.5$, N:P = 1:2.

As it can be deduced from figure 5.1.1.1, the cultures B and C, with a concentration of nitrates equal to 0.88 mM/L, show a diminution of the growth beginning after 72 h. Such event is referable to the exhaustion of nutrients, that determines a deceleration of primary metabolism and an accumulation of lipids as an energetic material storage for later uses by the same cells. Nutritional shortages, in particularly of nitrogenous substrates, determine the degradation of phycobiliproteins and chlorophyll pigments with a consequent prominence of the other pigments and the green-yellowish discoloration of the algal crops. Analyzing the growth rates reported in figure x.1. it is evident that the culture grown in the medium with increased nitrogen and with a N:P ratio of 20:1 shows a specific growth rate about 35% higher in comparison to the culture in lack of nutrients and N:P ratio 5:1.

The B and C cultures, characterised by low both species concentrations (culture B) and low nitrate concentration (culture C), exhibit comparable specific growth rates between them; the low concentration cause as a result that the specific growth rate is lower than that related to the standard conditions, but meaningfully different from zero.

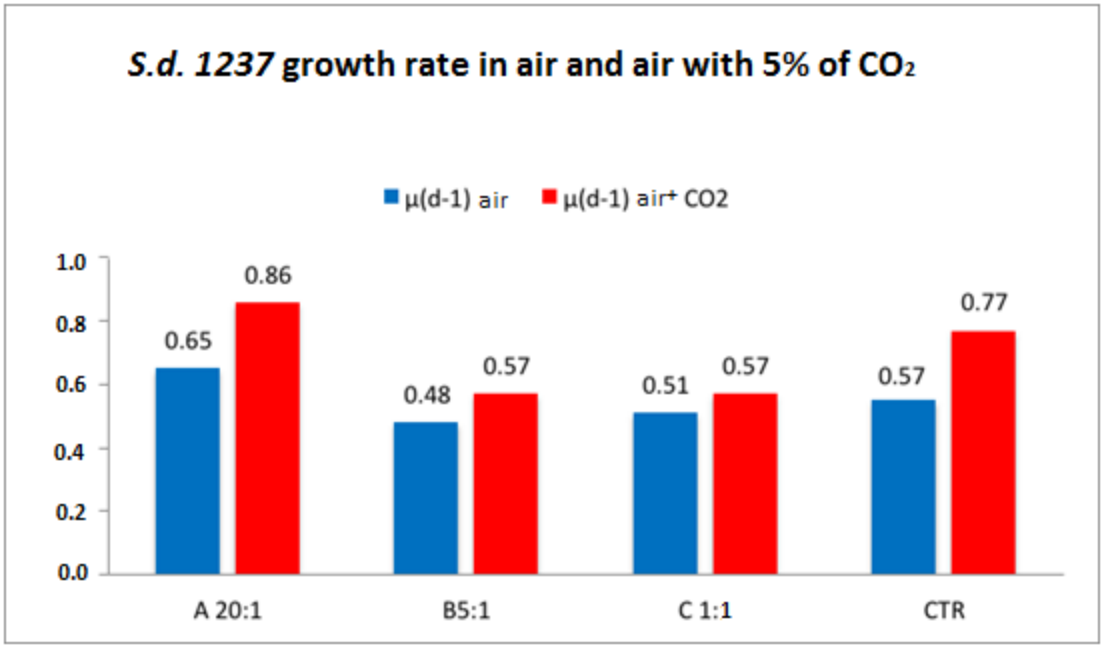

Figure 5.1.1.2. *S.d.1237* growth rates in synthetic medium insufflated with air and air with 5% of CO_2.

The growth rates of *S. dimorphus 1237* on the standard medium and on the A medium, in augmented CO_2, result to be 30% higher than the corresponding rates in standard air. The media that show a low concentration of nitrates (B and C) reveal a more limited increase, equal to 15%.

5.1.2. *Arthrospira platensis* growth

The relationship between cellular density (g/l) and the absorbance measured at a wavelength of 690 nm was determined by correlation line:

$$D = 0.81 * Abs \qquad R = 0.97$$

The growth rate in Zarrouk medium is 0.59 (d^{-1}) .

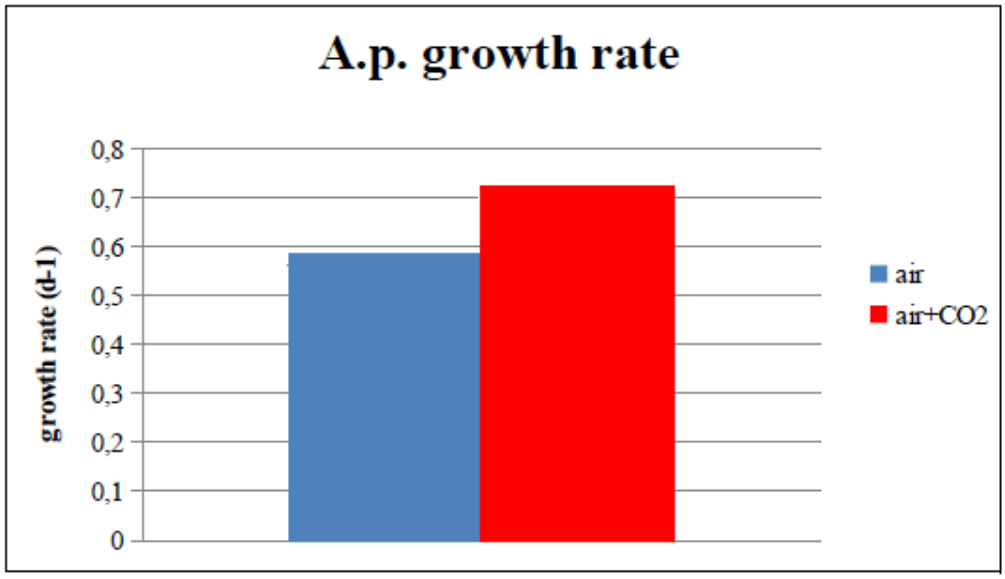

Figure 5.1.2.1. *A. platensis* growth rates in air and air with 5% of CO_2.

CO_2 being the substrate for the photosynthesis, increasing the concentration of the former has a positive effect on growth; in the specific case, the comparison between the growth rates in air and air enriched in CO_2 underlines an increase of almost 22% (Figure 5.1.2.1.).

5.2. Microalgal growth rates on olive oil mill wastewater (OMWW)

In order to evaluate the possibility to use OMWW for the microalgal cultivation and, at the same time, to appraise the efficiency of nutrients removal from OMWW, a set of test runs was carried using the microalga *S. dimorphus 1237* and the cyanobacterium *A. platensis* and, as culturing media, mixtures of OMWW and fractions thereof with both the species-specific relevant synthetic medium (modified 3NB medium and Zarrouk medium) and tap water.

Table 5.2.1. *A. platensis* and *S.d.1237* growth rates on different media: OMWW diluted with synthetic media (zarrouk and 3NB, respectively) and tap water.

samples	*A.p.* μ (d-1)	samples	*S.d.* μ (d-1)
1:1 omww/zarrouk	0.22	1:1 omww/3NB	0.35
1:5 omww/zarrouk	0.31	1:5 omww/3NB	0.46
1:10 omww/zarrouk	0.41	1:10 omww/3NB	0.48
1:1 omww/tap w.	-0.13	1:1 omww/tap w.	-0.13
1:5 omww/tap w.	-0.07	1:5 omww/tap w.	0.03
1:10 omww/tap w.	-0.01	1:10 omww/tap w.	0.29

In table 5.2.1. the growth rates of each microalgal species in the array of media resulting from mixing, at various mixing ratios, OMWW with the synthetic medium suited to each respective

species or tap water, are listed.
The resulting growth pattern is different between *A. platensis* and *S. dimorphus 1237* when OMWW is diluted with tap water. *A. platensis* did not grow, even at high dilution rates (cases 1:5 and 1:10). Nutrients (such as nitrate and phosphate) and organic substrates are indeed contained in the media, but cytotoxic effects (caused by other contained components) and light limitation (caused by some highly absorbing components, possibly the same) may be argued to have impaired growth at low dilutions; the very same toxicity has likely overcome the marginal growth potential which diluted nutrients would be able to support. *S. dimorphus 1237*, in turn, survived and was able to grow in media obtained from diluting OMWW with tap water to a high ratio (1:5 and 1:10); it possible to hypothesize this ability is due to a major dilution of toxic compounds.
When OMWW was diluted with synthetic medium, both *A. platensis* than *S. dimorphus* were able to grow. In the following, the 50% (1:1) dilution ratio was adopted as a basis for the detailed analysis of the growth behaviour of the two microalgal species in OMWW-based media (that is, OMWW after some specific pre-treatments, and fractions derived from it by membrane filtration processing, as described in the Materials and Methods Chapter).

5.2.1. Microalgal growth rates on OMWW and its fractions diluted with 50% of synthetic media: polyphenols and phenol analysis

OMWW fractions feedstocks are retentate streams produced by cross-flow filtration, enriched in all the molecules which do not permeate because of the membrane-specific pore size. They typically contain: proteins, polyphenols, and nitrate and phosphate ions; moreover, they feature high COD values. In order to evaluate the possibility of using OMWW and/or fractions obtained therefrom (see the Materials and Methods Chapter) as substrate for microalgal growth and appraise the efficiency of the concomitant nutritional removal, tests of growth were carried out using mixtures of treated OMWW and fractions thereof with the synthetic medium (3NB modified medium for *S. dimorphus 1237* and Zarrouk medium for *A. platensis*) as growth medium.
To help tracking and spotting the underlying motivation for such behaviour, normalised specific growth rates μ_n and growth rate reductions μ_{Rn} (with respect to the appropriate control for each species) were calculated for all the runs as follows:

$$\mu_n = \frac{\mu(mxxx)}{\mu(Ctr)} \qquad (1)$$

and

$$\mu_{Rn} = 1-\mu_n \qquad (2)$$

where $\mu(mxxx)$ and $\mu(Ctr)$ stand for the specific growth rate measured in medium mxxx and in control, respectively, so that both controls show normalised reductions of zero and any other run scores a value higher than zero.

Table 5.2.1.1. Specific growth rates of the two considered species in the tested media and normalised reductions thereof. Negative values of the specific growth rate and normalised reductions of the specific growth rate higher than unity indicate a net decay of the culture over the four-day monitored culturing period time.

Fraction 1:1 v/v medium	*S. dimorphus* 1237 [d^{-1}]	*S. dimorphus* 1237 (normalised reduction)	*A. platensis* [d^{-1}]	*A. platensis* (normalised reduction)
Ctr	0.57	0	0.59	0
OMWW	0.35	0.39	0.22	0.63
Ret. U. F.	0.1	0.82	-0.13	1.22
Ret. N F.	0.39	0.34	0.47	0.20

The data shown in table 5.2.1.1. are calculated using equations 1) and 2). As expected, by looking at the data reported in Table 5.2.1, both species grow at their maximum specific rate in their reference medium. *S. dimorphus* appears to be slightly less biomass productive than *A. platensis* in the optimal batch conditions, having a specific growth rate of 0.57 d^{-1} and 0.59 d^{-1}, respectively. Moreover, *A. platensis* appears to be more sensitive than *S. dimorphus* to media composition: indeed, it grows faster than *S. dimorphus* in the standard medium and in the NF concentrate, but slower (63%) in OMWW-based media. *A. platensis* totally fails to grow in UF concentrates, where a net biomass decay (23%) is observed instead.

The variables listed in Table 5.2.1.2. were used and measured in order to check and to justify the specific growth rate variations occurred during the cultures: initial phenolics (total, tyrosol and hydroxytyrosol, phenol, other), average phenolics (total, tyrosol and hydroxytyrosol, phenol), absolute and normalised phenolics reduction (total, tyrosol and hydroxytyrosol, phenol) (data partly not shown), nitrate and phosphate (average and reduction, data not shown), COD (initial, absolute reduction and normalised reduction). The normalised specific growth rate reduction was tested against each of the above variables and the fitting quality, expressed by the correlation coefficient, was ranked in paired (that is, considering both biomass species under culture) and split (only one biomass species under culture at a time) data sets. Paired data sets were ranked according to the average of the individual correlation coefficients for the observed relation.

Growth rate reduction, which may in general be the result of an imbalance between the rate of growth of new cells and the rate of death of living cells, might thus be due more to a reduction of the former (e.g. due to the energy expenditure for the degradation) than to an increase in the latter. Photoassimilation of phenol for *S. obliquus* and *Arthrospira maxima* has been described by Klekner and Kosaric (1992), who observed phenol degradation (400 mg/L in 6 days) in carbonated synthetic media only upon culture illumination and somewhat more quickly by *A.*

maxima. Moreover these authors noted that, following the initial adaptation, phenol degradation rate increased, but they did not estimate the biomass growth rate.

Table 5.2.1.2. Variation of the main composition parameters of the culture media during the microalgae growth and optical characteristics of the culture media.

	Unit	Time	Ctr	OMWW	Ret. UF	Ret. NF
Absorbance	A_{690}	Initial	0	0.238	0.583	1.4
S. dimorphus						
COD	mg/L	Initial	60	4960	8050	8210
		Final	100	5770	7310	5330
Polyphenols (PP)	mg/L	Initial	0	674	1303	766
		Final	0	277	518	344
Phenol	mg/L	Initial	0	238	411	381
		Final	0	64	41	232
A. platensis						
COD	mg/L	Initial	120	4070	5440	2550
		Final	210	5740	4010	2440
Polyphenols (PP)	mg/L	Initial	0	674	1303	766
		Final	0	490	356	541
Phenol	mg/L	Initial	0	238	411	381
		Final	0	181	0	316

Only the topmost eight relations for the paired data view are reported in Table 5.2.1.3.

Table 5.2.1.3. Suitability of a dependance for the description of the observed specific growth rate reduction. Sd and Ap stand for *S. dimorphus* and *A. platensis*; mu_Rn stands for normalised specific growth rate reduction; the "_red" suffix stands for "reduction"; the "_n" suffix stands for "normalised"; PP, Ph, HT and TYR stand for polyphenols, phenol, hydroxytyrosol and tyrosol, respectively.

Rank	*S. dimorphus* data view	*A. platensis* data view	Average r2	Sd slope	Ap slope	Ap slope / Sd slope
1	Sd: (mu_Rn) *vs* (PP_red_n)	Ap: (mu_Rn) *vs* (PP_red_n)	0.910	6.40E-01	1.68E + 00	2.62
2	Sd: (mu_Rn) *vs* (Ph_red_n)	Ap: (mu_Rn) *vs* (Ph_red_n)	0.893	5.27E-01	1.32E + 00	2.51
3	Sd: (mu_Rn) *vs* (PP_tot_in)	Ap: (mu_Rn) *vs* (PP_tot_in)	0.846	3.87E-04	8.23E-04	2.13
4	Sd: (mu_Rn) *vs* (PP_red)	Ap: (mu_Rn) *vs* (PP_red)	0.839	6.55E-04	1.37E-03	2.10
5	Sd: (mu_Rn) *vs* (COD_in)	Ap: (mu_Rn) *vs* (COD_in)	0.810	5.01E-02	1.91E-01	3.82
6	Sd: (mu_Rn) *vs* (COD_in_nonPP)	Ap: (mu_Rn) *vs* (COD_in_nonPP)	0.771	5.79E-02	2.54E-01	4.39
7	Sd: (mu_Rn) *vs* (PP_avg)	Ap: (mu_Rn) *vs* (PP_avg)	0.766	5.49E-04	1.09E-03	1.98
8	2.72		0.757	1.45E-03	3.19E-03	2.19
Average						0.89

Adopting the normalised specific growth rate reduction metrics, the reason for growth rate depression can be tracked down, primarily, to polyphenol (PP) presence. As it can be seen, the two topmost paired data views refer to (normalised) total phenol and phenol reduction. Albeit with a slightly lower fit quality, initial phenolics concentration still describes normalised specific growth rate reduction reasonably well. This means that growth rate is reduced proportionally to the extent of phenolics disappearance during the growth itself (Fig. 5.2.1.1.). The effect of all

tested parameter, as expressed by the slope parameter, is more pronounced for *A. platensis* than for *S. dimorphus*. For almost all the tested conditions, the ratio of slopes (*A. platensis*)/(*S. dimorphus*) is 2.57/0.65, showing that *A. platensis* is, in general, more sensitive to changes in the medium with respect to its control. However, the problem is simply shifted to the understanding of why phenolics are more or less metabolised, in order to anticipate and control this outcome. The reason for this erratic metabolism is not immediately apparent.

Figure 5.2.1.1. Specific growth rate reduction as a function of the total polyphenol concentration (left) and phenol degradation (right).

5.2.2. Microalgal growth rates on OMWW and its fractions diluted with 50% of synthetic media: biomass profiles and supernatant analysis

Microalgae *S. dimorphus 1237* and *A. platensis* were grown on pre-treated OMWW and its fractions diluted at 50% in the species-relevant synthetic medium. In this section we will consider components other than polyphenols. In the following tables the initial and final media pHs during the runs are listed; table 5.2.2.1 refers to *S.d.1237*; table 5.2.2.2. refers to *A. platensis.*

In *S.d.1237* the pH values are low and constant except for the case NFc 1:1 3NB, where the final pH increased up to 9.2. In this fraction, *S.d. 1237* grew better than in the others, alkalinizing the medium; pH in all cases starts at the natural acidic value of the blend, due to the acidity of both the synthetic medium and OMWW.

Analysing *A. platensis* cases, the pH value in OMWW diluted 1:1 in zarrouk medium settles at an average between the OMWW acidic pH and the zarrouk alkaline pH; the value increases in the ultrafiltration concentrate (UFc) fraction and decreases in the nanofiltration concentrate (NFc) fraction, due to the permeation of species that contribute to OMWW acidity through the UF membrane and their partial accumulation in the NF retentate.

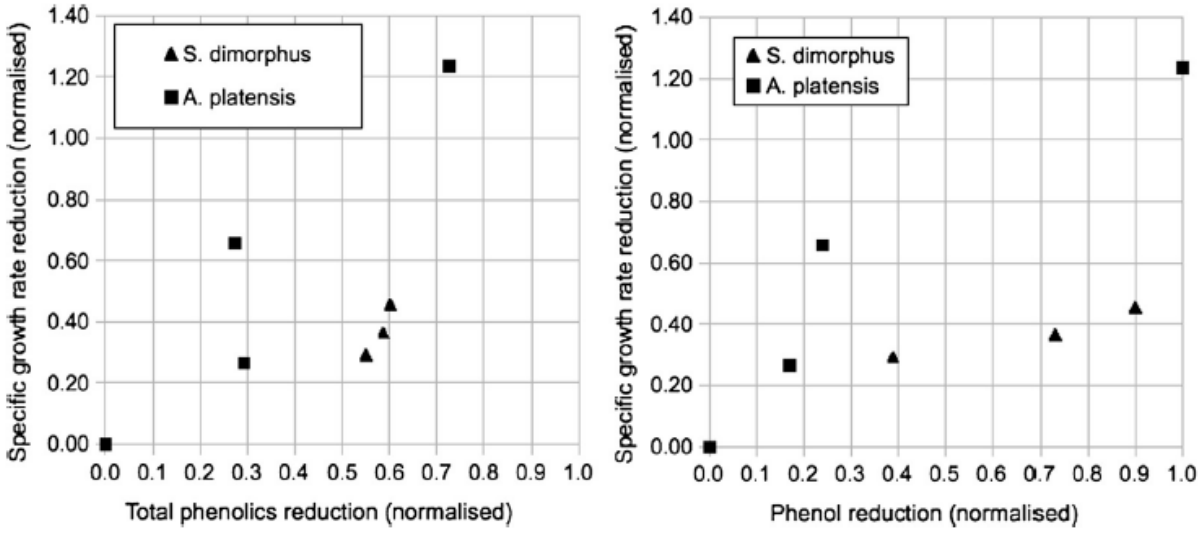

Table 5.2.2.1. pH at time 0 and 96 hours in *S. dimorphus 1237* growth test in OMWW and its fractions.

Sample	Initial pH	Final pH
control	6.3	10.2
omww1:1 3NB	6	6.1
Ufc 1:1 3NB	6	6.3
NFc 1:1 3NB	6.2	9.2

Table 5.2.2.2. pH at time 0 and 96 hours in *A. platensis* growth test in OMWW and its fractions.

Sample	Initial pH	Final pH
control	9.2	10.5
omww1:1 zarrouk	7.5	10.4
Ufc 1:1 zarrouk	9.7	10.5
NFc 1:1 zarrouk	8.9	10.4

5.2.3. *S. dimorphus 1237* growth in OMWW and its fractions diluted (1:1 v/v) with synthetic medium.

In standard conditions the biomass composition of *S.d. 1237*, obtained in our laboratory, is 22-31% carbohydrates, 47-53% proteins, 8-11% lipids, and 1-4% chlorophylls and carotenoids. These results are consistent with other published results, such as those by Hu (2004): 30–50% protein (average: 40%), 20–40% carbohydrate (average: 30%), and 8–15% lipid (average: 11.5%).

In all the experiments the metabolite classes of concern (carbohydrates, proteins, chlorophyll and carotenoids, and lipids) were quantified at the initial time of the run and after 96 hours. The fraction Y of each metabolite class j, expressed as the weight of metabolite per unit weight of biomass containing it, was recorded as $Y_{j,i}$ and $Y_{j,f}$, respectively.

The variation in the accumulated fraction for each fraction was then calculated over the entire

experiment run time separately as:

1. Percentage enrichment of biomass in fraction or metabolite j: $\Delta Y_j\% = [(Y_{j,f}-Y_{j,i}) / Y_{j,i}] \cdot 100$

In figure .2.3.1. the molecular profiles of the developed microalgal biomasses are graphically reported with respect to their physiological standard conditions.

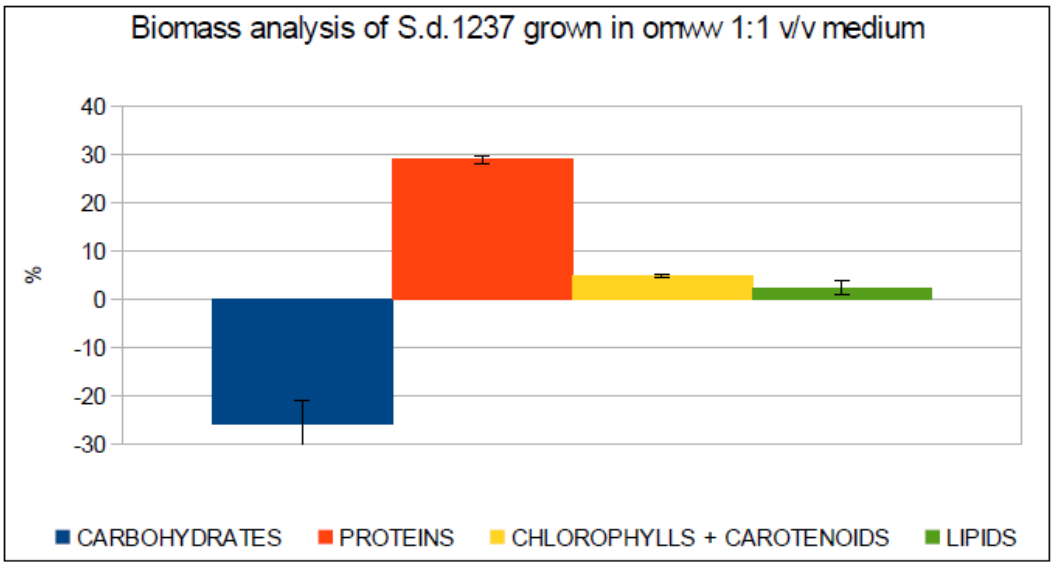

(A)

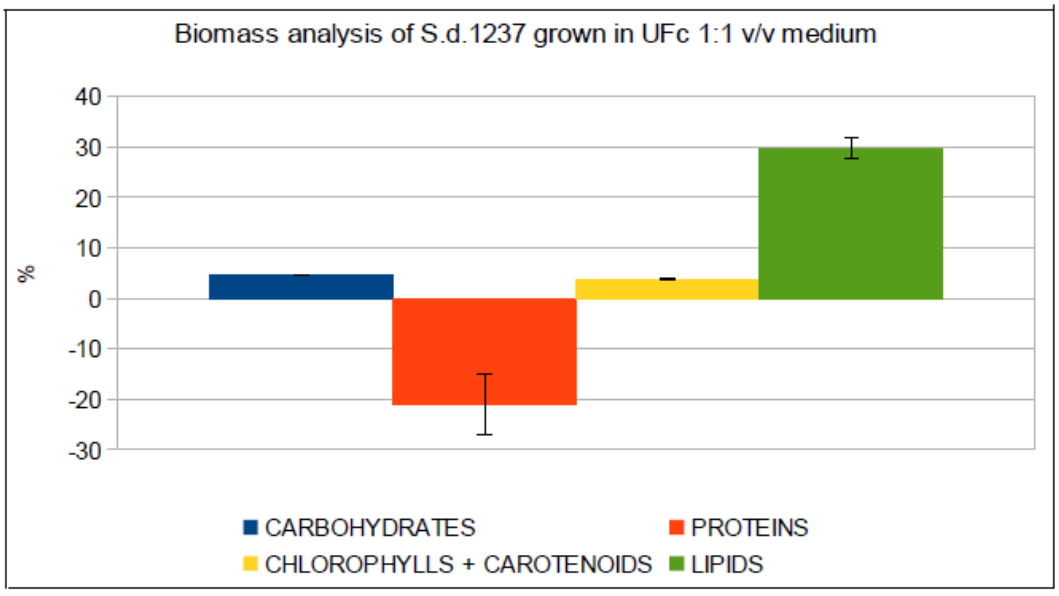

(B)

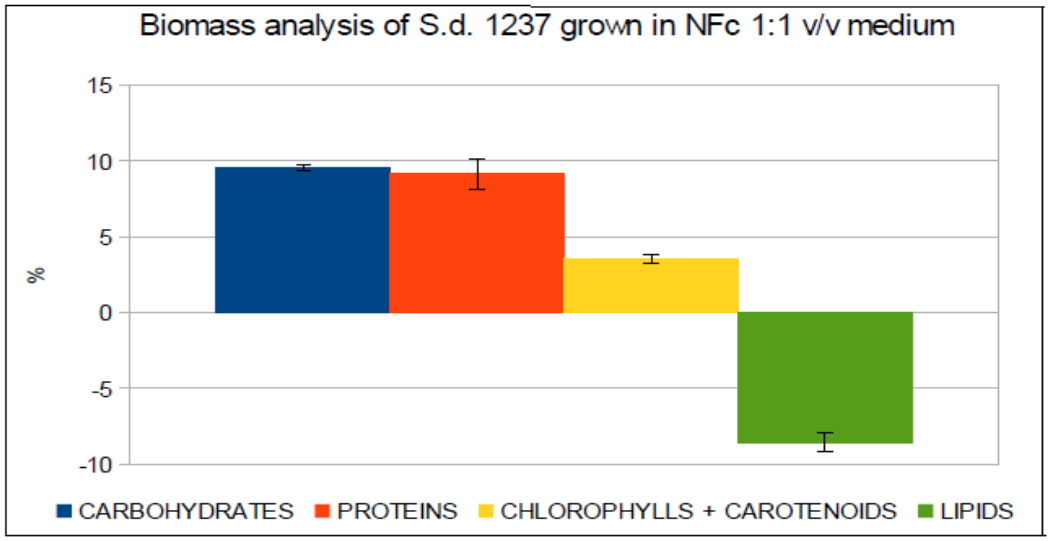

(C)

Figure 5.2.3.1. Percentage increment and reduction of the principal molecules extracted from biomass during *S. dimorphus* 1237 culturing in: A) OMWW diluted (1:1) with 3NB medium. B) UFc diluted (1:1) with 3NB medium. C) NFc diluted (1:1) with 3NB medium.

As figure .2.3.1. shows, after 96 hours of growth the biomasses exposed to the different media appear quite diversified; in UFc 1:1 3NB test (Figure 5.2.3.1.B), the biomass shows a limited growth (see table 5.2.1.1.) but after 72 hours the biomass concentration starts to decrease (data not shown). Several factors likely take part in this net biomass decay, namely scarce light penetration and phenolics toxicity. Nutrients deficiency, instead, does not seem a plausible cause, as nitrates and orthophosphates almost parallel, with a minor deficiency, the respective values measured in the control culture; chlorides, while higher than in the control, are lower than in the OMWW-based medium, which does not appear to suffer from it (table 5.2.3.1). Growth appears more pronounced in OMWW and NFc.
The OMWW-based medium promotes growth, at the expense of storage material (diminished carbohydrates); the UFc-based medium promotes carbon accumulation, in the form of lipids, at the expense of proteins, in a strongly depressed specific growth rate context; the NFc-based medium promotes growth and carbohydrate accumulation with a specific and significant increase in light-catching molecules (NFc is the most absorbing among all the tested fractions), at the expense of some accumulated lipids that are consumed to support such a metabolic change in a severe energy shortage context.

Table 5.2.3.1. Initial species concentrations in OMWW, UFc and NFc 50% 3NB *S. dimorphus 1237* growth tests.

Species	Ctr (mg/L)	omww 1:1 3NB (mg/L)	UFc 1:1 3NB (mg/L)	NFc 1:1 3NB (mg/L)
NITRATE	427.10	1402.60	374.55	485.10
ORTHOPHOSPHATE	172	433	148	439.30
NITRITE	0	0.05	0.05	0.05
CHLORIDE	33.10	141.80	108.40	48.50
AMMONIUM NITROGEN	0	2.70	0.44	0.55
COD	0	2110	885	1901
CARBOHYDRATES	0	210	49	81
PROTEINS	0	1302.59	286	439

(A)

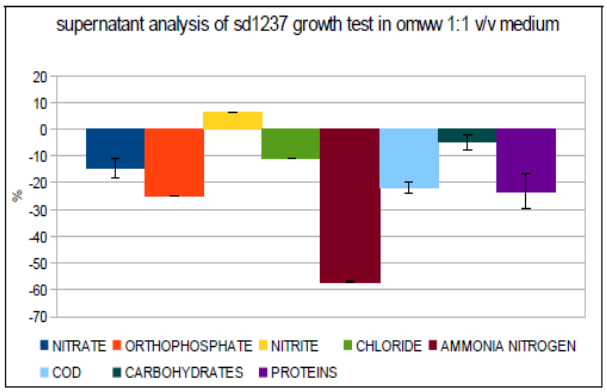

(B)

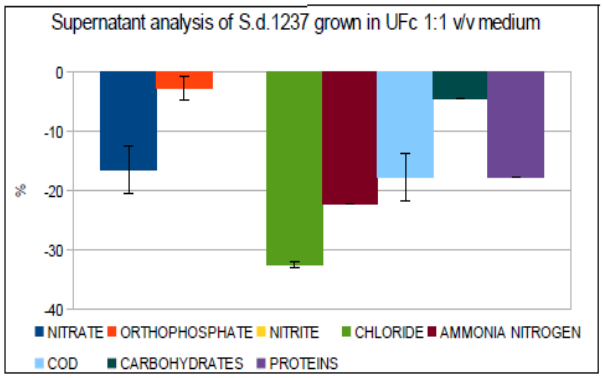

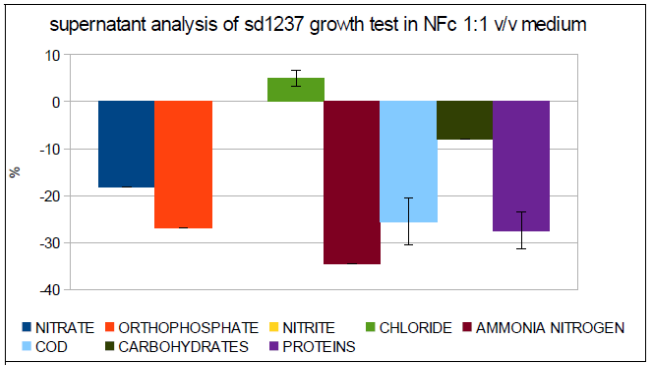

C)

Figure 5.2.3.2. Percentage reduction of the principal molecule classes during *S.d.1237* culturing in: A) OMWW 1:1 3NB medium. B) UFc 1:1 3NB medium. C) NFc 1:1 3NB medium.

In figure 5.2.3.2. a specific mention is in order for: nitrates (high in OMWW, aligned with the 3NB medium for the fractions mixtures), proteinaceous matter (high in OMWW, and significantly higher than zero for the fractions mixtures), chlorides (high in OMWW and UFc, and aligned with the 3NB medium for the NFc), orthophosphate (high in OMWW and UFc, and aligned with the 3NB medium for the NFc), COD (high in OMWW and NFc, significantly higher than zero for UFc).

From the N:P ratio standpoint, it can be observed that OMWW- and UFc-based media exhibit a balanced ratio with respect to the microalga nutrient uptake ratio, while NFc appears to be unbalanced (excess of orthophosphates). Therefore, irrespective of the actual removal obtained

during short-term growth tests, only partial phosphorous removal would be expected during long term (e.g., continuous) cultures. Strangely enough, however, the supernatant analysis displays the opposite, in that phosphorous removal appears less efficient in UFc-based than in NFc-based media. Furthermore, nitrate removal appears unchanged. However, it should be recalled that UFc-based media are growth-constraining and that the reported analysis shows that cells lose part of their proteins (and possibly need to rearrange their enzyme set). In addition, it is worth mentioning that OMWW generally contains polyphosphates (although a specific determination for the presence of polyphosphates in the OMWW used during the reported research was not carried out) and, if their hydrolysis has not completed by the time of their use and if they are not abated during pretreatments, they might concentrate at some step during membrane fractioning. The pretreatments undergone by the raw OMWW (acidic-thermal coagulation), the subsequent storage in frozen state, and the combined interplay among equipment- (the cut-size of membranes) and process-specific factors (the accumulated and the transient fouling deposition onto the membranes) might have contributed a non negligible concentration of non-readily available phosphates in the fraction itself.
It is easily noted that the COD decrease parallels the reduction in media content of proteinaceous matter for all the cultures. For the OMWW-based medium, the initial COD is very close to the value corresponding to the sum of the calculated oxygen demands (calculated according to the ThOD procedure and assuming all carbohydrates being equivalent to glucose and all proteinaceous material being equivalent to the aminoacid glycine) of proteinaceous material and carbohydrates.

5.2.4. *A. platensis* growth in OMWW and its fractions diluted (1:1 v/v) with synthetic medium

Due to the prevailing decay during *A. platensis* culture in UFc-based media, and to the consequent discharge of organic load into the medium, it was deemed unnecessary to characterise the final status of the remaining biomass.
In figure 5.2.4.1. the molecular profiles of the developed microalgal biomasses are graphically reported with respect to their physiological standard conditions.

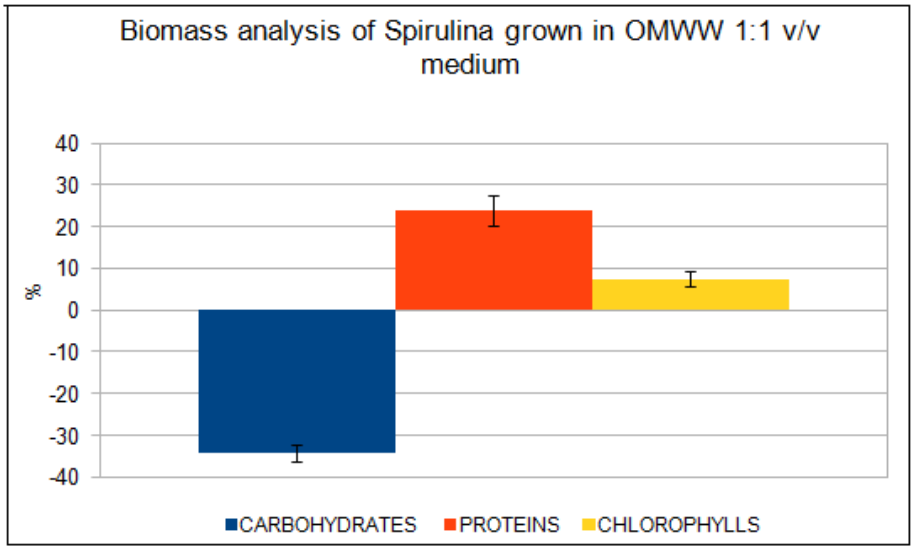

(A)

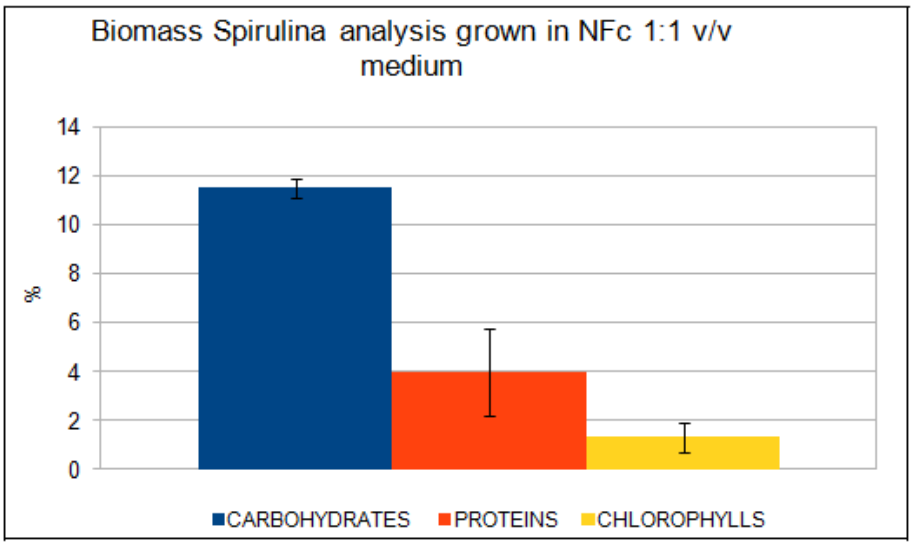

(B)

Figure 5.2.4.1. Percentage increment of the principal molecules extracted from biomass during *A. platensis* culturing in: A) OMWW 1:1 zarrouk medium. B) NFc 1:1 zarrouk medium.

Figure 5.2.4.1. shows that carbohydrates content changes in an opposite manner between OMWW and NFc. In NFc-based medium, proteins increase while carbohydrates undergo a massive breakdown; moreover, photoreceptors (chlorophylls) increase noticeably; in NFc-based medium, carbohydrates show a moderate increase, while proteins and photoreceptors remain almost stationary. An explanation for what occurred may be found if we consider that OMWW diluted 1:1 with synthetic zarrouk medium is a (moderately) dark culture medium; the constrained ability to fix CO_2 stimulates the production of photoreceptors to enhance the capture of the residual light. In NFc 1:1 diluted 1:1 with synthetic zarrouk medium, however, the culture is significantly darker than OMWW; however, the cyanobacterium does not activate any production of further photoreceptors and concentrates on the buildup of storage material

(carbohydrates in this case). The apparently contradictory behaviour can be explained by considering the fact that *A. platensis*, being a cyanobacterium, is an intrinsic mixotroph, that can use soluble organic carbon. In the presence of only minor toxic effects and in lack of a significant light supply, the cyanobacterium oriented its metabolism toward resource conservation (it is not worth to expend resources on a minimal enhancement of light capture) and behaved mostly as a bacterium, making the most out of ready-for-use soluble material (amino acids and substrates).

Among mixed media (Table 5.2.4.2.), NFc is well balanced according to its composition, but nitrate is consumed less than expected with regard to orthophosphate (N:P = 2.5:1) (Figure 5.2.4.2.C). In OMWW-based media, which is poor in phosphates, nitrate is consumed significantly more than expected with regard to orthophosphate (N:P = 11.6:1) (Figure 5.2.4.2.A).

Table 5.2.4.2. Initial species concentrations in OMWW, UFc and NFc 50% zarrouk *A.platensis* growth tests.

Species	Ctr (mg/L)	omww/zarrouk1:1 (mg/L)	UFc 1:1 zarrouk (mg/L)	NFc1:1 Zarrouk (mg/L)
NITRATE	597.8	1491.4	459.9	608.1
ORTHOPHOSPHATE	457	198	98	167
NITRITE	0	0.05	0.05	0.05
CHLORIDE	552.1	333.9	283.6	300.8
AMMONIUM NITROGEN	0	0.4	0,4	0.5
COD	0	1670	913	1918.5
CARBOHYDRATES	0	300	51	68.1
PROTEINS	0	3140	254	397.3

(A)

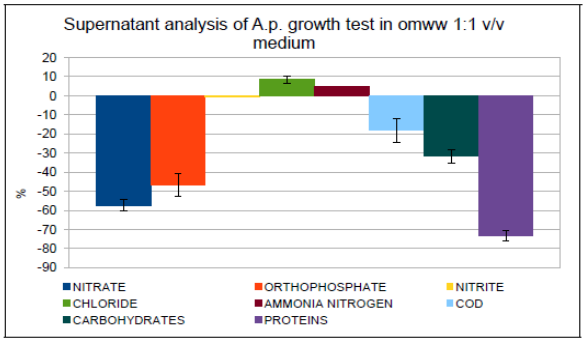

(B)

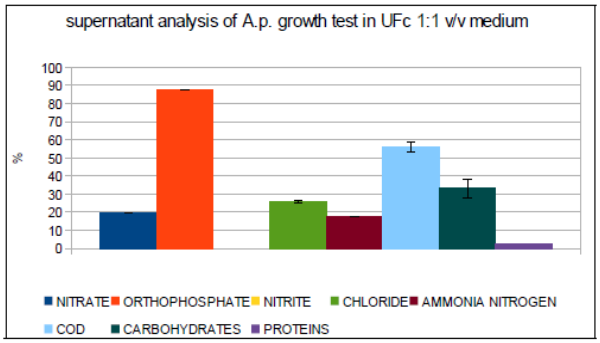

(C)

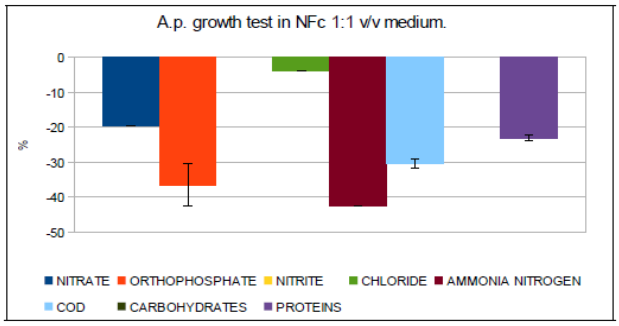

Figure 5.2.4.2. Percentage reduction and enlargement of the principal molecule classes during *A. platensis* culturing in: A) OMWW 1:1 3NB medium. B) UFc 1:1 3NB medium. C) NFc 1:1 3NB medium.

5.3. Preliminary data of *S. dimorphus 1237* and *Arthrospira platensis* growth rates in digestate

In order to evaluate the possibility to use digestate for the microalgal cultivation and, at the same time, to appraise the efficiency of nutrients removal from a waste water stream, a set of test runs was carried using the microalga *S. dimorphus 1237* and the cyanobacterium *A. platensis* and, as culturing media, mixtures of digestate with both the species-specific relevant synthetic medium (modified 3NB medium and Zarrouk medium) and tap water.

Table 5.3.1 *S. dimorphus* growth rates on media obtained from cattle digestate (c.d.) and 3NB medium (3NB) and tap water (tap w.), at different dilution ratios, under insufflation with air.

sample	μ (d-1)
1:1 c.d./3NB	0.4
1:5 c.d./3NB	0.5
1:10 c.d./3NB	0.54
1:1 c.d./tap w.	0.07
1:5 c.d./tap w.	0.09
1:10 c.d./tap w.	0.15

In table 5.3.1. the growth rates of *S. dimorphus 1237* in cattle digestate-based media at different dilutions are shown. Analysing the first three samples (cattle digestate diluted with synthetic medium), a specific growth rate increase corresponding to the dilution increase can be noticed. At dilutions 1:5 and 1:10 of cattle digestate with synthetic medium, similar results in terms of growth were obtained. Owing to their higher dilution, these cultures have a paler color than the 1:1 mixture which is considerably darker and, considering the size and tubular geometry of the photobioreactors used in the experiments, only permits a sufficient irradiation for cell maintenance and replication in a small fraction of the photobioreactor volume. Comparing the growth rates in cattle digestate diluted with tap water with that of cattle digestate diluted with synthetic medium, at the 1:10 dilution a strong limitation regarding light availability can be

observed.

Table 5.3.2. *A. platensis* growth rates on media obtained from cattle digestate (c.d.) and zarrouk medium (z.) and tap water (tap w.), at different dilution ratios, under insufflation with air.

sample	μ (d-1)
1:1 c.d./zarrouk	0.20
1:5 c.d./zarrouk	0.22
1:10 c.d./zarrouk	0.29
1:1 c.d./tap w.	-0.13
1:5 c.d./tap w.	-0.04
1:10 c.d./tap w.	0.01

A. platensis was found to be more sensitive to the combined effect of nutrient and light limitation and toxic effects than *S. dimorphus*. As it can be seen in table 5.3.2., this results very clearly from the fact that a low growth rate was exhibited by those diluted cultures which are most nutrient-limited, but also less light limited.

5.3.1. *S. dimorphus 1237* specific growth rates in digestate diluted at 50% by volume with synthetic medium

As a consequence of the preliminary growth results obtained, the dilution factor 1:1 of digestate/3NB and insufflation with air only were selected to study the growth potential of this species in the presence of digestate. A net biomass reduction during the run is then characterised by a normalised reduction greater than unity. In table 5.3.1.1. the normalised rate reductions are shown, confirming a decrease of the growth with a value of 30%.

Table 5.3.1.1. *S. dimorphus 1237* specific growth rate and normalised reduction thereof in medium obtained by 1:1 dilution of digestate with synthetic medium.

Fraction 1:1 v/v medium	*S.dimorphus 1237* μ (d^{-1})	*S.d. 1237* normalised reduction
Ctr	0.57	0
Digestate	0.4	0.30

In figure 5.3.1.1. carbohydrates, proteins, lipids and chlorophylls+carotenoids are shown; the microalgal biomass was analysed at times 0 h and 96 h and the values were represented as percentage ratio.
After 96 hours the biomass composition had changed showing a composition increase in carbohydrates and lipids and a decrease in proteins with respect to the initial concentration, leading to a pronounced accumulation of carbohydrates and lipids, and to a modest accumulation of chlorophylls and carotenoids (Figure 5.3.1.1.).

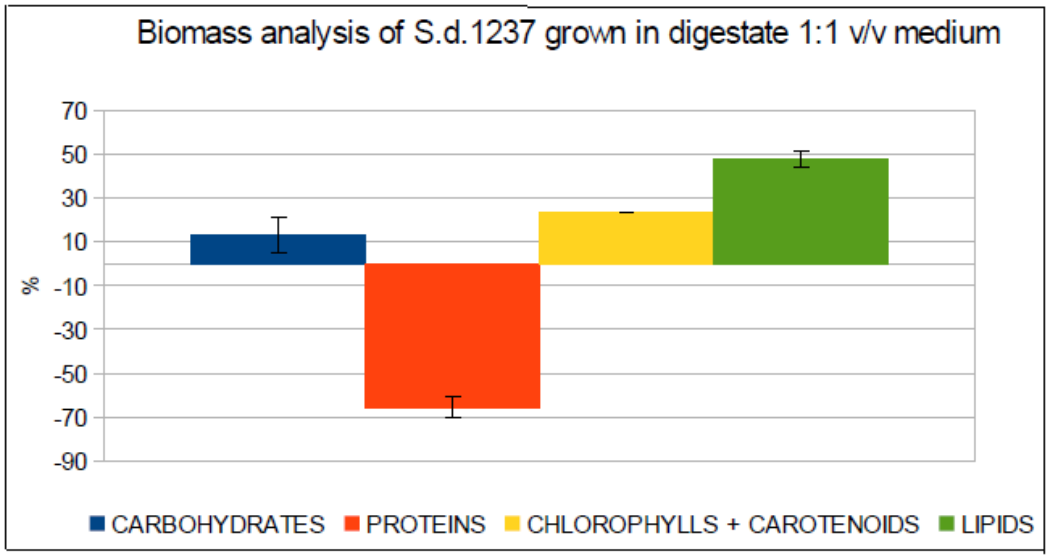

Figure 5.3.1.1. Percentage increment and reduction of the principal molecules extracted from biomass during *S. d. 1237* culturing in digestate diluted (1:1) with 3NB medium.

Light supply not only strongly influences microalgal growth, but is also capable of modifying the biochemical composition of the microalgal biomass; light supply could affect the metabolisms of fatty acid synthesis in stroma (Ho et al. 2012).

Lv et al. (2010) demonstrated that, when comparing low and high light intensity (i.e., low light- and light-saturation conditions), a light intensity of 60 umol/m^2s (i.e. a low light condition) might lead to changes in pH, NADPH, and Mg^{2+}, along with the raise of biomass and lipid concentration. Moreover, lipid content decreased while light intensity increased because lipids being major components of chloroplasts, an increase in light intensity overcomes the need for a high chloroplastidial activity.

The accumulation of energy-rich compounds, such as lipids and carbohydrates (e.g, starch), could occur in many microalgae species under such 'fattening' conditions as nitrogen limitation, phosphate limitation or high salinity.

In the 3NB synthetic medium NaCl concentration is 0.03 g/L, while in digestate 1:1 3NB NaCl concentration is 1 g/L (0.017 M); Kaewkannetra et al. (2012) demonstrated a strong growth inhibition only when NaCl concentration is higher than 0.05 M, which rules out a salt stress effect as a possible cause of the growth slowdown.

Anaerobic digestates normally are ammonium-rich waste waters where ammonium exceeds 2 g/L and nitrates are very low to absent. The medium that was supplied for testing the suitability for supporting microalgal growth underwent regular chemical analysis at the exit of the anaerobic digestor that was supplied to us. The media formulations were based on the chemical analysis sheet supplied by the Company running the digestor.

The media used for the cultures were subjected to analysis for the culture-relevant and environmental-relevant parameters, that showed that the medium was unusually rich in nitrates

(1 g/L) and very poor in ammonium (164 mg/L). Our pretreatment procedures, expecially thermal sterilisation, were carefully checked as to their influence on ammonium, and were found to have a minor influence on ammonium concentration decay.
The anaerobic digestor plant process flow and procedures was then investigated and it was found that the digestate discharged from the anaerobic digestor is normally stored by the plant operator in an open sump for several days. The sump is discharged discontinuously and partly, with a frequency lower than the loading frequency of the digestor, which provides a high residence time and does not force any microbiological washout. The digestate was declared to contain about 3 mg/L of nitrites (but none was later found by the initial analysis on the media). The digestate has significant alkalinity (1.2 g/kg) and a pH equal to 8. During the storage, the accumulated digestate is expected not to be devoid of dissolved oxygen, at least in the neighbourhood of its surface. As it flows out of the digestor, the digestate has about 3 g/L of BOD_5 and about 40 g/L of COD and is contaminated by a conspicuous yeast and mould population. COD reduces to a COD of 3 g/L after the sump storage and the adopted pretreatment (filtration and sterilisation).
Given the above, it may be argued that a non negligible nitrification has occurred in the upper layer of the accumulated digestate where it was collected by the plant operators.
In Table 5.3.1.2. the initial concentration values of the principal chemical fractions/species in the culture medium are listed; in figure 5.3.1.2. the percentage variation of the concentration of the monitored species in the developed biomass between the start of the experimental run and 96 h is reported. Park et al. (2010) demonstrated that Scenedesmus cells do not differentiate between nitrate and ammonium as a nitrogen source; *Scenedesmus sp*. is able to remove nitrogen from anaerobic digestion effluents as ammonium ions concentration < 100 ppm; from 200 to 500 ppm the growth shows similar levels of inhibition. The lower nitrogen (ammonia and nitrate) concentration of the cattle digestate-based media compared to the control participates in lowering the growth rate (further responsibility for this may be attributed to toxic effects) and is responsible for the higher production of carbohydrates and lipids by the developed biomass. Analysing the variation of the main compositional parameters of the medium between the start of the experimental run and 96 h (Figure 5.3.1.2.), a decrease of organic compounds can be observed and a reduction of nitrogenous and phosphorous species.

Table 5.3.1.2. Initial concentrations of the monitored species/fractions in 1:1 digestate:NB medium used for *S. dimorphus* 1237 growth tests.

	Cattle digestate 1:1 3NB (mg/L)	Ctr (mg/L)
NITRATE	256	427.1
ORTHOPHOSPHATE	339.0	148.0
NITRITE	0.1	0
CHLORIDE	572.8	33.1
AMMONIUM NITROGEN	82	0
COD	1556	0
CARBOHYDRATES	125	0
PROTEINS	1207	0

Table 5.3.1.3. pH at time 0 and 96 hours in *S.d.1237* growth test in digestate/3NB 1:1.

Sample	Initial pH (dig/medium 50%v/v)	Final pH (dig/medium 50%v/v)
S.d.1237	7.5	9.1
S.d. control	6.3	10.2

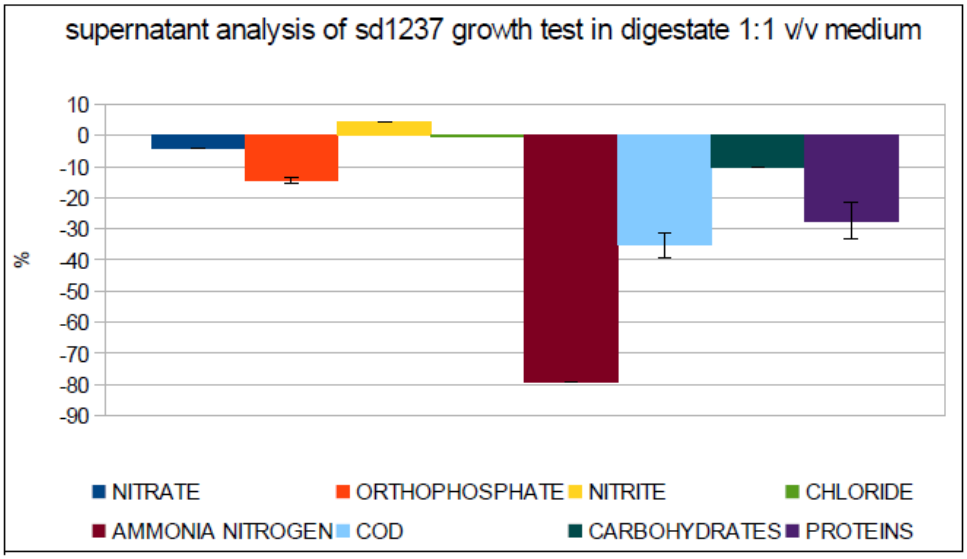

Figure 5.3.1.2. Variation of the concentrations of the monitored species/fractions in the supernatant after the *S. dimorphus 1237* grown in 1:1 digestate / 3NB.

In the 3NB medium bicarbonate and carbonate salts are absent; in digestate, the bicarbonate ion is at 0.9 g/L while the carbonate ion is at 0.3 g/L; at pH values between 7 and 10 the bicarbonate ion prevails on the other species. Park et al. (2010) found that the bicarbonate ion, which increases the alkalinity for anaerobic digestion, was successfully utilized as a carbon source by autotrophic microalgae grown in ammonium-rich wastewaters. In our case, where the cultures were insufflated with air only, algal cells were forced to utilize dissolved inorganic carbons in the wastewater.

5.3.2. *A. platensis* growth rates in digestate diluted at 50% in volume with synthetic medium

A. platensis was inoculated in pretreated digestate diluted at 50% by volume with Zarrouk synthetic medium. The biomass growth was monitored daily spectrophotometrically (absorbance at 690 nm).

Table 5.3.2.1. *A. platensis* growth rate and its normalised reduction in digestate 1:1 zarrouk medium.

Fraction 1:1 v/v medium	*A.platensis* μ (d^{-1})	*A.platensis* normalised reduction
Ctr	0.59	0
Digestate	0.20	0.66

Digestate exerts an inhibitory effect on *A. platensis* growth reducing its growth rate by 66%. Analysing biomass components it can be the organism reacts at this stress producing especially carbohydrates and lipids (data not shown).

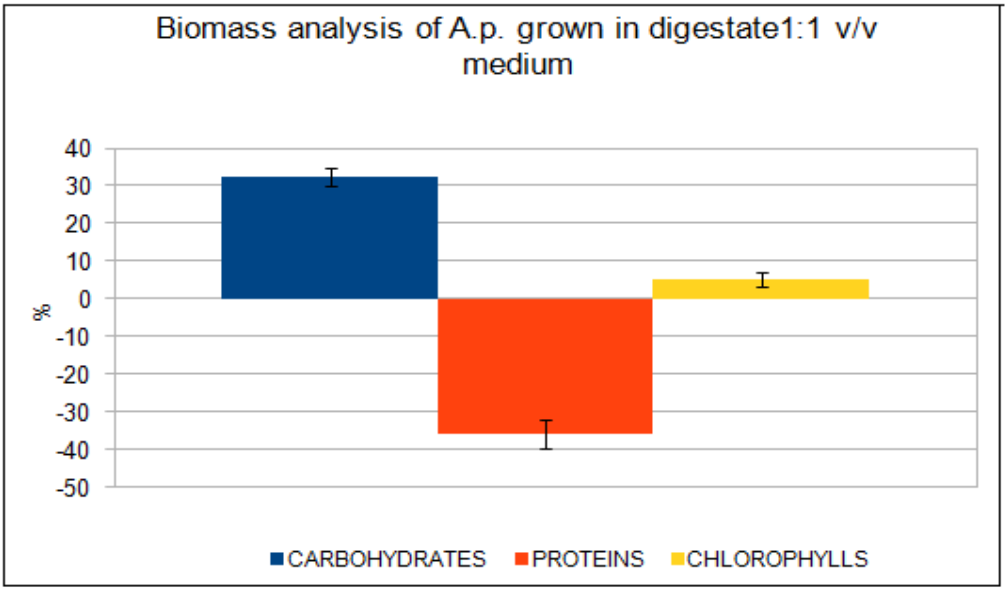

Figure 5.3.2.1. Percentage increment and reduction of the principal molecules extracted from biomass during *A. platensis* culturing in digestate diluted (1:1) with Zarrouk medium.

Ammonia nitrogen exists in aqueous solution as either NH_4^+ ion or NH_3 gas depending on the pH and temperature of the medium; at pH 10.5 and 20°C more than 90% of ammonia nitrogen is in the gas phase, while at pH 9.0 and 10°C only 20% of it is volatile. Thus, batch cultures with an initial concentration of 1 mM ammonia, incubated at 32°C and left under uncontrolled pH regime, are expected to have a large loss of this ion, by stripping, to the atmosphere (Olguin et al. 2001).

Table 5.3.2.2. Initial species concentrations in digestate at 50% dilution with zarrouk medium. *A. platensis* growth tests.

	Cattle digestate 1:1 zarrouk (mg/L)	Ctr (mg/L)
NITRATE	770	597.8
ORTHOPHOSPHATE	383	457
NITRITE	0.05	0
CHLORIDE	1605.3	552.1
AMMONIUM NITROGEN	82	0
COD	1450	0
CARBOHYDRATES	165	0
PROTEINS	1010	0

Table 5.3.2.3. pH at time 0 and 96 hours in *A. platensis* growth test in digestate/zarrouk 1:1.

Sample	Initial pH (dig/medium 50%v/v)	Final pH (dig/medium 50%v/v)
A.platensis	8.8	9.8
A.p. control	9.2	10.5

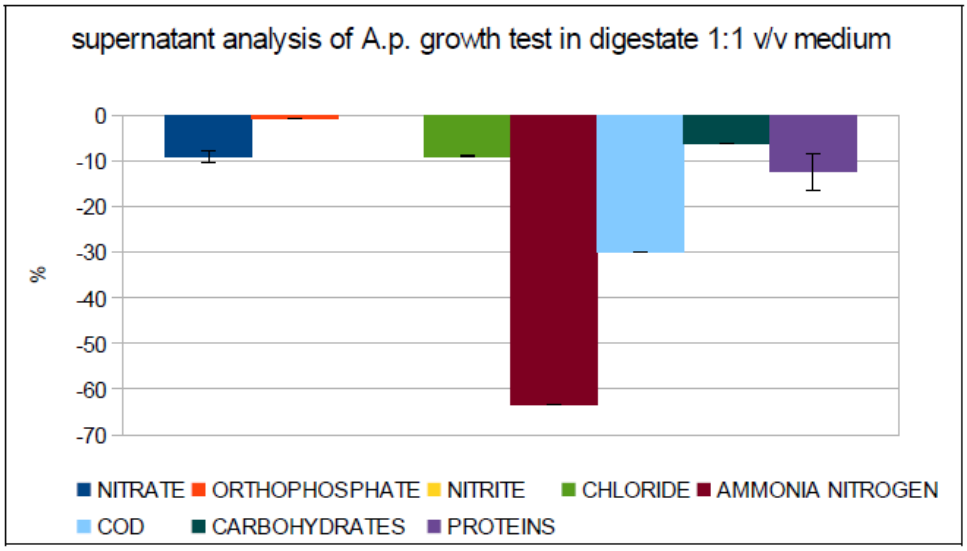

Figure 5.3.2.2. % of decrease of supernatant chemical parameters in *A. platensis* grown in digestate diluted 1:1 with Zarrouk medium.

Arthrospira platensis is capable of utilizing ammonia as the sole source of nitrogen even at pH 10 and above (Boussiba 1989), in contrast to the general notion that at high pH values ammonia is toxic to photosynthesis (Abeliovich and Azov 1979). In the thylakoids, where ammonium ions would tend to accumulate as a result of the lower pH of that compartment, the concentration of ammonia would be much higher. Nevertheless, the proton gradients appeared to be maintained, and this stability may be the reason that explains the ability of *A. platensis* to evolve O_2 at high pH values in the presence of ammonia (Belkin et al. 1991). On the other hand, in the presence of

sodium chloride, ammonia volatilization is diminished and more nitrogen remains available for algal assimilation (Chiu et al. 1980).

In synthetic medium Zarrouk the presence of Na^+ is 5.5 g/L, 0.43 g/L which comes from NaCl; in digestate 1:1 zarrouk NaCl concentration is 1.21 g/L (0.02M) while total Na^+ content is 6.65 g/L (0.2 M). For *A. platensis*, exposure to a salt stress (0.5- 1 M of NaCl) results in an immediate inhibition of both the photosynthetic and the respiratory systems, as shown by Reed et al. (1985). They showed that a short term increase in the cellular sodium concentration was due a transfer increase in the permeability of plasma membrane during the first seconds of exposure to high salt concentrations. It has been suggested that the inhibition of photosynthesis arising from the rapid entry of sodium, might be the result of the detachment of phycobilisomes from the thylakoid membranes (Blumwald et al., 1984). Elevated activities of dark respiration in cyanobacteria because of salinity stress have previously been reported (Vonshak and Richmond, 1981; Fry et al., 1986; Molitor et al., 1986). This high activity may be associated with the increased level of maintenance energy required for pumping out the toxic sodium ions. In digestate 1:1 zarrouk the Na concentration is 0.2 M and is salt stress effect on growth is therefore plausible. For supporting Spirulina growth on digested wastes the addition of sodium bicarbonate at concentrations of 9 to 17 g/L is necessary; some works show that bicarbonate addition in the range of 3 to 4 g/ L is sufficient (Fedler et al. 1993; Becker et al. 1982). In the zarrouk medium the bicarbonate ion (which is present only as sodium bicarbonate) concentration is 12.4 g/L; in digestate 1:1 zarrouk bicarbonate ion is 6.6 g/L; while carbonate ion in digestate 1:1 zarrouk is 0.15 g/L; at pH values between 7 and 10 the species carbonate has converted in species bicarbonate for a total of 7.8 g/L. Therefore it is possible to conclude that the inhibition of *A. platensis* growth principally depends on low light intensity inside the culture. *A.platensis*, being a cyanobacterium, is a mixotrophic microorganism and is able to degrade some organic substrates; therefore, it may have played a direct role in the observed 30% reduction of the medium COD.

5.4. Analysis of extracted species-specific metabolites: lipids from *S. dimorphus 1237* and C-phycocyanin from *A. platensis*

Productivity of metabolite j:

$P_j = (M_f Y_{j,f} - M_i Y_{j,i}) / (V \Delta t)$ $\quad [P_j] = [g_j L^{-1} d^{-1}]$

Table 5.4.1. lipid content extracted from *S.d.1237* and biomass productivities in all waste waters.

Fraction 1:1 v/v medium	Lipids productivity (g/L d)	Biomass productivity (g/L d)
Ctr	0.08	0.91
OMWW 1:1 3NB	0.00	0.11
Ufc 1:1 3NB	0.03	0.07
Nfc 1:1 3NB	0,00	0.21
c.d. 1:13NB	0.10	0.22

In standard condition lipids productivity is 0.08 g/Ld.; generally in *Scenedesmus sp.* lipids productivity changes from 0.04 to 0.06 g/Ld, considering the species variety (Mata et al. 2010). Analysing the results (Table 5.4.1.) it is possible to see how the biomass productivities in samples from OMWW- and NFc-based media are lower than in the control culture, although the nitrate concentrations are higher than in the synthetic medium. In the cattle digestate-based medium case, where the nitrate concentration is half with respect to the control culture and the light penetration in the culture is very scarce, the lipid productivity is very high; however, the biomass productivity is very low.

Table 5.4.2. C-phycocyanin (C-P) content extracted from *A. platensis* biomass grown in all waste waters.

Sample	C-Phycocyanin content (g/L d)	Biomass productivity (g/L d)
control	0.08	0.64
digestate1:1 z.	3.4*10-3	0.03
omww 1:1 z.	7.9*10-3	0.09
Nfc 1:1 z.	8.5*10-3	0.07

As possible to see in table 5.4.2. in standard condition, according with Chen et al. (2013), biomass productivity is 0.64 g/Ld and C-phycocyanin content is 0.08 g/L d; in all tests with wastewaters the productivity obtained is very low. Chen et al. (2013) demonstrated that the c-phycocyanin productivity can be enhanced using a flat panel PBR where the culture can be receive a high solar irradiation intensity (700 μmol photons/m^2 s) and CO_2 availability. In wastewaters tests the limiting light inside the culture determined a low C-P productivity. Furthermore in cultivations under nitrate limitation, when it is exhausted, phycocyanins begin to be degraded and are used as nitrogen reserve for synthesis of other proteins (Cornet et al. 1998).

5.5. Light supply and microalgal growth

When it comes to growing microalgae for low-valued applications, the impact of every cost item should be minimised and any growth promotion potential should be exploited. Byproducts from agro-food processing are prime candidate for reuse both because they convey nutrients and sometimes organic carbon which are required (or may be used) by the microalgal biomass and because they need to be treated before discharge anyway.

Most microalgae grow in photoautotrophy and some benefit from mixotrophy. Therefore their growth essentially depends on the effective available light intensity. Within a photobioreactor, photosynthetically active light is maximum near the liquid boundary facing light supply and reduces at a distance from it. The reduction of useful irradiance is due to absorption from the microalgae capture itself, but non-transparent media (both due to dissolved and suspended material) add up to the absorbance contribution of the former to a non negligible degree.

Non transparent media are frequently obtained as the byproduct of processing in the agro-food

and in ancillary domains, and they are frequently assayed for their suitability as growth media for various microbial biomasses, including microalgae. However, the suitability of such media, judged by the specific growth rate obtained therein may be misleading due to the low transparency of the byproduct itself and to the length of the light path even in laboratory scale photobioreactors.

So far, only the relation between reduced growth rate and compositional features has been highlighted. However, it should be noted that OMWW (and the fractions derived therefrom) and digestate are strongly coloured and have a significant absorbance at 690 nm, which is the primary wavelength at which energy capture occurs. Light decays rapidly below the surface in such media just as it happens in concentrated cultures, thus reducing the photic fraction of the overall photobioreactor volume.

In order to separate the nutritional/toxic effects from the energetic effect (deriving from different illumination) of media composition, residual light intensity in a cylindrical photobioreactor was expressed as a function of the radial position. Then, the instantaneous specific growth rate in the reactor volume was calculated by integration. The average specific growth rate during the whole run was calculated by substituting the instantaneous specific growth rate calculated at the average absorbance of the culture (medium + microalgae) to the integral over the culture lifetime of the instantaneous specific growth rate at the prevailing optical density. The synthetic culture medium was considered transparent. The reference wavelength for the calculation of absorbance and local specific growth rate was assumed to be 690 nm, which is very close to the absorbance peak of chlorophyll, and the wavelength at which experimental determinations are usually carried out. in order to cancel out unknown constants in the Monod form of specific growth rate (μ_{max} e K_I) the calculated average specific growth rate was normalised by dividing it by the value of the average specific growth rate calculated for the culture developed on the synthetic medium.

Cornet et al. (1995) introduced the concept of working illuminated volume, based on a semi-rigorous estimation of both scattering/absorption effects of microalgal biomass in an illuminated volume in an otherwise clear growth medium. Other authors followed along this way. Compared to the Lambert-Beer equation, which is an approximation completely valid in the limit, this approach lacks easy mathematical tractability and does not easily lend itself to considering the simultaneous absorption effects determined by the suspended biomass and by a coloured culturing medium. Therefore, in an attempt to show the potential benefits of such a modelling and experimental data post-processing that such an approach might warrant, the development of the mathematical model will make use of the Lambert-Beer dependence of light transmittance upon culture absorbance and light penetration depth. As a consequence of the Lambert-Beer law, the light intensity at depth *x* in a suspension can be expressed as:

$$I = I_o \cdot e^{-A \cdot x} \qquad (1)$$

Within a cylindrical photobioreactor light intensity decreases by effect of depth and increases by effect of its distribution on an area which is *r*/R times smaller than peripheral surface, so that the

following applies:

$$I(r,t) = I_o \cdot \frac{R}{r} e^{-A(t)\cdot(R-r)} \qquad (2)$$

where *r* is the generic radial position and R is the internal radius of the cylindrical photobioreactor. The instantaneous specific growth rate can be written as:

$$\mu(r,t) = \mu_{max} \frac{I(r,t)}{K_I + I(r,t)} \qquad (3)$$

where:

$$\mu^* = \mu_{max} \cdot \frac{S_N}{K_{S_N} + S_N} \cdot \left(1 - \frac{S_t}{S_{t,max}}\right) \quad (4)$$

where N refers to the limiting nutrient compound and t to the most toxic compound which is present in the raw wastewater. For a wastewater which contains an excess of nutrients and no toxic compounds, which we will assume initially, μ^* equals μ_{max}. For an illumination intensity below the saturation value, Eq. (4) may thus be approximated by:

$$\mu(r,t) \sim \mu_{max} \frac{I(r,t)}{K_I} \qquad (5)$$

The volume-averaged instantaneous specific growth rate can be calculated by integration:

$$\bar{\mu}(t) = \frac{\int_0^R \mu(r,t)\cdot 2\pi r\cdot dr}{\int_o^R 2\pi r\cdot dr} = \frac{2\cdot\mu_{max}\cdot I_o}{\pi R^2\cdot K_I} \cdot \int_0^R \frac{R}{r} e^{-A(t)\cdot(R-r)} \cdot 2\pi r \cdot dr \qquad (6)$$

which simplifies into:

$$\bar{\mu}(t) = \frac{2\cdot\mu_{max}\cdot I_o}{A(t)\cdot R \cdot K_I} \cdot \left[1 - e^{-A(t)\cdot R}\right] \quad (7)$$

Assuming the cultural medium absorbance to be constant along the culture lifetime, and denoting:

$$\bar{A} = A_{CM} + \frac{A_B(t=t_o) + A_B(t=t_f)}{2} \qquad (8)$$

as the average absorbance of the culture during the experimental run, the time-averaged specific growth rate during the experimental run can be expressed as:

$$\bar{\mu} = \frac{2 \cdot \mu_{max} \cdot I_o}{\bar{A} \cdot R \cdot K_I} \cdot \left(1 - e^{-\bar{A} \cdot R}\right) \qquad (9)$$

The estimated growth rate estimate relevant to the generic medium mxxx can be normalised by dividing it by the estimated value at infinite dilution in the same medium, i.e., that in the synthetic medium (Ctr); in the absence of any limitation and toxic effect coming from the wastewater, μ_{max} can be simplified and a (dimensionless) Semi-Theoretical Normalised Specific Growth Rate (STNSGR) can be defined:

$$\mu_n(mxxx) = \frac{\bar{A}(Ctr)}{\bar{A}(mxxx)} \cdot \frac{\left[1 - e^{-\bar{A}(mxxx) \cdot R}\right]}{\left[1 - e^{-\bar{A}(Ctr) \cdot R}\right]} \qquad (10)$$

It should be noted that the only experimental quantity in this expression is the average absorbance defined by Eq. (8). In analogy, we can calculate a ratio of the measured specific growth rates at the various dilutions to the specific growth rates at the maximum dilution ratio, that is, the Experimental Normalised Specific Growth Rate (ENSGR in the following).
If we assume that the only discrepancy between the theoretical and the experimental growth behaviours resides in toxic and nutrient scarcity effects, the ratio of the measured specific growth rate to the specific growth rate at the maximum dilution ratio for the experimental growth should equal:

$$\mu_n^e(mxxx) = \frac{\frac{S_{N,w} \cdot D + S_{N,d} \cdot (1-D)}{K_{S_N} + S_{N,w} \cdot D + S_{N,d} \cdot (1-D)} \cdot \left(1 - \frac{S_t \cdot D}{S_{t,max}}\right)}{\frac{S_{N,w} \cdot D_{min} + S_{N,d} \cdot (1-D_{min})}{K_{S_N} + S_{N,w} \cdot D_{min} + S_{N,d} \cdot (1-D_{min})} \cdot \left(1 - \frac{S_t \cdot D_{min}}{S_{t,max}}\right)} \frac{\bar{A}(Ctr)}{\bar{A}(mxxx)} \cdot \frac{\left[1 - e^{-\bar{A}(mxxx) \cdot R}\right]}{\left[1 - e^{-\bar{A}(Ctr) \cdot R}\right]} \qquad (11)$$

where D is the volume fraction of the wastewater in the medium employed for the culture, $S_{N,w}$ and $S_{N,d}$ denotes the concentration of the limiting nutrient in the wastewater and the concentration of the same nutrient in the synthetic medium, S_t is the actual concentration of toxic component and $S_{t,max}$ the concentration of the toxic component that annihilates growth. μ_n^e accounts for light and nutrient scarcity effects, and toxic effects.
To cancel out light limitation effects we can take the ratio of ENSGR (Eq. 11) to STNSGR (Eq. 10). Denoting the ratio by the symbol μ_R, we can write:

$$\mu_R = \frac{\frac{S_{N,w} \cdot D + S_{N,d} \cdot (1-D)}{K_{S_N} + S_{N,w} \cdot D + S_{N,d} \cdot (1-D)} \cdot \left(1 - \frac{S_t \cdot D}{S_{t,max}}\right)}{\frac{S_{N,w} \cdot D_{min} + S_{N,d} \cdot (1-D_{min})}{K_{S_N} + S_{N,w} \cdot D_{min} + S_{N,d} \cdot (1-D_{min})} \cdot \left(1 - \frac{S_t \cdot D_{min}}{S_{t,max}}\right)} \qquad (12)$$

It should be noted that, since the actual nutrient concentration in the diluted medium corresponds to the product $S_{N,w} \cdot D + S_{N,d} \cdot (1-D)$, the maximum dilution in a series of experimental runs is obtained when D takes its minimum value, indicated here as D_{min}. By definition, $\mu_R \rightarrow 1$ for $D \rightarrow D_{min}$.

It might be argued that the soundest choice for the normalising function would be the value at infinite dilution in the dilution medium. However, while this choice is perfectly acceptable when the dilution medium is represented by the species-specific control medium, this would be meaningless if the wastewater base of the final medium is diluted with water. It should be considered that this latter approach might be attempted in the cases where the wastewater is sufficiently rich, but exceedingly concentrated, in all the components required for growth support. In order to allow such a practice, the choice was made to divide by the values relevant to the most diluted culture, irrespective of the nature of the diluting medium.
When plotting μ_R as a function of D, it is useful to expand the abscissa near the maximum dilution by taking the natural logarithm of D.
The meaning and use of the introduced quantities is illustrated in Figure 5.5.1. The data reported by Cicci et al. (2014) were used to calculate the quantities themselves. The semi-theoretical growth rates reflect the expected growth rate, normalised by the value at the maximum dilution considered.

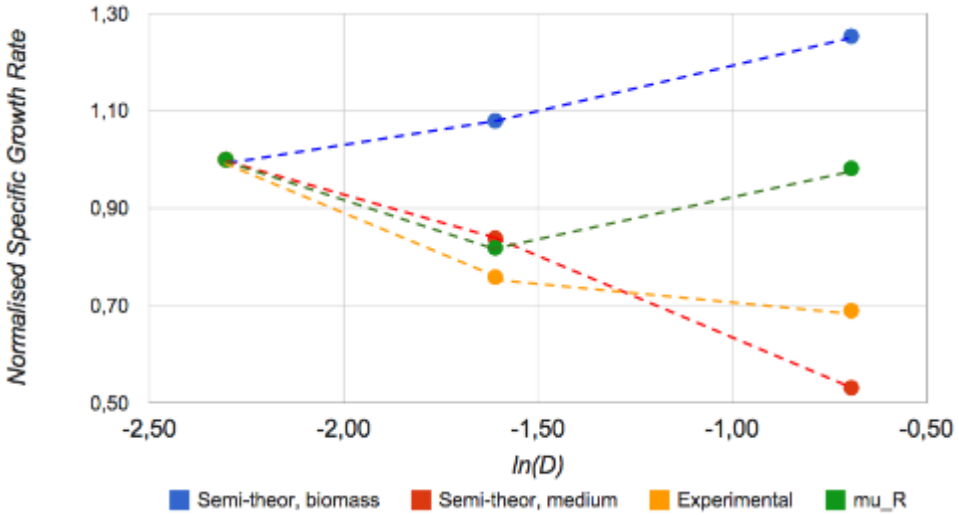

Figure 5.5.1. Illustration of the various normalised specific growth rate quantities involved in the analysis as a function of culture medium dilution. The semi-theoretical normalised growth rate has been split into the two contributions deriving from the biomass and from the medium. 'Experimental' stands for the normalised experimental value of specific growth rate.

For any non-transparent wastewater fraction, the medium offers an opacity to light transmission which depends upon its dilution (assumed with a transparent medium, as synthetic media generally are). Biomass absorbance adds up to medium absorbance to yield total absorbance which dictates the effective growth-enabling irradiance.
It is expected that a photosynthetic microalgal culture grown in a non-transparent medium, obtained by diluting it with a transparent balanced medium (i.e., the synthetic medium) grows at a slower rate. It is therefore expected that growth proceeds at a progressively reduced pace when dilution with such transparent balanced medium is reduced.

In figure 5.5.1 the two separate contributions to biomass- and medium-related absorbance effects on reducing the expected volume-averaged growth rates are shown, but their sum is not shown.
As far as the biomass contribution is concerned, the figure shows that at the lowest dilution the expected growth pace is higher than at the highest dilution; this might seem incorrect, but is justified by the fact that in the less diluted media the *experimental value* of biomass concentration is lower; being less absorbing toward light, the *calculated* growth rate is higher than the calculated value in the most diluted medium, where the experimental value of biomass concentration is higher. As far as the medium contribution to normalised specific growth rate, instead, a downward trend is obtained, as expected.
Plotting *experimental* normalised specific growth rate vs dilution, a downward trend should therefore be obtained. If the only 'interference' from the medium being diluted were on light supply (and not from nutrient carence, toxic effects, or promotion effects deriving from external substrates feeding the heterotrophic path of a mixotrophic microorganism), this downward broken line should exactly overlap with the calculated average specific growth rate as a function of dilution. Therefore, their point ratio (i.e., μ_R) would be unity. However, the two broken lines will, in general, split apart from each other, so that the point ratio will follow a non horizontal path which will suggest an interpretation on the possible role of light and nutrients/substrates on the overall microalgal growth.
Eximining the plot in figure 5.5.1 from the left to the right, it can be observed that μ_R initially decays, meaning that the *experimental* value of growth rate decays with decreasing dilution *more than it is expected from a light restriction point of view*. However, at a higher concentration in the wastewater used as the base medium, μ_R increases again, meaning that it grows *faster* than it can be expected from a light supply point of view.
In (Figure 5.5.2.) the μ_R's were calculated as a function of the dilution and were compared to the experimental values for both *Scenedesmus dimorphus* 1237 and *Arthrospira platensis*.

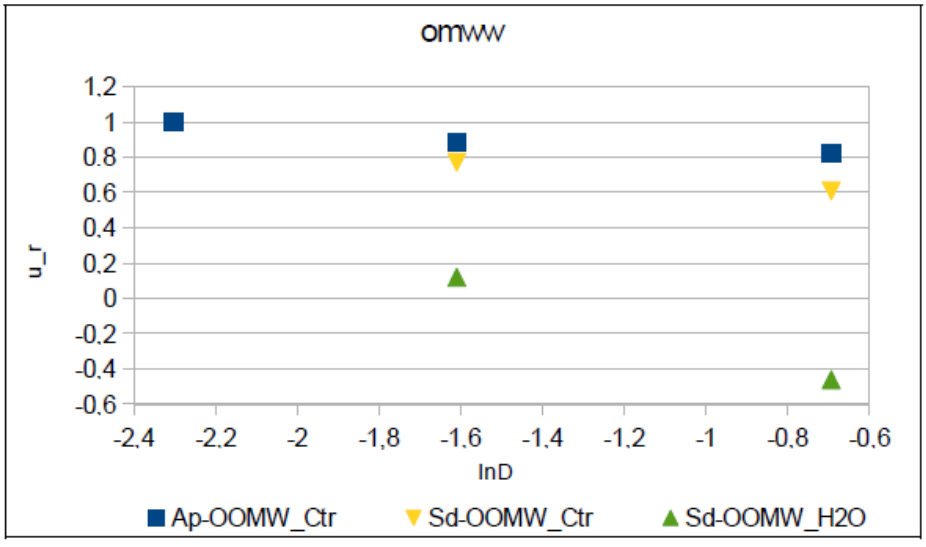

(A)

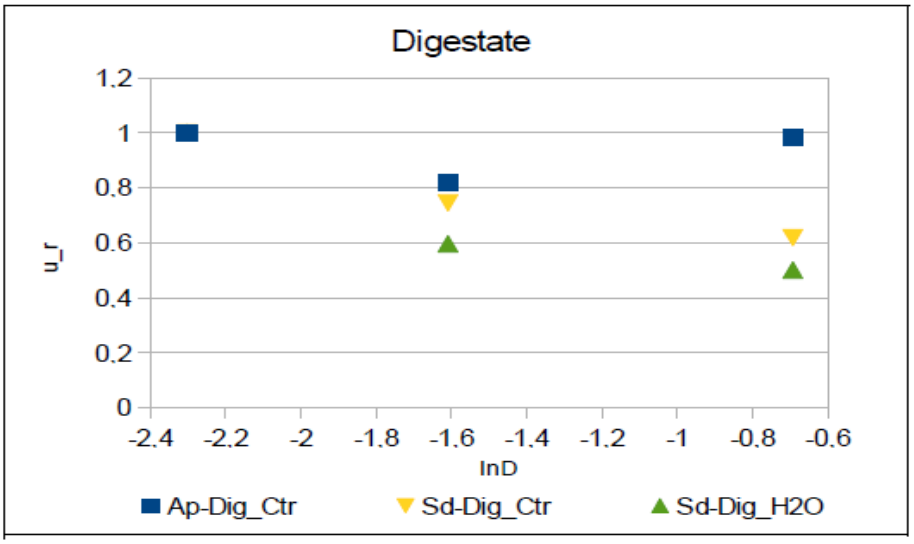

(B)

Figure 5.5.2. Normalised specific growth rates of *S. dimorphus* and *A. platensis* in balanced medium and tap water diluted with: A) OMWW; B) digestate.

The first observation comes from the two opposite trends concerning *A. platensis* cultures obtained under dilution by water. The opposite trend is actually deriving from the fact that while the culture showed a decay (negative specific growth rate) at all concentrations with OMWW-based media, it exhibited a very limited growth (positive specific growth rate) at the maximally diluted digestate-based medium, therefore leading to opposite trends for an otherwise clearly downward trend of specific growth rate in both cases. Such a case does not lend to a useful interpretation upon analysis with the presently defined parameters.

In all the other cases, the trend is regular, or exhibits slope changes that can be attached a process-relevant meaning.

All OMWW trends in figure 5.5.2 (A) are monotonically decreasing. The slope is maximum for *S. dimorphus 1237* under dilution with water, intermediate for *S. dimorphus 1237* under dilution with the control medium and minimum for *A. platensis* under dilution with the control medium. The steeper the slope, the faster the decay of the experimentally measured specific growth rate with respect to the average illumination received by the biomass, meaning that the gain from the increase of the concentration of soluble components (lower dilution) is more than offset by the lower light availability. This may happen either because the wastewater exhibits some toxicity, or because the diluent is too dilute in nutrients.

Two out of three trends digestate trends in figure 5.5.2 (B) are monotonically decreasing. The slope is higher for *S. dimorphus 1237* under dilution with water and lower for *S. dimorphus 1237* under dilution with the control medium. Actually, *A. platensis* shows an initially decreasing trend at an even lower slope, and a slope reversal, leading to a minimum. The subsequent increase of μ_R's toward the minimum dilution, that is, the maximum value of `ln(D)`, means that at increased concentration of the wastewater the specific growth rate decreases *less than it would be expected from light considerations* or, that is equivalent, that some gain can be exected by some character of the wastewater itself at that concentration.

This aspect suggest two observations, that should be taken care of separately. The former, is that at the highest concentration the biomass is actually performing (from the growth rate point of view) better, and similarly to the highest dilution, than at the intermediate concentration. Therefore, one might expect that by enhancing illumination, e.g. reducing the light path, this benefit might be fully exploited. The latter observation has to do with the way the volume-averaged specific growth rate has been calculated. Indeed, by adopting the Lambert-Beer model neglects scattering, so that the irradiance deep into the bioreactor might have been underestimated. However, from the one hand our in-situ determination of illumination at the centre of the photobioreactor do not indicate that this approach would actually be required. If a more sophisticated light model had to be implemented, the present easy tractability would be lost. Furthermore, models incorporating scattering require the knowledge of more parameters which are not very easy to determine. This complication might offset the advantages that come from the cleanliness of the mathematical analysis of specific growth rate vs dilution in the present form and that might come from its potential developments (such as the study of the shape of the function expressing the semitheoretical normalised growth rate and so on).

5.6. Fluid dynamic study of Local Recirculating PBR (LR-PBR) by particle tracking velocimetry (FT)

After carrying out and recording at fast image rate the seeded experimental runs, as described in the Materials & Methods Chapter, the collected image sequence was analysed by software to extract kinematical features and to estimate the expected process-relevant differences compared to other reactor.

Operatively, first the Feature Tracking algorithm computes the Harris matrix for each pixel of the image with a window of 3x3 pixels. The partial derivatives are calculated with a central difference scheme. Second, the matrix eigenvalues are determined. A set of eigenvalues for each pixel of the image is then produced. Those are listed for decreasing value of the second eigenvalue (λ_2) and those pixels that do not satisfy the minimum criterion for λ_2 are rejected. The threshold for λ_2 is set as a percentage of the maximum among all the minimum eigenvalues. The requirement of significant values for λ_2 strengthens the reliability of the trajectories reconstructed. To estimate the displacement vector associated to the validated feature, a window of different dimensions is introduced which is strictly related to the velocity field, i.e., the length of the window sides should be at least twice the displacement of the feature between two consecutive frames. The iterative application of the feature detection-velocity prediction procedure allows tracking the tracer particles. Fig. 5.6.1. presents a scheme of the measurement chain for a reference image.

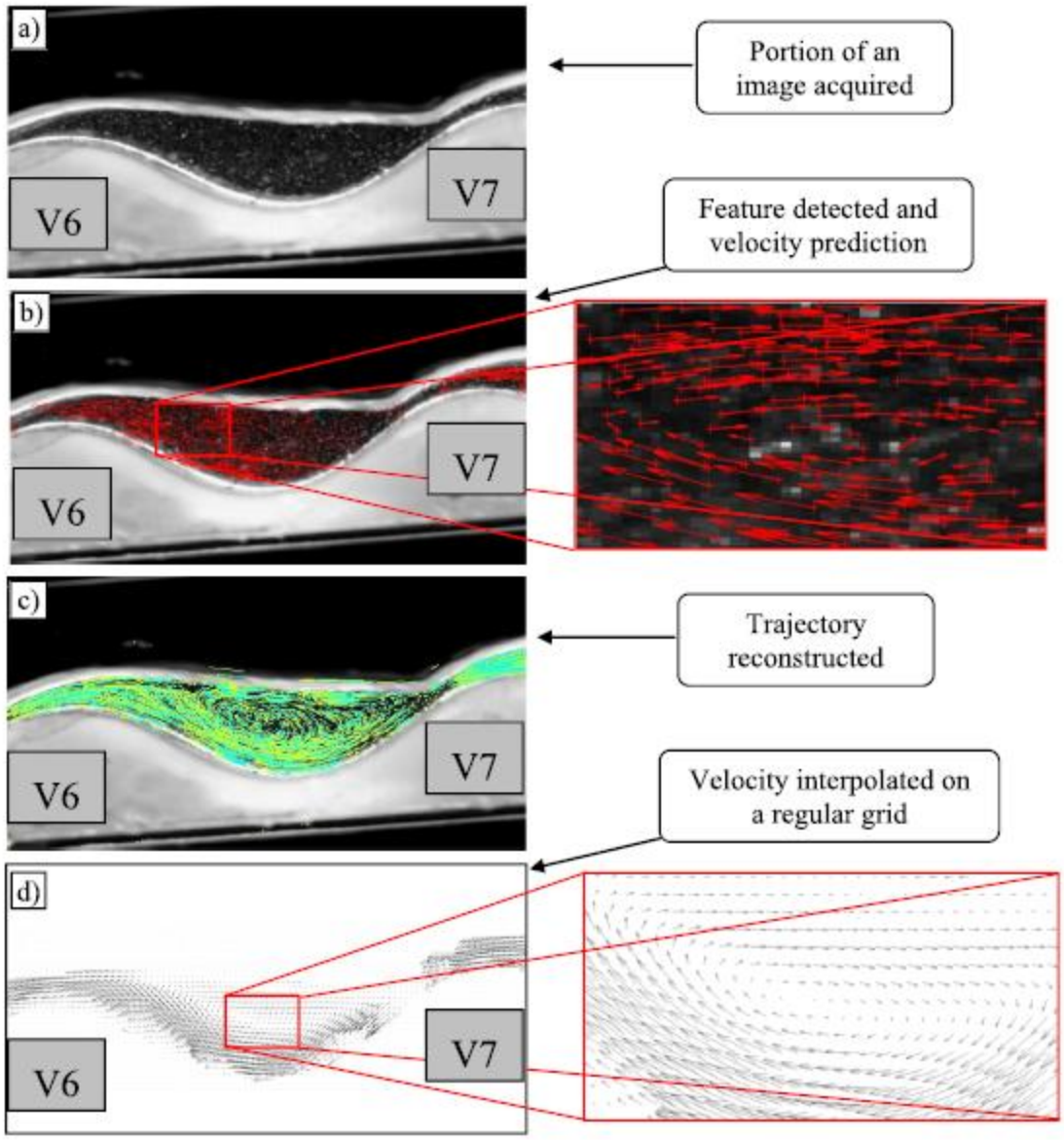

Figure 5.6.1. Scheme of the whole measurement chain used to process the raw data, from the acquired images to the velocity interpolated to a regular grid. a) Portion of an image acquired; b) Feature detected and velocity vectors; c) Samples of trajectories reconstructed by the Feature Tracking algorithm; d) Example of velocity field interpolated on a regular grid.

The interpolation step is necessary to map randomly spaced Lagrangian data onto regular grids, i.e., to compute instantaneous or time-averaged Eulerian velocity fields, to replace erroneous vectors with values computed from the neighboring vectors or to refine the original grid. A two dimensional orthogonal reference system (xez), where x is the horizontal axis (positive upslope) and z is vertical axis (positive upward), is introduced. The origin of the reference system is set in correspondence of the image left bottom corner. The mean velocity components along x and z, U and W, are evaluated in the knots of a regular grid of 60 rows and 256 columns (cell sizes of about 1x1 mm^2). An adaptive Gaussian arithmetic average method, which combines the well-

known inverse distance and the Gaussian interpolation methods, was employed. Fig. 5.6.1.d presents a snapshot of velocity vectors interpolated on the regular grid.
Table 5.6.1 shows the flow rates per unit width measured for each slope of the bottom plate and height of the tank. The last rows of the table present the average and the maximum differences of the flow rate values for the same height of the tank and different bottom plate slopes. Q1, Q2 and Q3 to indicate the tank heights and the corresponding specific flow rates.

Table 5.6.1. Specific flow rates per unit width measured for each slope and height of the tank (values in L/s/m).

Slope	Q1 (L/s/m)	Q2 (L/s/m)	Q3 (L/s/m)
0°	0.713	0.941	1.174
3°	0.715	0.943	1.167
6°	0.705	0.939	1.169
9°	0.711	0.944	1.169
Average	0.711	0.943	1.169
Maximum difference	0.006	0.004	0.005

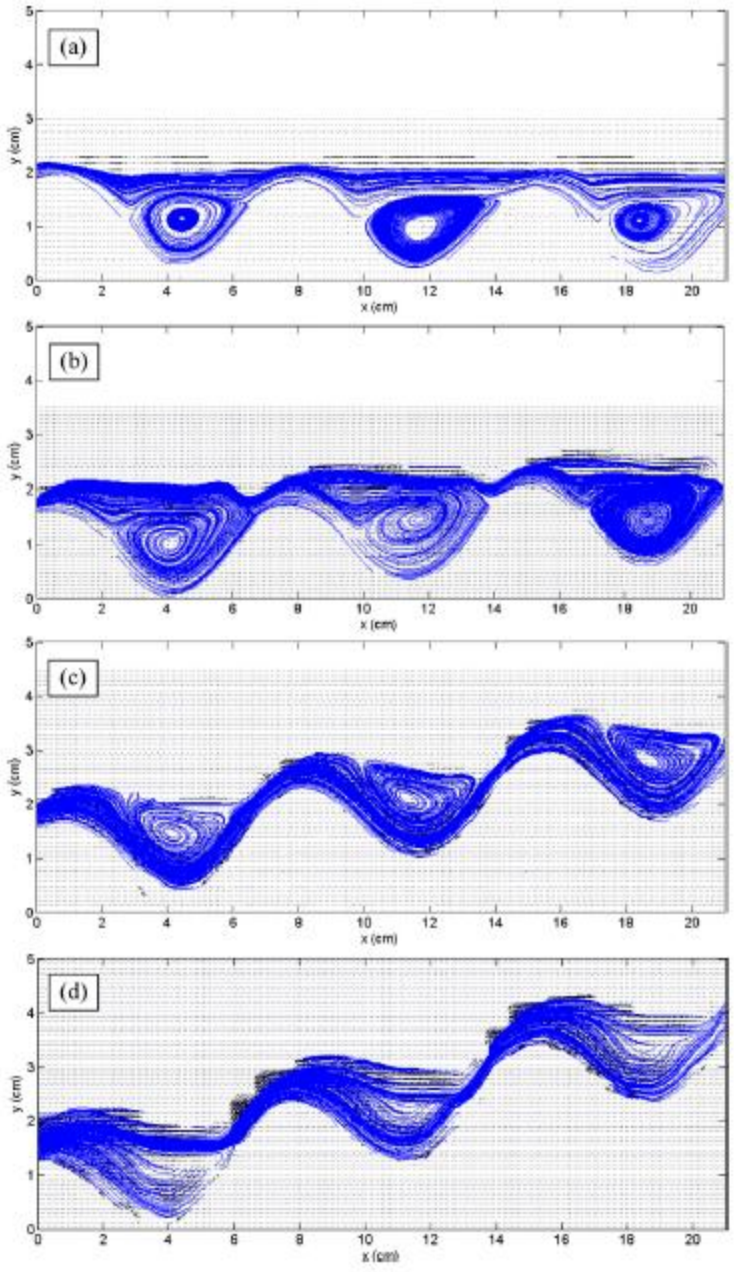

Figure 5.6.2. Flow streamlines at the maximal flow rate for slope (a) 0, (b) 3, (c) 6, (d) 9.

Fig. 5.6.2. presents the streamlines at the maximal flow rate for each tested inclination angle of the channel bottom. The streamlines allow visualizing the average characteristic arrangement of the fluid flowing through the photobioreactor, characterized by the presence of a principal stream and a recirculation area. The slope of the photobioreactor bottom plate influences the location of the recirculation region. For small slopes, i.e., 0 and 3, a thick layer of fluid flows at the free surface whereas a recirculation area is located within each vane of the channel. As a matter of facts, the upper layer reduces the amount of light effectively reaching the recirculating portion. For a slope of 6, the recirculation area moves upward while the principal stream flows at the

channel lower
boundary. In this case, microalgae entrained by both the recirculation areas and the main current undergo light/dark cycles. Finally, for the highest investigated slope, 9, though recirculation areas occasionally appear close to the free surface, on average the fluid flows through the principal transport current extending from the channel bottom to the free surface.
Fig. 5.6.3. presents a sample of the processed experimental results showing the velocity vectors overlapped with the color map of the horizontal (Fig. 5.6.3.a) and vertical (Fig. 5.6.3.b) velocity components and streamlines (Fig. 5.6.3.c), respectively, for the 6° slope and the entire set of flow rates investigated. Two regions can be easily visualized, i.e., a principal current flowing close to the channel bottom and one recirculation area in clockwise motion of increasing extent with the flow rate establishing in the vane up to the current free surface.

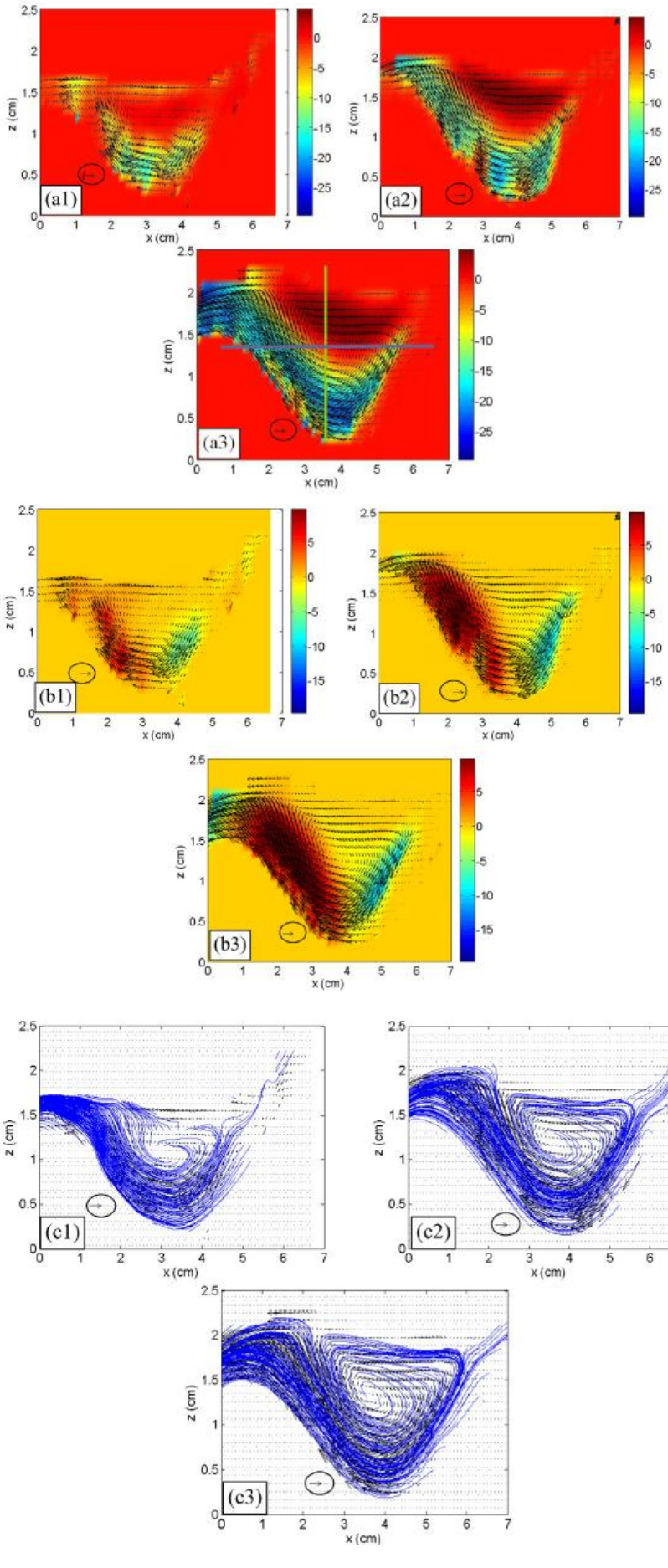
(a1)
(a2)
(a3)
(b1)
(b2)
(b3)
(c1)
(c2)
(c3)
z (cm)
x (cm)

Figure 5.6.3. Velocity vector field overlapped with (a) the color map of the horizontal velocity component; (b) the color map of the vertical velocity component; (c) the flow streamlines. The lines in a3 indicate the profiles passing through the center of the vortex.

After determining the velocity field, all the potential sources of high frequency light/dark alternation within the vanes of the photobioreactor exposed to sunlight were spotted and analysed by using the velocity fields themselves. Two major sources were identified:
1. the recirculatory area, where a significant portion of the entrapped liquid circulates (theoretically, all but the stationary center) and is exposed to different illumination intensity due to Lambert Beer intensity reduction as a function of depth in the liquid;
2. the liquid stream flowing close to the wavy bottom, i.e., again, alternatively, close to the liquid surface or below a thick liquid layer and, therefore, exposed at varying illumination regimens.
For the recirculatory area, the recirculation time was determined. For this purpose, by following the vertical line passing through the center of the vortex, a velocity profile was created (see Fig. 5.6.3.(a3) for the location of the line) beginning from the top surface of the liquid down to the vane bottom.
For the 6 slope and Q3, Fig. 5.6.4.a presents three profiles of the horizontal component of the velocity field drawn through vanes V5, V6 and V7.

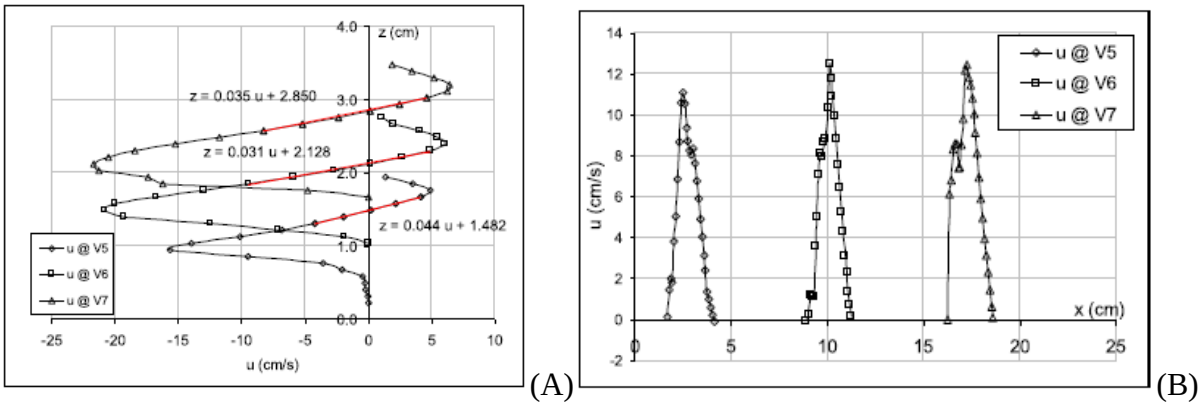

(A) (B)

Figure 5.6.4. e (a) Vertical and (b) horizontal sectional views of the velocity field for all points along the vertical and horizontal profiles drawn through the vortex center in Fig. 5.6.3. a3 and the maximal velocity.

A positive value of velocity in the plots indicates that the local velocity is oriented upstream, a negative value means that the velocity vector is oriented downstream. The three profiles show the consistence of the shapes of the velocity absolute values among the three vanes. The three profiles exhibit a vertical displacement with respect to each other in the plot, which is due to the different elevation of the three vanes, in turn consequent to the inclination of the wavy bottom.
Each profile starts at the liquid air interface with a positive velocity. First velocity increases with increasing depth, determining a velocity difference higher than expected, and then decreases down to the center of the vortex, where it becomes null. The velocity profile then increases in the negative direction up to an absolute value which is higher than the maximum in the positive

direction. This region is relevant to the stream flowing next to the bottom of the channel and does not recirculate but, rather, flows directly to the next vane by overpassing the curved weir.
Within each plot, a reasonably linear zone can be noted (marked in red along each curved profile), which indicates that the gradient is constant within a relatively ample zone; this both the vertical and horizontal directions; therefore three zeros are required to brace the vortex characteristic sizes.
Table 5.6.2. shows the recirculation times and horizontal and vertical sizes of the recirculation regions corresponding to different slopes and flow rates. The recirculation time gradually decreases for increasing flow rate and decreasing slope of the bottom surface.

Table 5.6.2. Sizes of the vortex streams and local recirculation time in the three tested flow rate conditions.

Q (L/s/m)	Recirculation time (s)	Vertical size (cm)	Horizontal size (cm)
Slope 6			
0.943	0.324	1.250	4.225
0.711	0.331	0.355	3.722
Slope 3			
1.169	0.422	1.979	5.036
0.943	0.494	1.909	3.938
0.711	0.571	1.723	3.791
Slope 0			
1.169	0.589	1.889	3.777
0.943	0.604	1.818	3.485
0.711	0.857	1.911	3.184

A comparison based on the average local recirculating liquid speed (which defines the fast light-darkness alternation frequency) and fraction of photobioreactor exposed to light (which defines the fast light-darkness alternation duty-cycle) was carried out. Two different photobioreactor types were selected for comparison: bubble columns (BC PBR) and circulated tubular photobioreactors (PBR). Our reference equivalence criterion was equal fraction of the high frequency light cycle time that cells spend exposed to high light, according to the definition by Brindley et al. (2011), that is, also, equal average irradiance inside the photobioreactor volume. This position defines the equivalence of continuously, and even randomly, varying local irradiation to regular, under a rectangular-shape applied irradiation of such duty-cycle. At a frequency higher than 1 Hz Brindley et al. (2011) showed that not only equivalence can be approached, but higher photosynthetic efficiency than that warranted by complete light integration (as defined by Terry, 1986) can be observed. Irradiance decay was approximated by the Lambert Beer law. For cylindrical photobioreactors, a light distribution inside the tube volume equivalent to the simplified light distribution model published by Molina Grima et al. (2000) was obtained. The reference adopted suspension biomass load was such that absorbance

at 690 nm is 3.0, corresponding to 2 g/L of microalgae (depending on the species and the physiologic condition of the culture) Average irradiance was numerically calculated in each geometry over 100 sub-intervals of the main size coordinate of each photobioreactor geometry (that is, the distance between two crests for the local recirculation (LR) PBR, and the diameter for the cylindrical geometries). For the local recirculation photobioreactor, a duty cycle of 0.23 was calculated. For the two cylindrical geometries an equal average internal irradiance was imposed and an equivalent (based on the above criterion) diameter was calculated, equal to 1.75 cm. While this diameter is unpractical for bubble column units, which should observe a reasonable aspect ratio (that is, length to diameter ratio), here it will be adopted anyway for the sake of the comparison. The average circulation velocity (m/s) in a bubble column photobioreactor, vlc, was estimated along with Joshi (1980):

$$v_{lc} = 1.31 \cdot \left[g \cdot D \cdot \left(v_{gs} - \varepsilon_g \cdot v_{bs} \right) \right]^{1/3} \qquad (1)$$

where D is the diameter of PBR (m), g is the gravity acceleration (m/s^2), εg is the fractional gas holdup calculated according to Chisti (1989):

$$\varepsilon_g = 2.47 \cdot v_{gs}^{0.97} \qquad (2)$$

and the slip velocity of gas bubbles, vbs (m/s), was set equal to the stationary rise velocity (Heijnen and Van't Riet, 1984):

$$v_{bs} = 0.25 \qquad (3)$$

The circulation time, tc (s), was calculated as:

$$t_c = \frac{2 \cdot D}{v_{lc}} \qquad (4)$$

considering that the circulation cell length is about twice the pipe diameter. The average circulation velocity in a tubular photobioreactor, vlc (m/s), according to Davies (1972) is:

$$v_{lc} = 0.2 \cdot \left(\frac{v_L^7 \cdot \mu}{2 \cdot R \cdot \rho} \right)^{1/8} \qquad (5)$$

where is the velocity of liquid in the reactor (m/s), m is the viscosity, R is the tube radius (m), r is the density (kg/m3). The circulation time has calculated as:

$$t_c = \frac{D}{v_{lc}} \qquad (6)$$

At an air insufflation rate of 1 vvm (gas Volume liquid Volume minute) for the bubble column

this latter features a fast light:dark alternation frequency of 1.63 Hz. Adopting an average liquid velocity of 0.5 m/s in the circulated tubular photobioreactor, a fast light:dark alternation frequency of 1.60 Hz can be calculated. This compares to 4.35 Hz found for the main locally recirculating volume in the LR PBR. The 1:2 light to darkness duty cycle relationship published by Grobbelaar (2006) was adopted:

$$PA = -22.5 \cdot \ln(\tau) + 263.5 \qquad (7)$$

where PA is photosynthetic activity (mmol O_2/ mg Chl a*h) and t is the light/dark alternation time. Photosynthetic activity was averaged over the vane surface by taking into account the separate contribution of the vorticose and the non-vorticose zone. Given the linear dependence of growth rate on photosynthetic activity when no other factor is limiting growth itself (e.g. CO_2 and nutrients supply, O_2 expulsion etc), the obtained increases in PA have the meaning of increases in photobioreactor productivity.
Calculated values were reported in Table 5.6.3; performing the calculations for the three geometries, it is easily seen that one may expect from the LR PBR installed at 6 inclination and operated at 600 L/h performance gains in the order of 13% over the bubble column and circulated tubular photobioreactors. It should be noted, also, that these gains only refer to the intrinsic photosynthetic efficiency. Other performance gains over each of the two considered PBR geometries may come from minimization of oxygen concentration buildup (with respect to circulated tubular photobioreactors) and conserved photic volume ratio (with respect to full scale bubble column photobioreactors with an acceptable aspect ratio).

Table 5.6.3. Photosynthesis activity comparison among Tubular PhotoBioReactor (TPBR), Bubble column PhotoBioReactor (BCPBR) and Local Recirculating PhotoBioReactor (LPBR).

Wavy bottom channel inclination (°)		PBR		Light/dark alternation time	
		Tubular PhotoBioReactor (TPBR)		119	ms
		Bubble column PhotoBioReactor (BCPBR)		123	ms
		Flow rate (L/s/m)			
		0.711 (Q1)	0.943 (Q2)	1.109 (Q3)	Unit
0	V vortex	19.1	19.9	22.4	cm^3/cm
	V layer	3.2	3.9	4.0	cm^3/cm
	Locally recirculating volume fraction	86	84	85	%
	Non-locally recirculating volume fraction	14	16	15	%
	Vortex frequency	1.17	1.66	1.70	Hz
	Layer frequency	10.00	10.00	10.00	Hz
	PA vortex	112	119	120	mmol O_2/g Chl a*h
	PA layer	160	160	160	mmol O_2/g Chl a*h
	PA average	118	126	126	mmol O_2/g Chl a*h
	PA (LRPBR) vs PA (BCPBR)	96	102	102	%
	PA (LRPBR) vs PA (TPBR)	96	102	102	%
3	V vortex	20.5	23.6	31.3	cm^3/cm
	V layer	2.1	3.1	3.6	cm^3/cm
	Locally recirculating volume fraction	91	88	90	%
	Non-locally recirculating volume fraction	9	12	10	%
	Vortex frequency	1.75	2.02	2.37	Hz
	Layer frequency	10.00	10.00	10.00	Hz
	PA vortex	121	124	127	mmol O_2/g Chl a*h
	PA layer	160	160	160	mmol O_2/g Chl a*h
	PA average	124	128	131	mmol O_2/g Chl a*h
	PA (LRPBR) vs PA (BCPBR)	101	104	106	%
	PA (LRPBR) vs PA (TPBR)	101	104	106	%
6	V vortex	4.1	16.6	20.1	cm^3/cm
	V layer	4.2	4.0	4.4	cm^3/cm
	Locally recirculating volume fraction	50%	81%	82%	%
	Non-locally recirculating volume fraction	50%	19%	18%	%
	Vortex frequency	3.02	3.09	4.35	Hz
	Layer frequency	1.57	2.16	2.43	Hz
	PA vortex	133	133	141	mmol O_2/g Chl a*h
	PA layer	118	125	128	mmol O_2/g Chl a*h
	PA average	126	132	139	mmol O_2/g Chl a*h
	PA (LRPBR) vs PA (BCPBR)	102	107	113	%
	PA (LRPBR) vs PA (TPBR)	102	107	113	%

5.7. Microalgal growth tests in the Local Recirculation PhotoBioreactor (LR-PBR)

LRPBR described in materials and methods was installed on the roof of the Dept. building and was tested with both the species (*A. platensis, S. dimorphus*).

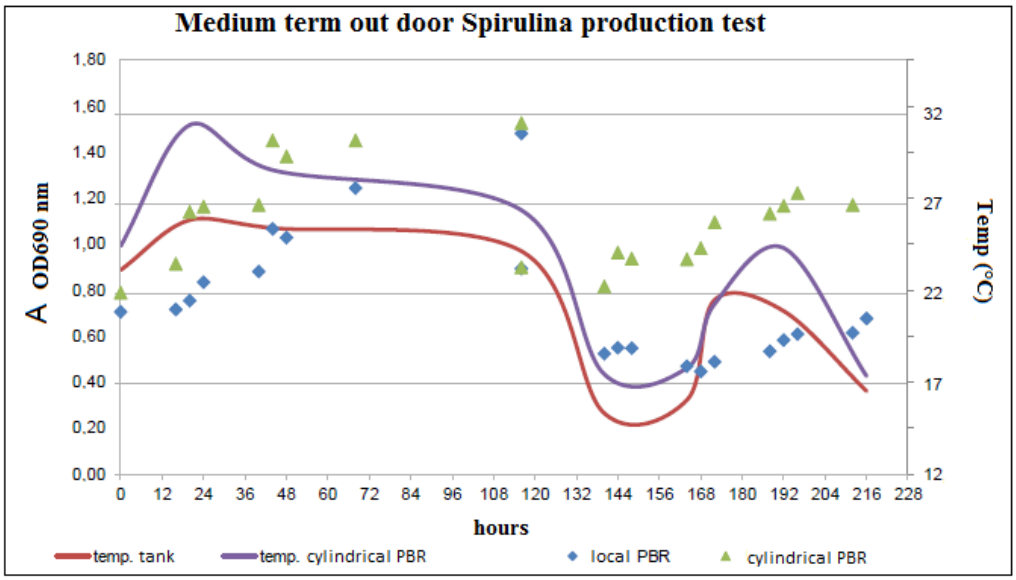

(A)

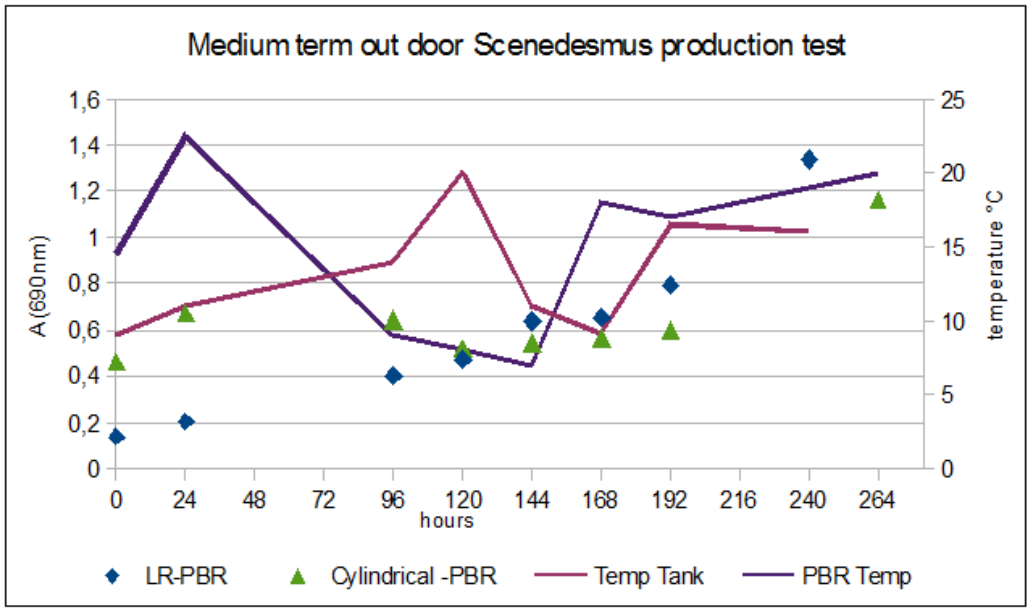

(B)

Figure 5.7.1. Microalgal growth and temperatures relative at two photobioreactors: cylindrical and local recirculation; (A*) A. platens*is run test. *B) S.d.123*7 run test.

The outdoor growth test of *Spirulina* was carried out between the end of September to mid-October, while the growth test of *S.d.12*37 was carried out in March. The cultures were initially grown in a 15-cm diameter cylindrical photobioreactor (bubble column, hereinafter denoted as TPBR) in the laboratory growth chamber at a temperature ranging from 24-28 °C, and under controlled artificial illumination. Then, the cylindrical PBR itself was moved to the building roof for culture acclimation, as described in Materials & Methods Chapter.

In Figure 5.7.1. (A) Spirulina growth curves, both in LR-PBR and T-PBR, the temperatures in PBRs are shown; initially we have an increment of the biomass owing to to the constant and

fairly favourable temperatures, approximately 26 °C. After a few days from the onset of the culture, a repentine drop of external temperature caused a collapse of growth rate (Table 5.7.1.). Temperature is among the major factors controlling the multiplication of Spirulina (Oliveira et al. 1999); optimum temperature for Spirulina growth lies in the range of 30 to 35 °C, temperatures frequently encountered in North and Northeast regions of Brazil. These tropical lands are affected by the Atlantic coast and the Equatorial region, resulting in a humid climate with favourable conditions of temperature and light exposure time, for algal cultivation throughout the year. These climatic conditions particularly favour the commonly practised outdoor industrial algal production. Therefore, geographical regions where winter temperatures will be below 15 °C are unsuitable for Spirulina growth (Richmond et al. 1990).

Table 5.7.1. *A. platensis* and *S. dimorphus 1237* growth rates and biomass productivities.

Species	μ(d^{-1})	Temp. °C	Biomass productivity outdoor (g/L d)	Biomass productivity (ton/ha y)
A.platensis	0.19	25	0.23	16
	0.11	19	0.14	10
S.d.1237	0.17	15	0.24	17

Oliveira et al. (1999) studied *A. platensis* growth in the range of 15 to 20 °C; they observed that microalgal growth increased with temperature and a great reduction of metabolic activity occurred for temperatures below 17 °C. Also, at temperatures of 15 and 45 °C, the absence of growth was associated with the disappearance of green pigmentation. In Table 5.8.1. biomass productivities are listed; for *A. platensis* there are two different specific growth rates, corresponding to the two different average temperature ranges prevailing during the initial and the final part of the test, respectively. At temperature of 19°C *A. platensis* demonstrated to be able to survive and to restart growth when the temperature rises again; it can be argued that this ability is due to acclimatization of the culture at external environmental conditions before to be inculated in the LR-PBR. Biomass productivity in the first part of the test, when temperature was 25 °C, is 16 t/ha y (Table 5.7.1) corresponding to 4.5 g/m^2 d and at 19 °C is 10 t/ha y (2.8 g/m^2 d) ; in open pond system maximal productivity obtained is 26 g/m^2 d (Spring-Summer seasons) while in Fall-Winter (covering the pond) is 13 g/m^2 d (Richmond et al. 1990). In *S. dimorphus 1237* growth test it is possible to see (Fig. x.7.1.B) how the biomass responds to a temperature shock by slowing its growth that has not an exponential profile but follows a linear trend; *Scenedesmus sp.* is a microalga that naturally grows in continental climate, it is able to grow in a wide range of temperatures, from 10°C (*S. sp.* LX1, Xin et al. 2011) to 30°C; above 30 °C its growth is inhibited (Martinez et al. 1999). Biomass productivity at 15 °C is 17 ton/ha y (Table 5.7.1) corresponding to 4.7 g/m^2 d; in an inclined surface open PBR at the maximal productivity obtained is 26 g/m^2 d in spring (Tredici et al. 1992). These low growth rates and productivities showed some criticities of the current implementation of the local recirculation photobioreactor that were detrimental during the low outdoor temperature significant heat transfer and high evaporation rate (from its openness), need of further reducing holdup volumes held in dark conditions to fully exploit the flash effect.

6. Conclusions

The present thesis work dealt with the evaluation of the potential for exploitation of olive oil mill wastewaters and anaerobic digestates in supporting microalgal growth for the production of biomass, biocommodities, biofuels, and for bioremediation. Furthermore, a novel photobioreactor aiming at pushing microalgae photosynthetic efficiency closer to its theoretical limits was characterised. The largest part of the thesis work is experimental, but the overall work carried out includes a non negligible part of data analysis and post-processing in both the aspects which have been dealt with.

As far as the exploitation of wastewaters in supporting microalgal growth is concerned, *S. dimorphus 1237* and *A. platensis* specific growth rates in their standard media aerated with air and air enriched in CO_2 5% v/v were characterized. For both *S. dimorphus 1237* and *A. platensis* the promotion of specific growth rate which can be obtained by supplementing the insufflated air with CO_2 was evaluated and was found to be 35% and 22%, respectively.

S.dimorphus 1237 is an oleaginous microalga, capable of producing lipids in nitrogen limitation; aiming at understanding the growth trends in response to the culturing conditions, a set of diverse nitrate and phosphate concentrations, corresponding to different ratios of these two species, were tested. The best specific growth rate result was obtained when the nitrate/phosphate ratio was 20:1, with a growth promotion of 14% respect to the control culture. In medium with nitrate and phosphate decrease of ten fold in concentration respect to control, but ratio 5:1 nitrate:phosphate, the growth rate decrease of 19%.

The microalga *S. dimorphus* and the cyanobacterium *A. platensis* are able to grow in downstream processing fractions of olive wastewater.

The use of pre-treated OMWW and its fractions as media, gave best results with *S. dimorphus* 1237, where the growth rate maintained at a fairly high value (0.39 d^{-1}) in fairly concentrated nanofiltration retentate (diluted 1:1 in synthetic medium). *A. platensis* showed a major sensibility to the medium and, while the best growth rate obtained (again, in equally diluted nanofiltration concentrate) was even higher (0.47 d^{-1}), biomass productivity was found to be ten fold lower than in the control (best case). Microalga *S. dimorphus 1237* productivity was much lower than that of the control culture as well (one fourth; best case). The reduction of productivity, given that the best case specific growth rate undergoes a much smaller reduction, can be identified in the lower (average) biomass density of the culture. Physiological stresses induced by ions, such as sodium, and oxidant molecules, such as polyphenols may likely team with reduced light curtailing specific growth rate (and productivity). It is unlikely that productivity might be enhanced by increasing the biomass load within the culture, because the scarce penetration of light in photobioreactors of usual thickness (some centimeters) would further reduce light availability and measured growth rate. In the OMWW nanofiltration concentrate, where phenol and polyphenols concentrations are low, both species grow better than in (pretreated) OMWW,

producing carbohydrates and proteins in a balanced way. OMWW ultrafiltration concentrate showed marked toxic effects, due to high polyphenol and phenol levels.
Testing optically thick wastewaters as a substitute medium for the growth of microalgae generally shows some impairment with respect to a balanced culture in a transparent medium. This work showed that by taking into account the lower light availability, the variation of the growth rate at different dilution ratios could offer some insight as to the reasons (carence/toxicity) for such reduction, signal productivity gains opportunities and suggest the geometry to adopt to exploit it.
Preliminary growth tests in the liquid fraction of an anaerobic digestate mixed with synthetic media were carried out; both the adopted species are able to growth in digestate diluted 1:1 with (species-specific) synthetic medium, showing a specific growth rate reduction of 30% for *S. dimorphus 1237*, and 66% for *A. platensis*.
During the growth runs in all wastewaters, dissolved nitrogen, phosphorous (organic also) and carbonaceous substrates are reduced, both organic and inorganic mechanisms, thereby contributing to wastewater remediation.
The cyanobacterium *A. platensis* produces the C-phycocyanin (C-PC) protein, with vast applications (natural food colorant in food industries and in cosmetic industries and beyond, due to its antioxidant, anti-inflammatory and neuroprotective properties). In nanofiltration concentrate diluted 1:1 with synthetic medium C-phycocyanin productivity was reduced to one tenth of that in standard conditions (best case). Low illumination and nitrogen concentration limit the C-phycocyanin production.
The microalga S. *dimorphus* 1237 is an oleaginous species, able to produce lipids which are suitable for biodiesel production; in digestate diluted 1:1 with synthetic medium *S. dimorphus* 1237 produces 47% (d.w.) of lipids, corresponding to a productivity of 0.10 g/L d; however biomass productivity is to one fourth of the control value.
Results obtained in limiting light regime stimulate to verify the potential biomasses ability to grow in wastewaters, using thin layer photobioreactors, after adaptation time in the wastewaters media.

A novel geometry of photobioreactor was investigated in two phases:

- ➢ an experimental fluid-dynamic study to permittee to determine the detailed liquid flows and showed that a significant portion of the liquid volume recirculates.
- ➢ experimental growth tests were carried out on this photobioreactor with living cultures.

In the first part of the study, several experimental conditions were tested, varying the slope of the reactor bottom and the flow rate through the apparatus (the maximum flow rate being capped by a limit of the available detection equipment and being lower than the flow rate that can be experimentally used). Flow at 0 and 3 inclination features a bottom vortex and an upper relatively undisturbed layer; flow at 6 features an upper vortex and a liquid layer following the bottom of the PBR surface. The size of vorticose volume, the recirculation and the straight flow characteristic times in each vane were identified by software analysis. At the maximum tested

flow rate, the local recirculation period inside the vanes was measured to be shorter than 250 ms. The photosynthetic activity expected from a biomass growing in such fast light-dark alternation frequency was estimated by resorting to interpolating functions available in the open literature (Grobbelaar, several titles) and derived from an ample experimentation. The photosynthetic activity increase that can be expected from the "flash effect", was estimated to range between 2 and 13% with respect to tubular and bubble column PBRs operating at an equivalent L:D ratio.

In the second part of this study the LR-PBR was installed on the roof at an angle of 6 degrees and a liquid flow rate of 1100 L/h. Two different growth rates were obtained for *A. platensis*, corresponding to two different temperature ranges (consequent to a repentine meteorological change): 0.19 d^{-1} (at 25 °C) and 0.11 d^{-1} (at 19 °C). In the *S. dimorphus 1237* growth study, 0.17 d^{-1} was obtained (at 19°C). The calculated biomasses productivities are: for *A. platensis*, at the temperature of 25 °C, productivity was 16 ton/ha y; at 19 °C it was 10 ton/ha y. In *S. dimorphus 1237* the productivity a 15°C was 17 ton/ha y.

These low growth rates and productivities showed some criticities of the current implementation of the local recirculation photobioreactor: significant heat transfer and high evaporation rate (from its openness), need of further reducing holdup volumes held in dark conditions to fully exploit the flash effect.

7. References

Abeliovich A., Azov Y. (1979). Toxicity of ammonia to algae in sewage oxidation ponds. Appl. Environ. Microbiol. 31: 801-806.

Acie´n Ferna´ndez, F.G., Ferna´ndez Sevilla, J.M., Molina Grima, E.,2013. Photobioreactors for the production of microalgae. Rev. Environ. Sci. Bi/Technol. 12: 131-151.

Becker E.W., Venkataraman L.V. (1982). Biotechnology and Exploitation of Algae: The Indian Approach, Deutsche Gesellschaft für Technische Zusammenarbeit (GTZ), Germany

Belay A. (2008). Spirulina (Arthrospira): production and quality assurance. In: Gershwin ME and Belay A (eds) Spirulina in human nutrition and health. pp1-25, CRC Press Taylor & Francis group, London, UK, pp.312.

Belay A. (2009). Spirulina (*Arthrospira*): Potential as an Aqua Feed. Algae Biomass Summit. October 7--9, 2009.

Belkin S., Boussiba S. (1991). Resistance of Spirulina platensis to Ammonia at High pH Values. Plant Cell Physiol. 32, 7: 953-958.

Ben-Amoz A., Avron M. (1983). On the factors which determine massive beta-carotene accumulation in the halotolerant alga Dunaliella bardawil. Plant Physiol 72: 593-597.

Bennett A., Bogorad L. (1973). Complementary chromatic adaptation in a filamentous blue-green alga. J. Cell Biol, 58: 419-435.

Berland B.R., Bonin D.J., Cornu A.L. (1972). The antibacterial substances of the marine alga Stichochrysis immobilis (Chrysophyta). J. Phycol. 8: 383-392.

Bjornsson W.J., Nicol R.W., Dickinson K.E., McGinn P.J. (2013). Anaerobic digestates are useful nutrient sources for microalgae cultivation: functional coupling of energy and biomass production. Journal of Applied Phycology, 25:1523–1528.

Bonjouklian R., Smitka T.A., Doolin L.E., Molloy R.M., Debono M., Shaffer S.A., Moore R.E., Stewart J.B., Patterson G.M.L. (1991). Tjipanazoles, new antifungal agents from the blue-green alga Tolypothrix tjipanasensis. Tetrahedron 47: 7739-7750.

Boussiba S. (1989). Ammonia uptake in the alkalophilic cyanobacterium Spirulina platensis. Plant Cell Physiol. 30: 303-308.

Boussiba S., Affalo C. (2005). An insight into the future of microalgal biotechnology. Innovations in Food Tehnology (www.innovfoodtech.com).

Bozarth A., Maier U. G., Zauner S. (2009). Diatoms in biotechnology: modern tools and applications. *Applied Microbiology and Biotechnology, 82*(2), 195-201.

Bravi M., Cicci A., Torzillo G. 2012. Quality Preservation and Cost Effectiveness in the Extraction of Nutraceutically-Relevant Fractions from Microbial and Vegetal Matrices. In *Scientific, Health Social Aspects of the Food Industry*, Edited by: Valdez, B., Schorr, M. and Zlatev, R. 463–488. Rijeka, , Croatia: InTech.

Brindley C., Acie´n Ferna´ndez F.G., Ferna´ndez-Sevilla J.M. (2011). Analysis of light regime in continuous light distributions in photobioreactors. Bioresour. Technol. 102: 3138-3148.

Brouers M., Hall D.O. (1986). Ammonia and hydrogen production by immobilized cyanobacteria. J Biotechnol 3, 307–321.

Carvalho A.P., Meireles A.L., Xavier Malcata F.. (2006). Microalgal reactors: a review of enclosed system designs and performances. Escola Superior de Biotecnologia, Universidade Catòlica Portuguesa, Porto.

Chisti, M.Y. (1989). Airlift Bioreactors. Elsevier, London, p. 339

Chisti Y. (2007). Biodiesel from microalgae. *Biotechnol Adv, 25: 294–306*.

Chisti Y. (2013). Constraints to commercialization of algal fuels. Journal of Biotechnology, 167, 3, 10: 201–214.

Chiu R.J., Liu H.I., Chen C.C., Chi Y.C., Shao H., Soong P., Hao P.L.C. (1980).The cultivation of Spirulina platensis on fermented swine manure. In CHANG PO (Ed.) Animal Wastes Treatment and Utilization, Proc. Int. Symp. on Biogas, Microalgae and Livestock, Taiwan, p. 435.

Chiu S. Y., Tsai M. T., Kao C. Y., Ong S. C., Lin C. S. (2009). The air-lift photobioreactors with flow patterning for high-density cultures of microalgae and carbon dioxide removal. *Engineering in Life Sciences*, *9*(3), 254-260.

Christenson L., Sims R. (2011). Production and harvesting of microalgae for wastewater treatment, biofuels, and bioproducts. Biotechnology Advances, 29: 686–702

Cicci A., Stoller M., Bravi M. (2013). Microalgal biomass production by using ultra- and nanofiltration membrane fractions of olive mill wastewater. Water Research, 47: 4710-4718.

Cicci A., Bravi M. (2014). Production of the freshwater microalgae *Scenedesmus dimorphus* and *Arthrospira platensis* by using cattle digestate. Chemical Engineering Transactions, 38: xxx-xxx.

Cornet J.F., Dussap C.G., Gros J.B., Binois C., Lasseur C. (1995). A simplified monodimensional approach for modeling coupling between radiant light transfer and growth kinetics in photobioreactors. Chem Eng Sci 50, 9: 1489−1500.

Cornet J.F., Dussap C.G., Gros J.B.(1998). Kinetics and energetics of photosynthetic micro-organisms in photobioreactors. Advances in Biochemical Engineering Biotechnology, 59:155–224.

Correll DL. (1998). Role of phosphorus in the eutrophication of receiving waters: a review. J Environ Qual, 27:261–6

Davies J.T. (1972). Turbulence Phenomena: an Introduction to the Eddy Transfer of Momentum, Mass and Heat, Particularly Interfaces. Academic Press, New York, p. 412.

De Cano M.M.S., De Mule M.C.Z., De Calre G.Z., De Halperin D.R. (1990). Inhibition of Candida albicans and Staphylococcus aureus by phenolic compounds from the terrestrial cyanobacterium Nostoc muscorum. J. appl. Phycol. 2: 79-81.

Doucha J., Straka F., Lıvansky K. (2005). Utilization of flue gas for cultivation of microalgae (*Chlorella* sp.) in an outdoor open thin-layer photobioreactor. *Journal of Applied Phycology* 17: 403–412.

Doucha J., Livansky K. (2009). Outdoor open thin-layer microalgal photobioreactor: potential productivity. *Journal of Applied Phycology*, 21, 1: 111-117.

Dubois M., Gilles K. A. , Hamilton J. K., Rebers P. A., Smith F. (1956). Colorimetric Method for Determination of Sugars and Related Substances. Anal. Chem., *28*, 3: 350–356.

Duff D.C.B., Bruce D.L., Antia N.J. (1966). The antibacterial activity of marine planktonic algae. Can. J. Microbiol. 12: 877-884.

Eriksen N. T. (2008). The technology of microalgal culturing. *Biotechnology Letters, 30*(9): 1525-1536.

Evens T. J., Chapman D. J., Robbins R. A., D'Asaro E. A. (2000). An analytical flat-plate photobioreactor with a spectrally attenuated light source for the incubation of phytoplankton under dynamic light regimes. *Hydrobiol*ogia, 434(1-3): 55-62.

Felder C.B., Pulluoglu M.A., Parker N.C. (1993). Integrating livestock waste recycling with production of microalgae. In Techniques for Modern Aquaculture, American Society of Agricultural Engineers, Publication 02–93.

Friedrickson A.G., Tsuchiya H.M. (1970). Utilization of the effects of intermittent illumination on photosynthetic microorganisms. In: Prediction and Measurement of Photosynthetic Productivity. Wageningen Centre for Agricultural Publishing and Documentation: 519-541.

Gouveia L., Oliveira A. C. (2009). Microalgae as a raw material for biofuels production. *Journal of Industrial Microbiology & Biotechnology*, *36*(2): 269-274.

Graham L.E., Graham J., Graham J.M., Wilcox L.W. (2009). Algae. Benjamin Cummings.

Greque de Morais M., Vieira Costa A., (2007). Biofixation of carbon dioxide by *Spirulina* sp. and *Scenedesmus obliquus* cultivated in a three-stage serial tubular photobioreactor. *Journal of Biotechnolog,y* 129: 439–445.

Grobbelaar J.U. (2006). Photosynthetic response and acclimation of microalgae to light fluctuations. In: Subba-Rao, D.V. (Ed.), Algal Cultures Analogues of Blooms and Applications. Science Publishers, Enfield, N.H., USA: 671-683.

Grzanna R., Polotsky A., Phan P.V., Pugh N., Pasco D., Frondoza C.G.(2006). Immolina, a High–Molecular-Weight Polysaccharide Fraction of Spirulina, Enhances Chemokine Expression in Human Monocytic THP-1 Cells. J.l of Alternative and Complementary Medicine.12(5): 429-435

Guschina I. A., Harwood J. L. (2006). Lipids and lipid metabolism in eukaryotic algae. Progress in Lipid Research, 45: 160–186.

Harun R., Singh M ., Forde G.M. and Danquah M. K. (2010). Bioprocess engineering of microalgae to produce a variety of consumer products. Renewable and Sustainable Energy Reviews 14:1037–1047.

Heijnen J.J., Van't Riet K., (1984). Mass transfer, mixing and heat transfer phenomena in low viscosity bubble column reactors. Chem. Eng. J. 28: 21-42.

Issarapayup K., Powtongsook S., Pavasant P. (2009). Flat panel airlift photobioreactors for cultivation of vegetative cells of microalga Haematococcus pluvialis. *Journal of Biotechnology, 142* (3-4): 227-232.

Jorquera O., Kiperstok A., Sales E.A., Embiruçu M., Ghirardi M.L. (2010). Comparative energy life-cycle analyses of microalgal biomass production in open ponds and photobioreactors. Bioresource Technology 101: 1406–1413.

Joshi J.B. (1980). Axial mixing in multiphase contactors a unified approach. Trans. IChemE 58: 155-165.

Kaewkannetra P., Enmak P., Chiu T.Y. (2012). The Effect of CO2 and Salinity on the Cultivation of Scenedesmus obliquus for Biodiesel Production. Biotechnology and Bioprocess Engineering 17: 591-597.

Khozin I., Adlerstein D., Bigongo C., Heimer Y.M., Cohen Z. (1997). Elucidation of the biosynthesis of eicosapentaenoic acid in the microalga Porphyridium cruentum. 2. Studies with radiolabeled precursors. *Plant Physiol, 114: 223–30.*

Kim J. D. and Lee C. G. (2005). Systemic optimization of microalgae for bioactive compound production. *Biotechnol Bioprocess Eng, 10: 418-424.*

Klekner V., Kosaric, N. (1992). Degradation of phenols by algae. Environmental Technology 13: 493-501.

Kok.B. (1953). Experiments on photosynthesis by Chlorella in flashing light. In: Burlew JS (ed.), Algal Culture from Laboratory to Pilot Plant. Carnegie Institution of Washington, Washington, D.C.:63-158.

Kok B. (1957). Absorption changes induced by the photochemical reaction of photosynthesis. Nature 179: 583-584.

Findlay J.A., Patil A.D. (1984). Antibacterial constituents of the diatom Navicula delognei. Lloydia 47: 815-818.

Harder R., Opperman A. (1953). Uber antibiotische Stoffe bei den Griinalgen Stichococcus bacillaris und Protosiphon botryoides. Arch. Mikrobiol. 19. 398-401.

Ho S.H., Chen C.Y., Chang J.S. (2012). Effect of light intensity and nitrogen starvation on CO2 fixation and lipid/carbohydrate production of an indigenous microalga Scenedesmus obliquus CNW-N. Bioresource Technology, 113: 244–252.

Hu Q. (2004). Environmental effects on cell composition. In: Richmond, A. (Ed.), Handbook of Microalgal Culture. Blackwell Science Ltd., Oxford OX2 0EL, UK, 5: 83–93.

Lau A.F., Siedlecki J., Anleitner J., Patterson G.M.L., Caplan F.R., Moore R.E. (1993). Inhibition of reverse transcriptase activity by extracts of cultured blue-green algae (Cyanophyta). Planta Med. 59: 148-151.

Lee Y. K. (1997) Commercial production of microalgae in the Asia-Pacific rim. J Appl Phycol 9: 403-4511.

Legendre L., Rochet M., Demers .S (1986.) Sea-ice microalgae to test the hypothesis of photosynthetic adaptation to high frequency light fluctuations. J. exp. mar. Biol. Ecol. 97: 321-326.

Lehr F., Posten C. (2009). Closed photo-bioreactors as tools for biofuel production. *Current Opinion in Biotechnology, 20* (3): 280-285.

Loubiere K., Olivo E., Bougaran G., Pruvost J., Robert R., Legrand J. (2009). A New Photobioreactor for Continuous Microalgal Production in Hatcheries Based on External-Loop Airlift and Swirling Flow. *Biotechnology and Bioengineering, 102* (1): 132-147.

Lowry O.H., Rosenbrough N.J., Farr A.L.Randal R. 1951. Protein determination using Folin Ciocalteu reagent. J Biol Chem, 193: 265-278.

Luo H. P., Kemoun A., Al-Dahhan M. H., Sevilla J. M. F., Sanchez J. L. G., Camacho F. G. (2003). Analysis of photobioreactors for culturing high-value microalgae and cyanobacteria via an advanced diagnostic technique: CARPT. *Chemical Engineering Science, 58*(12): 2519-2527.

Lv J.M., Cheng L.H., Xu X.H., Zhang L., Chen H.L. (2010). Enhanced lipid production of Chlorella vulgaris by adjustment of cultivation conditions. Bioresource Technology, 101 (17): 6797–6804.

Mallick N. (2002). Biotechnological potential of immobilized algae for wastewater N, P and metal removal: A review. BioMetals 15: 377–390.

Markou G., Georgakakis D. (2011). Cultivation of filamentous cyanobacteria (blue-green algae) in agro-industrial wastes and wastewaters: A review. Applied Energy 88, 10: 3389–3401.

Martinez M.E.,Jimenez J.M., El Yousfi F. (1999). Influence of phosphorus concentration and temperature on growth and phosphorus uptake by the microalga *Scenedesmus obliquus.* Bioresource Technology, 67: 233-240.

Masojidek J., Prasil O. (2010). The development of microalgal biotechnology in the Czech Republic. J Ind Microbiol Biotechnol 37:1307–1317.

Mata M.T., Martins A.T., Nidia. Caetano S. (2010). Microalgae for biodiesel production and other applications: A review. Renewable and Sustainable Energy Reviews 14: 217–232.

Mehta S. K., Gaur J. P. (2005). Use of Algae for Removing Heavy Metal Ions From Wastewater: Progress and Prospects. Critical Reviews in Biotechnology 25, (3): 113-152.

Molina Grima E., Acie´n Ferna´ndez F.G., Garcı´a Camacho F., Camacho Rubio F., Chisti Y. (2000). Scale-up of tubular photobioreactors. J. Appl. Phys. 12: 355-368.

Moroni M., Cenedese A. (2005). Comparison among feature tracking and more consolidated velocimetry image analysis techniques in a fully developed turbulent channel flow. Meas. Sci. Technol. 16: 2307-2322.

Morweiser M., Kruse O., Hankamer B., Posten C. (2010). Developments and perspectives of photobioreactors for biofuel production. Appl. Microbiol. Biotechnol. 87: 1291-1301.

Nedbal L., Tichy´ V., Xiong F., Grobbelaar J.U.(1996). Microscopic green algae and cyanobacteria in high-frequency intermittent light. J. Appl. Phycol. 8: 325–333.

Olguin E.J., Galicia S., Angulo-Guerrero O., Hernandez E. (2001). The e€ ect of low light lux and nitrogen deficiency on the chemical composition of Spirulina sp. (Arthrospira) grown on digested pig waste. Biores. Technol. 77: 19-24.

Oliveira M.A.C.L., De Monteir M.P.C., Robbs P.G., Leite S.G.F.(1999).Growth and chemical composition of Spirulina maxima and Spirulina platensis biomass at different temperature Aquaculture International 7: 261–275.

Oswald WJ. (1988). Microalgae and wastewater treatment. In: Borowizka MA, Borowizka LJ, eds Microalgal Biotechnology. NY: Cambridge University Press:305-328.

Oswald WJ. (2003). My sixty years in applied algology. J Appl Phycol, 15:99–106.

Park K.H., Lee C.G. (2001). Effectiveness of flashing light for increasing photosynthetic efficiency of microalgal cultures over a critical cell density. Biotechnol. Bioproc. Eng. 6: 189-193.

Park J., Jin H.F.,Lim B.R., Park K.Y., Lee k. (2010). Ammonia removal from anaerobic digestion effluent of livestock waste using green alga Scenedesmus sp.Bioresource Technology 101: 8649–8657.

Pedersen M., DaSilva E.J. (1973). Simple brominated phenols in the bluegreen alga Calothrix brevissima West. Planta 115: 83-96.

Pesando D., Gnassia-Barelli M., Gueho E., Rinaudo M,. Defaye J. (1980) Isolement, etucle structurale et proprietes antibiotiques et antifongiques d'un comosant polysaccaridique de la diatome marine Chaetoceras lauderi Ralfs. Oceanis. Fasc. Hors.-Ser.:561-568.

Posten C. (2009). Design principles of photo-bioreactors for cultivation of microalgae. *Engineering in Life Sciences, 9* (3): 165-177.

Pratt, R., and Fong, J. (1940). Studies on Chlorella vulgaris. Further evidence that chlorella cells form a growth inhibiting substance. Am. J. Bot. 27, 431-436.

Pulz O. (2001). Photobioreactors: production systems for phototrophic microorganisms. Appl Microbiol Biotechnol 57: 287–293.

Pulz O., Gross W. (2004). Valuable products from biotechnology of microalgae.Appl Microbiol Biotechnol, 65: 635–648.

Ras M., Lardon L., Sialve B., Bernet N., Steyer J.P. (2011). Experimental study on a coupled process of production an anaerobic digestion of *Chlorella vulgaris*. Bioresource Technology 102: 200–206.

Reed R.H., RIichardosn D.L., STewart W.D.P. (1985). Na+ uptake and extrusion in the cyanobacterium Synechocystis PCC 6714 in response to hyper-saline treatment. Evidence for transient changes in plasmalemma Na+ permeability, Biochim. Biophys. Acta, 814, 347.

Richmond A.., Lichtenberg E., Stahl B., Vonshak A. (1990). Quantitative assessment of the major limitations on productivity of Spirulina platensis in open raceways, Journal of Applied Phycology 2: 195–206.

Richmond A., Cheng-Wu Z., ZarmiY. (2003).Efficient use of strong light for high photosynthetic productivity:interrelationships between the optical path, the optimal population density and cell-growth inhibition.Biomolecular Engineering 20: 229-236.

Rinehart K.L., Shaw P.D., Shield L.S., Gloer J.B., Harbour G.C., Koker M.E.S., Samain D., Schwartz R.E., Tymiak A.A., Weller D.L., Carter G.T., Munro M.H.G., Hughes R.G., Renis H.E., Swynenberg E.B., Stringfellow D.A., Vavra J.J., Coats J.H., Zurenko G.E., Kuentzel S.L., Li L.H., Bakus G.J., Brusca R.C., Craft L.L., Young D.N., Connor J.L. (1981) Marine natural products as sources of antiviral, antimicrobial, and antineoplastic agents. Pure appl. Chem. 53: 795-817.

Ryll J., Scheper T., Lotz M. (2003). Biotechnological production of -1,3-Glucan in a technical pilot plant. Abstr. Eur. Workshop Microalgal Biotechnol., Germany, p. 56.

Sánchez E., Ojedaa K., El-Halwagib M. and Kafarova V. 2011. Biodiesel from microalgae oil production in two sequential esterification/transesterification reactors: Pinch analysis of heat integration. *J. of chem. eng., 176-177:211-216.*

Sato T., Yamada D., Hirabayashi, S. (2010). Development of virtual photobioreactor for microalgae culture considering turbulent flow and flashing light effect. Energ. Convers. Manage. 51: 1196-1201.

Shen Y., Pei Z., Yuan W. and Mao E. (2009). Effect of nitrogen and extraction method on algae lipid yield. *Int J Agric & Biol Eng, 2, (1): 51-57.*

Sieburth J.M. (1959). Acrylic acid, an 'antibiotic' principle in Phaeocystis blooms in Antarctic waters. Science 132: 676-677.

Sili C., Torzillo G., Vonshak A. (2012). Arthrospira platensis.Ecology of Cyanobacteria II: 677-705.

Spolaore P., Joannis-Cassan C.,Duran E., Isambert A. (2006). Commercial Applications of Microalgae. JOURNAL OF BIOSCIENCE AND BIOENGINEERING ,101, 2: 87–96.

Tchobanoglous G., Burton F.L. (1991). Wastewater engineering: treatment, disposal, and reuse. McGraw-Hill.

Terry K. (1986). Photosynthesis modulated light: quantitative dependence of photosynthetic enhancement on flashing rate. Biotechnol. Bioeng. 28 (7): 988-995.

Tredici M., Materassi R. (1992). From open ponds to vertical alveolar panels: the Italian experience in the development of reactors for the mass cultivation of phototrophic microorganisms. Journal of Applied Phycology 4: 221-231.

Taylor R.F., Ikawa M., Sasner J.J., Thurberg F.P., Andersen K.K. (1974). Occurrence of choline esters in the marine dinoflagellate Amphidinium carter. J. Phycol. 10: 279-283.

Torzillo G., Vonshak A. (2003) Biotechnology for algal mass cultivation. In: Recent advances ion marine biotechnology (Fingerman M., Nagabhushanam R. eds) Volume 9 Biomaterials and Bioprocessing, Science Publishers, Inc. Enfield (NH), USA, 45-77.

Torzillo G., Giannelli L., Verdone N., De Filippis P., Scarsella M.,Martı´nez-Rolda´ n A.J., Bravi M., (2010). Microalgae culturing in thin-layer photobioreactors. Chem. Eng. Trans. 20: 265-270.

Wang B., Li Y. Wu N., Lan C.Q. (2008). CO2 bio-mitigation using microalgae. Appl Microbiol Biotechnol, 79: 707–718.

Wang L., Yecong L., Chen P., Min M., Chen Y., Zhu J., Ruan R. (2010). Anaerobic digested dairy manure as a nutrient supplement for cultivation of oil-rich green microalgae Chlorella sp. Bioresource Technology 101:2623–2628.

Wellburn A. (1994). The spectral determination of chlorophylls a and b, as well as total carotenoids, using various solvents with spectrophotometers of different resolution. J. Plant Physiol 144: 307-313.

Weller S., Franck J. (1941) Photosynthesis in flashing light. J Physiol Chem 45 (9), 1359-1373.

Wijffels R.H. and Barbosa M.J. 2010. An Outlook on Microalgal Biofuels. *Science, 329: 796-799.*

Xin l., Hong-ying H., Yu-ping Z. (2011). Growth and lipid accumulation properties of a freshwater microalga Scenedesmus sp. under different cultivation temperature. Bioresource Technology 102: 3098–3102.

Yoshimoto N., Sato T., Kondo Y. (2005). Dynamic discrete model of flashing light effect in photosynthesis of microalgae. J. Appl. Phycol. 17: 207-214.

Zarrouk C. (1996). Contribution a l'etude d'une cyanobacterie: influence de divers facteurs physiques et chimiques sur la croissance et la photosynthese de *Spirulina maxima* (Setchell *et* Gardner) Geitler. Ph.D. thesis, University of Paris, France.

Thanks

Ringrazio tutti i professori del corso di dottorato, in particolar modo Prof.ri Chianesee Di Palma; ringrazio il Dott. Marco Stoller, la prof.ssa Monica Moroni, il Prof. Giuseppe Torzillo e la dott.ssa Cecilia Faraloni, per il sostegno e le conoscenze che mi hanno trasmesso.
Ringrazio tutti i tecnici del Dipt.d'ingegneria chimica, in particolar modo Massimo Giugnoli e Stefania Pontecorvo.
Ringrazio i miei genitori, per tutto l'aiuto e il tempo che mi hanno dedicato.